JAERI-M
85-115

PRE-TEST PREDICTION OF FIX II INTERMEDIATE BREAK EXPERIMENT WITH THYDE-P1

(CSNI INTERNATIONAL STANDARD PROBLEM NO. 15)

August 1985

Masashi HIRANO and Masayuki AKIMOTO

日本原子力研究所
Japan Atomic Energy Research Institute

JAERI-Mレポートは，日本原子力研究所が不定期に公刊している研究報告書です。
入手の問合わせは，日本原子力研究所技術情報部情報資料課（〒319-11茨城県那珂郡東海村）あて，お申しこしください。なお，このほかに財団法人原子力弘済会資料センター（〒319-11 茨城県那珂郡東海村日本原子力研究所内）で複写による実費頒布をおこなっております。

JAERI-M reports are issued irregularly.
Inquiries about availability of the reports should be addressed to Information Division Department of Technical Information, Japan Atomic Energy Research Institute, Tokai-mura, Naka-gun, Ibaraki-ken 319-11, Japan.

編集兼発行　日本原子力研究所
印　　刷　㈱高野高速印刷

JAERI-M 85-115

Pre-Test Prediction of FIX II Intermediate Break Experiment with THYDE-P1 (CSNI International Standard Problem No. 15)

Masashi HIRANO and Masayuki AKIMOTO

Department of Reactor Safety Research
Tokai Research Establishment, JAERI

(Received July 15, 1985)

This report contains the results from the pre-test prediction calculation of FIX II Intermediate Break Experiment with the THYDE-P1 computer code. The experiment simulated the conditions corresponding to an intermediate size break loss-of-coolant accident (LOCA) in one of the recirculation lines of a boiling water reactor (BWR) with external pumps. The test was the first LOCA experiment in the FIX II facility and was chosen as the OECD CSNI International Standard Problem No 15.

Although an extensive verification calculations have been performed with THYDE-P1 for pressurized water reactors (PWRs), the present calculation is the first application to BWR. The major purposes of the present calculation are to verify the applicability of THYDE-P1 to BWR and to identify the model deficiencies for further code modification.

After the experimental data being released, the predicted results with THYDE-P1 have been compared with the experimental data. The comparison shows that the present calculation has adequately predicted the important phenomena observed in the experiment.

Key Words: THYDE-P1, LOCA, Pre-Test Prediction, FIX II, Intermediate Break, CSNI International Standard Problem No. 15, BWR External pump, Verification

ＴＨＹＤＥ－Ｐ１によるＦＩＸ　ＩＩ中破断実験の実験前予測計算
（ＣＳＮＩ国際標準問題№１１）

日本原子力研究所東海研究所原子炉安全工学部
平野雅司・秋元正幸

（１９８５年７月１５日受理）

ＴＨＹＤＥ－Ｐ１コードによるＦＩＸ　ＩＩ中破断実験の実験前予測計算結果を報告する。本実験は，外付き再循環ポンプ沸騰水型軽水炉（ＢＷＲ）に於ける再循環ライン中破断冷却水喪失事故（ＬＯＣＡ）を模疑した実験である。本実験はＦＩＸ　ＩＩ実験装置での初めてのＬＯＣＡ実験であり，ＯＥＣＤ　ＣＳＮＩ国際標準問題№１５に採用された。

これまでＴＨＹＤＥ－Ｐ１の検証計算を，加圧水型軽水炉に対して広範に行って来たが，本計算がＢＷＲへの初めての適用である。本計算の目的は，ＴＨＤＥ－Ｐ１がＢＷＲに適用可能であることを検証すると同時に，今後のコードの改良のためにモデルの不備を検討することにある。

実験結果が公開された後，予測結果と実験結果の比較を行った。その結果，本予測計算は，実験で観測された重要な事象を適切に予測したことが示された。

Contents

1. Introduction 1

2. Description of FIX II Intermediate Break Experiment 1

2.1 System Description 1
2.2 Test Procedure 2
2.3 Initial Conditions and Boundary Conditions 3

3. Analytical Models 3

3.1 Nodalization 3
3.2 CHF and Heat Transfer Correlations 4
3.3 Break Flow Model 5
3.4 Relief Valve Model 5
3.5 Pump Model 5
3.6 Pressure Loss Coefficients 6
3.7 Ambient Heat Loss 6
3.8 Material Properties 7
3.9 Phase Separator Model 7

4. Calculated Results and Discussions 8

4.1 Pressure Transient 8
4.2 Cladding Surface Temperature Transient 8
4.3 Core Hydraulics 9
4.4 Downcomer Behavior 10
4.5 Break Flow Transient 11
4.6 Bypass Hydraulics 11

5. Concluding Remarks 13

References 14

Appendix A List of Input Data 57
Appendix B Description and Geometrical Data of components in FIX II Loop 66
Appendix C Brief Description of Code Characteristics and Information on Computer Resources Utilized in Present Calculation 71
Appendix D Pump Characteristic Curves Used in Present Calculation 75

目　　次

1. 序 …… 1
2. ＦＩＸ　ＩＩ　中破断実験の記述 …… 1
2.1 実験装置 …… 1
2.2 実験手順 …… 2
2.3 初期条件及び境界条件 …… 3
3. 解析モデル …… 3
3.1 ノード分割 …… 3
3.2 ＣＨＦ及び熱伝達モデル …… 4
3.3 破断流モデル …… 5
3.4 逃し弁モデル …… 5
3.5 ポンプモデル …… 5
3.6 圧損係数 …… 6
3.7 系外への熱損失 …… 6
3.8 物性値 …… 7
3.9 気水分離器モデル …… 7
4. 計算結果及び議論 …… 8
4.1 圧力の過渡変化 …… 8
4.2 被覆管表面温度の過渡変化 …… 8
4.3 炉心流動 …… 9
4.4 ダウンカマ挙動 …… 10
4.5 破断流の過渡変化 …… 11
4.6 バイパス流動 …… 11
5. 結論 …… 13
参考文献 …… 14
付録　Ａ　入力データリスト …… 57
Ｂ　ＦＩＸ　ＩＩループの記述及び形状データ …… 66
Ｃ　コードの簡単な記述及び本計算に使用した計算機資源 …… 71
Ｄ　本計算で使用したポンプ特性曲線 …… 75

List of Figures

Figure No.	Title	Page
Fig. 2.1.1	Lay-out of FIX II loop	23
Fig. 2.1.2	Schematic diagram of central loop section	24
Fig. 2.1.3	Split break simulation	25
Fig. 2.1.4	Horizontal cut view of test section and radial power distribution	26
Fig. 2.1.5	Structure of fuel rod simulator	27
Fig. 2.1.6	Axial power distribution and instrumentation location	28
Fig. 2.1.7	Structure of bypass and control rod guide tube volume	29
Fig. 2.1.8	Axial power distribution of bypass channel	30
Fig. 2.1.9	Structure above test section	31
Fig. 2.3.1	Planned core and bypass power histories	32
Fig. 2.3.2	Measured core and bypass power histories	32
Fig. 2.3.3	Planned pump speed histories	33
Fig. 2.3.4	Measured pump speed histories	33
Fig. 3.1.1	Nodalization chart	34
Fig. 3.5.1	Pump characteristic curve for pump P1	35
Fig. 3.5.2	Pump characteristic curve for pump P2	35
Fig. 3.6.1	Flow diagram of FIX II loop	36
Fig. 3.6.2	Pressure losses at core and bypass	37
Fig. 3.8.1	Specific heat of fuel rod simulator filler material	38
Fig. 3.8.2	Thermal conductivity of fuel rod simulator filler material	38
Fig. 3.9.1	Schematic diagram of phase separation	39
Fig. 4.1.1	Pressure at steam dome	39
Fig. 4.1.2	Mass flow rate through steam relief valve	40
Fig. 4.1.3	Schematic diagram of valve actions	40
Fig. 4.1.4	Measured fluid temperatures at lower plenum and upper plenum	41
Fig. 4.2.1	Vertical distribution of calculated cladding surface temperature	42
Fig. 4.2.2	Three-Dimensional view of calculated cladding surface temperature	43

Fig. 4.2.3 Experimental cladding surface temperatures in upper part part of core 43
Fig. 4.2.4 Experimental cladding surface temperatures in lower part part of core 44
Fig. 4.2.5 Effect of lower plenum flashing on cladding surface temperature 45
Fig. 4.2.6 Cladding surface temperature at level 1 45
Fig. 4.2.7 Cladding surface temperature at level 3 46
Fig. 4.2.8 Cladding surface temperature at level 5 46
Fig. 4.2.9 Cladding surface temperature at level 7 47
Fig. 4.2.10 Cladding surface temperature at level 9 47
Fig. 4.2.11 Cladding surface temperature at level 10 48
Fig. 4.2.12 Cladding surface temperature at level 12 48
Fig. 4.2.13 Cladding surface temperature at level 15 49
Fig. 4.3.1 Bundle inlet mass flow rate 49
Fig. 4.3.2 Differential pressure through core 50
Fig. 4.3.3 Mass flow rate through pumpP1 50
Fig. 4.3.4 Mass flow rate through pump P2 51
Fig. 4.3.5 Calculated mass flow rates at core inlet and both inlet and outlet of lower plenum 51
Fig. 4.3.6 Calculated void fractions at core 52
(a) Lower part of core 52
(b) Upper part of core 52
Fig. 4.4.1 Differential pressure through downcomer 53
Fig. 4.4.2 Fluid temperature at downcomer inlet 53
Fig. 4.5.1 Break flow 54
Fig. 4.5.2 Integrated break mass flow 54
Fig. 4.5.3 Calculated mass flow rates at break, vessel side and pump side of broken recirculation line 55
Fig. 4.5.4 Calculated mass flow rates at lower plenum inlet, vessel side of broken recirculation line and intact recirculation line 55
Fig. 4.6.1 Differential pressure through bypass 56
(a) Calculated 56
(b) Measured 56

List of Tables

Table No.	Title	
Table 2.2.1	Planned performance chronology	16
Table 2.2.2	Measured performance chronology	16
Table 2.3.1	Planned initial conditions	17
Table 2.3.2	Planned initial conditions and rated values for recirculation pumps	17
Table 2.3.3	Measured initial conditoins	18
Table 3.1.1	Description of nodes and heat slabs	19
Table 3.6.1	Loss coefficients in loop	20
Table 3.7.1	Ambient heat losses evaluated before experiment	21
Table 3.7.2	Measured ambient heat losses	21
Table 4.1	Chronology of key events	22

1. Introduction

The THYDE-P1 (1-10) code is a computer code which is applicable to various types of transient including a loss-of-coolant accident (LOCA) in both pressurized water reactors (PWRs) and boiling water reactors (BWRs). Although an extensive verification calculations have been performed for PWRs using the experimental data such as Loss-Of-Fluid Test (LOFT)(11) data, the present calculation is the first application to BWR.

The experiment(12-14) has been performed in May 1983 as the very first LOCA experiment in the FIX II facility, which has simulated the Swedish Oskarshamn 2 reactor, a 570 MWe BWR with external recirculation pumps. The volume scaling is 1:777. Components are included to steam dome, downcomer, two recirculation lines with one pump each, lower plenum, core with a 36-rod full-length bundle, control-rod guide tube volume, core bypass, upper plenum and steam separators.

The transient performed has simulated the conditions corresponding to an intermediate size split break in one of the main recirculation lines. The general objective with the test program is to obtain data for heat transfer between rod cladding and coolant during specified LOCAs and transients included in the studies of Swedish BWRs.

The test has been chosen as the OECD CSNI International Standard Problem No. 15 (ISP No.15). A blind calculation has been performed with THYDE-P1 based on the information provided about the test loop geometry, data on flow resistance, initial conditions and the test procedure(12).

In the present pre-test prediction calculation, the system characteristics is unknown because the experiment is the very first LOCA experiment in the facility. In addition, the planned initial conditions and chronology of performance can be different from those actually realized in the experiment. In these points of view, the present calculation can be said what is called a double-blind calculation. In spite of the difficulties expected to this type of calculation, the calculated results are reasonably in agreement with the expermental data.

2. Description of FIX II Intermediate Break Experiment

The intermediate break experiment, denoted Experiment 3025, has been conducted as the first LOCA experiment in the FIX II facility. The test facility is utilized for loss-of-coolant heat transfer experiment during the blowdown phase in an external recirculation pump BWR.

2.1 System Description

Figure 2.1.1 shows the lay-out of the FIX II loop. The description and the geometrical data of each component shown in this figure are summarized in App. B. The principal outline of the central loop section is schematically shown in Fig. 2.1.2. The test apparatus comprises the following main parts:

1. Introduction

The THYDE-P1 (1-10) code is a computer code which is applicable to various types of transient including a loss-of-coolant accident (LOCA) in both pressurized water reactors (PWRs) and boiling water reactors (BWRs). Although an extensive verification calculations have been performed for PWRs using the experimental data such as Loss-Of-Fluid Test (LOFT)(11) data, the present calculation is the first application to BWR.

The experiment(12-14) has been performed in May 1983 as the very first LOCA experiment in the FIX II facility, which has simulated the Swedish Oskarshamn 2 reactor, a 570 MWe BWR with external recirculation pumps. The volume scaling is 1:777. Components are included to steam dome, downcomer, two recirculation lines with one pump each, lower plenum, core with a 36-rod full-length bundle, control-rod guide tube volume, core bypass, upper plenum and steam separators.

The transient performed has simulated the conditions corresponding to an intermediate size split break in one of the main recirculation lines. The general objective with the test program is to obtain data for heat transfer between rod cladding and coolant during specified LOCAs and transients included in the studies of Swedish BWRs.

The test has been chosen as the OECD CSNI International Standard Problem No. 15 (ISP No.15). A blind calculation has been performed with THYDE-P1 based on the information provided about the test loop geometry, data on flow resistance, initial conditions and the test procedure(12).

In the present pre-test prediction calculation, the system characteristics is unknown because the experiment is the very first LOCA experiment in the facility. In addition, the planned initial conditions and chronology of performance can be different from those actually realized in the experiment. In these points of view, the present calculation can be said what is called a double-blind calculation. In spite of the difficulties expected to this type of calculation, the calculated results are reasonably in agreement with the expermental data.

2. Description of FIX II Intermediate Break Experiment

The intermediate break experiment, denoted Experiment 3025, has been conducted as the first LOCA experiment in the FIX II facility. The test facility is utilized for loss-of-coolant heat transfer experiment during the blowdown phase in an external recirculation pump BWR.

2.1 System Description

Figure 2.1.1 shows the lay-out of the FIX II loop. The description and the geometrical data of each component shown in this figure are summarized in App. B. The principal outline of the central loop section is schematically shown in Fig. 2.1.2. The test apparatus comprises the following main parts:

- A pressure vessel with a 36-rod test section and a steam dome,
- A piping system with recirculation pumps and arrangements for break simulations,
- An external piping and auxiliary systems for steady-state operation of the loop, and
- Power supply and power control systems.

The downcomer is simulated by the external piping. Two recirculation lines simulate 4 recirculation lines in BWR. The one simulates the three intact lines and the other simulates one broken line. Thus, 1/4 of the total flow is circulated through the broken line. The valves v103, v117, v120 and v123 are used to simulate the break. In Experiment 3025, a simulated split break is acomplished by opening the valve 120 to the break flow receiver as shown in Fig. 2.1.3. The valve 103 is closed when simulating a double-ended break.

For the removal of the heat generation during the steady state operation, a portion of the downcomer flow is circulated through the cooler. The flow is fed back to the system as feed water and as spray to the top of the steam dome. During the steady-state operation, the valve v112 is closed and all the steam generated at the core is condensated by the spray flow. The flow path through the cooler is closed immediately after the break.

Figure 2.1.4 shows the horizontal cut view of the test section and the radial power distribution. The test section consists of a container with a 6x6 bundle of electorically heated fuel rod simulators. The measurment lines from the test section are cooled by circulating water in the gap between the teflon filling and the pressure vessel. This causes a heat loss, which will be discussed later.

Figure 2.1.4 shows the horizontal cut view of the test section and the radial power distribution. The test section consists of a container with a 6 × 6 bundle of electorically heated fuel rod simulators. The measurement lines from the test section are cooled by circulating water in the gap between the teflon filling and the pressure vessel. This causes a heat loss, which will be discussed later.

The core bypass and guide tube volume are simulated by separate pipes outside the pressure vessel as shown in Fig. 2.1.7. An electrically heated rod is installed within the core bypass. Its axial power distribution is shown in Fig. 2.1.8.

Figure 2.1.9 shows the structures above the test section. A spray condensor is located on top of the test section. A simplified steam separator is located in the lower part of the condensor, and its upper part is used as a steam dome, to which the steam relief line is connected.

2.2 Test Procedure

Table 2.2.1 shows the planned chronology of performance, which has been provided for the blind calculation for ISP No. 15. Table 2.2.2 shows the chronology of performance actually measured in the

experiment. When these tables are compared, it is clear that the planned chronology of performance is a little different from that actually measured in the experiment. The difference in these two tables will be discussed in detail later. Here, the test procedure is stated based on the measured chronology of performance shown in Table 2.2.2. The test has been initiated by opening the break valev at 0.0 s. The steam relief valve has started to open at 0.4 s and been fully open at 1.0 s. The steam relief valve has started to close again at 1.6 s. The flow through the cooler has been closed by 2 s into the transient. The steam relief valve has started to open for the second time at 12.05 s. The experiment has been terminated by closing the steam relief valve and the break valve at 76 s.

2.3 Initial Conditions and Boundary Conditions

Table 2.3.1 shows the planned initial conditions provided(12) for the blind calculation. Also the initial conditions for the pumps and the rated pump values are summarized in Table 2.3.2. Table 2.3.3 shows, on the other hand, the initial conditions actually measured in the experiment. The planned initial conditions are also slightly different from those measured in the experiment. For example, the planned initial core power is about 3 % larger than the actual power and the planned bypass power is also 8 % larger than the actual value.

Figure 2.3.1 shows the planned core and bypass power histories. Corresponding to this figure, the measured power histories are shown in Fig. 2.3.2. The planned normalized core power, for example, at 10 s is, in turn, about 10% smaller than the measured value. Then, considering the difference in the initial power, it is concluded that the power level used in the calculation at 10 s is slightly smaller than the actual power applied in the experiment, and the difference is small.

Figures 2.3.3 and 2.3.4 show planned and measured pump rotational speeds, respectively. Aparrent difference appears after 50 s for pump P2. Except this point, the planned speeds are in good agreement with those measured in the experiment.

3. Analytical Models

As to the detailed description of the methods and the models of THYDE-P1, Ref. (1) should be refered. The brief summary of the code characteristics and the options applied are shown in Table C.1 in App. C.

3.1 Nodalization

Figure 3.1.1 shows the nodalization diagram. The description of the nodes and the heat slabs are shown in Table 3.1.1. The present calculation has been performed with 54 nodes and 50 junctions. The test section is represented by a single channel. The focal point in the present calculation is the core heat trans-

experiment. When these tables are compared, it is clear that the planned chronology of performance is a little different from that actually measured in the experiment. The difference in these two tables will be discussed in detail later. Here, the test procedure is stated based on the measured chronology of performance shown in Table 2.2.2. The test has been initiated by opening the break valev at 0.0 s. The steam relief valve has started to open at 0.4 s and been fully open at 1.0 s. The steam relief valve has started to close again at 1.6 s. The flow through the cooler has been closed by 2 s into the transient. The steam relief valve has started to open for the second time at 12.05 s. The experiment has been terminated by closing the steam relief valve and the break valve at 76 s.

2.3 Initial Conditions and Boundary Conditions

Table 2.3.1 shows the planned initial conditions provided(12) for the blind calculation. Also the initial conditions for the pumps and the rated pump values are summarized in Table 2.3.2. Table 2.3.3 shows, on the other hand, the initial conditions actually measured in the experiment. The planned initial conditions are also slightly different from those measured in the experiment. For example, the planned initial core power is about 3 % larger than the actual power and the planned bypass power is also 8 % larger than the actual value.

Figure 2.3.1 shows the planned core and bypass power histories. Corresponding to this figure, the measured power histories are shown in Fig. 2.3.2. The planned normalized core power, for example, at 10 s is, in turn, about 10% smaller than the measured value. Then, considering the difference in the initial power, it is concluded that the power level used in the calculation at 10 s is slightly smaller than the actual power applied in the experiment, and the difference is small.

Figures 2.3.3 and 2.3.4 show planned and measured pump rotational speeds, respectively. Aparrent difference appears after 50 s for pump P2. Except this point, the planned speeds are in good agreement with those measured in the experiment.

3. Analytical Models

As to the detailed description of the methods and the models of THYDE-P1, Ref. (1) should be refered. The brief summary of the code characteristics and the options applied are shown in Table C.1 in App. C.

3.1 Nodalization

Figure 3.1.1 shows the nodalization diagram. The description of the nodes and the heat slabs are shown in Table 3.1.1. The present calculation has been performed with 54 nodes and 50 junctions. The test section is represented by a single channel. The focal point in the present calculation is the core heat trans-

fer during the blowdown and therefore the phase separation phenomenon is considered to be very important. In order to simulate the phase separation phenomenon adequately, the test section should be discretized vertically by many nodes because a drift flux model is applied in THYDE-P1 and a water level tracking model is not implemented. In the present calculation, the test section and the downcomer are nodalized 12 and 11 nodes, respectively. The average rod and the highest power rod are simulated separately by the heat slabs. The power ratio of the highest power rod to the average rod is 1.034 based on the radial power disdribution shown in Fig. 2.1.4.

The core bypass and the control rod guide tube volume are simulated by the flow path parallel to the test section. The heater in the core bypass is also modeled by the heat slabs.

The flow path through the cooler with the circulation pump P3 and several controling valves are also modeled to simulate the steady-state operation in the experiment. The spray line is, however, assumed to be directly connected to the lower part of the steam dome. It is because that, in the present version of THYDE-P1, the velocity difference between the phases are not yet considered at the steady state calculation. This means the node average enthalpy is set equal to the average enthalpy upstream of the node, if the heat source does not exist. Then, the spray line from the evaporation cooler, which is filled with subcooled water, cannot be connected at the top of steam dome, filled with saturated steam. This simulation method may not affect adversely the overall trend of the calculation, beause the spray valve starts to close just after the test initiation, i.e. 1.78 s after break in the planned sequence.

The list of the input data used in the present calculation is shown in App. A.

3.2 CHF and Heat Transfer Correlations

In the present calculation, the correlations for the heat transfer coefficients and the critical heat flux (CHF) are selected by options as follows:

- The Dittus-Boeltler correlation(18) for the forced convection condition,
- The Thom correlation(19) for the nucleate boiling,
- The Bromley-Pomeranz correlation(20, 21) for the low flow film boiling,
- The Groenevelt(22) and Dougal-Rohsenow(23) correlations for high flow film boiling, and
- The McEligot(24) correlation for the forced convection due to superheated steam.

The CHF correlations applied in the present calculation are:

- The Biasi correlation(25) for the high flow condition, and
- The Zuber correlation(26) for the low flow condition.

3.3 Break Flow Model

The modified Zaloudek equation(16) and the Moody correlation(15) are applied under the subcooled condition and the saturated condition, respectively. The discharge coefficient for the Moody correlation is assumed to be 0.6. The modified Zaloudek equation is as follows:

$$G_c = cd\sqrt{2\rho(P-c_2 P_{sat})} \qquad \text{Eq. 3.3.1}$$

where

G_c : Critical mass flow ($kg/s.m^2$)
P : Pressure upstream of break (pa)
P_{sat} : Saturation pressure (pa)
ρ : Fluid density (kg/m^3)
Cd : Discharge coefficient (=0.6)
C_2 : Constant (=0.8)

The transition quality is assumed to be 0.02. When the coolant is subcooled, the modified Zaloudek equation is used and when it becomes larger than 0.02, the Moody correlation is used. When the quality is between 0.0 and 0.02, the critical flow is linearly interpolated between them.

3.4 Relief Valve Model

The boundary condition at the steam outflow is very important to determine the pressure transient. In the experiment, the steam flow is calibrated to give 1 kg/s at a steam dome pressure of 70 bars. This is done by the adjustment of the valve flow area.

In the present calculation, the following model(13) is tentatively implemented in THYDE-P1 and used:

$$W_s = A\sqrt{\kappa\left(\frac{2}{\kappa+1}\right)^{\frac{\kappa+1}{\kappa-1}}\cdot\sqrt{\rho_{fs}\cdot P}} \qquad \text{Eq. 3.4.1}$$

where

W_s : Steam mass flow (kg/s),
A : Valve flow area (m),
P : Pressure upstream of valve (pa),
ρ_{fs} : Fluid saturation density (kg/m^3),
κ : Ratio of isobaric specific heat to specific heat at constant volume (-).

The flow area A is adjusted to give 1 kg/s at a steam dome pressure of 70 bar corresponding to the flow calibration in the experiment. It is because the relief valve model in THYDE-P1 is yet to be developed.

3.5 Pump Model

Figures 3.5.1 and 3.5.2 show so called Q-H curves for recirculation pumps p1 and p2, respectively. These are the only data available from the experimental basis. In the transient analysis, however, the full pump characteristic curves are necessary including those for two-phase flows.

Although the two-phase pump characteristics are very important to predict the core hydraulics, no experimental data are available for the recirculation pumps. The pump characteristic curves for both single phase flow and two-phase flow used in the present calculation are shown in App. D. These data are recommended(13) to be used for blind calculations because of lack of data, in spite of the fact that the two-phase data are to be used for the different pump from that installed in FIX II test facility.

3.6 Pressure Loss Coefficients

Table 3.6.1 shows the data table provided(12) for the pressure loss coefficients for the blind calculation. It is found that there is a inconsistency in this table. Figure 3.6.2 schematically shows the pressure drops calculated based on the items 1 to 3 and 9 in Table 3.6.1. Since the wall frictional pressure drops through the test section and the bypass are small in comparison with the pressure losses at the flow restrictions, they are not necessary to be considered here. As shown in this figure, the pressure loss through the bypass is much larger than that through the core. Thus, we can conclude that some data are missing for the pressure losses at the test section or the loss coefficient at the bypass inlet is errorneous, i.e. too large. In the present blind calculation, the loss coefficient at the bypass inlet is reduced and adjustment has been perforemed at the steam separator and the pumps to obtain a consistent presure distribution at the steady state.

3.7 Ambient Heat Loss

The detailed information on the structures in the test loop has not been provided for the blind calculations. In the present calculation, therefore, the structual heat and ambient heat loss are not taken into consideration.

The major heat losses from the loop are caused by the cooling of the measurment lines and heat losses from exposed surfaces. As stated in Subsec. 2.1, the measurement lines from the test section are cooled by circulating water in the gap between the teflon filling and the pressure vessel. The heat loss from this section estimated before the experiment is 250 kw. The other heat losses estamated are shown in Table 3.7.1. The total heat loss is evaluated more than 10% of the rated core power. Table 3.7.2 shows the measured heat loss from the measurment lines. The evaluated heat loss from this section is turned out to be the same order of magnitude as that measured.

3.8 Material Properties

Figures 3.8.1 and 3.8.2 show the specific heat capacity and the thermal conductivity of the compacted magnesium oxide as a function of temperature provided(12) for the blind calculation. These data are used in the present calculation.

3.9 Phase Separator Model

In the pesent version of THYDE-P1, a phase separator model yet to be developed. Therefore, in the present calculation, a very simple model is tentatively implemented into THYDE-P1 and used. The modeling is schematically explained in Fig. 3.9.1. In this model, the integration scheme of the enthalpy transportation term in the energy conservation equation is changed only at the phase separator as follows:

(1) If mixing junction 42 (mj42) is saturated and the node 14 (n14) inlet flow is positive, only saturated fluid is transported from mj42 to n14.

(2) If mj42 is saturated and the n50 inlet flow is positive, only saturated steam is transported from mj42 to n 50.

(3) If n14 is saturated and the n14 inlet flow is negative, only the saturated steam is transported from n14 to mj42.

(4) If n14 is saturated and the n14 inlet flow is positive, only saturated fluid is transported from n14 to mj44.

(5) In the other cases than (1) to (4), the integration method is the same as that for the other nodes and junctions.

4. Calculated Results and Discussions

The calculated chronology of key events are compared with the measured data in Table 4.1. In the following subsections, the predicted results with THYDE-P1 are compared with the experimental data and discussed with special attention to the key events shown in the table.

4.1 Pressure Transient

The calculated pressure transient at the steam dome is shown in Fig.4.1.1 along with the experimental data. In the early stage, the pressure is overestimated but is underestimated in the late stage. In order to clarify the reasons for the difference, the valve actions in the calculation should be compared with those actually performed in the experiment because the steam flow rate through the relief valve is very important to determine the pressure history especially in the early stage of the blowdown. Figure 4.1.2 shows the comparison between the calculated mass flow rate through the relief valve and the corresponding experimental data. Overall trend of the calculated steam mass flow rate is in good agreement with the experimental data. This means the model stated in Subsec. 3.4 gives a good approximation to the steam mass flow rate. Although it is not clear in this figure, the relief valve is closed earlier in the calculation than in the experiment. Figure 4.1.3 shows the valve actions both in the calculation and experiment. The valve actions in the calculation are based on the planned sequence of events, which is different from the measured one. The steam relief valve (v 112) is closed about 0.5 s earlier in the calculation than in the experiment. In addition, both spray flow valve (v 106) and feed water valve (v 104) are also clculated to be closed earlier than in the experiment. These differences in the boundary condition are considered to be one of the reasons for the overestimated pressure in the early stage of the blowdown.

The other reason for the difference may come from the ambient heat loss. As stated in Subsec. 3.7, the ambient heat loss during the steady state operation is evaluated more than 10 % of the rated power. This value is comparable to the decay power. When the ambient heat losses are not taken into account by modeling the structures, the pressure may be overestimated in the early stage and be underestimated in the later stage. It is because that they behave as heat sinks at the begining and as the heat sources later on. In fact, in the experiment, superheated steam was observed after about 50 s at the upper plenum due to the structural heat as shown in Fig. 4.1.4.

4.2 Cladding Surface Temperature Transient

The focal point of the experiment is the core heat transfer during the blowdown. Figure 4.2.1 shows the vertical distribution of the cladding surface temperatures. The level numbers denoted right sides of the curves are corresponding to the levels of the

thermo-couples in the test section shown in Fig. 2.1.6. The dotted lines descriminate the area where the cladding temperature stays at the saturation temperature. The effect of the lower plenum flashing is clearly shown in this figure. Figure 4.2.2 shows the three-dimensional view of also the calculated cladding surface temperatures. The first DNB is calculated to occur at 16 s at the top of core and the core wide drys out at about 38 s. At the lower part of the test section, temperature excursion is not calculated to occur. The distributions of the measured cladding temperatures in the upper part and lower part of the core are in Figs 4.2.3 and 4.2.4, respectively. The DNB ocuured just after the break at the top of core and the cladding temperature soon returns to the saturation temperature. The core uncovery occurs first at about 50 s at the top of core. The experimetal data imply a clear water level has been formed and it slowly moved down to the bottom within about 10 s. It should be noted that in Fig. 4.2.4, a small peak has been observed at level 7. This is caused by the lower plenum flashing just after the dryout. Figure 4.2.5 shows the cladding surface temperature calculated at level 7 along with the experimental data. With respect to the small peak, a very good agreement was obtained. This means the core hydraulics related to the lower plenum flashing is properly predicted by the calculation.

Figures 4.2.6 to 4.1.13 show the calculated cladding surface temperatures at the different levels with the corresponding experimental data. The tendencies shown in these figures are summerized as follows:

(1) The observed small peak of the cladding temperature at the beginning of the blowdown is not predicted to occur,

(2) The observed small peak just before the lower plenum flashing is well predicted by the calculation,

(3) At the upper part of the test section, the temperature excursion is calculated to start earlier than in the experiment and at the lower part, on the other hand, it is delayed in the calculation.

(4) In the experiment, the whole test section is uncovered within 10 s starting at about 50 s. In the calculation, however, the cladding temperature at the lower part of the core stays almost at the saturation temperature.

One of the reasons for (1),(3) and (4) seems to be that the model for the phase separation, i.e. the drift flux model, does not correctly predict the phase separation in the core. These figures imply the present drift flux model overpredicts the relative velocity between the phases, resulting in higher void fraction in the upper part and lower void fraction in the lower part in comparison with the experiment, which will be shown in the next subsection.

4.3 Core Hydraulics

The calculated bundle inlet mass flow rate and the differential pressure through the core are shown in Figs. 4.3.1 and 4.3.2, respectively, along with the experimental data. A good agreement is obtained in both core inlet flow and the differential pressure through the core. In the experiment, the core inlet flow suddenly decreses just after the break and reaches very close to zero, i.e. flow stagnation. This instantaneous flow stagnation brings about the initial dryout. In the calculation, on the other hand, the core flow also suddenly decreases but does not reach close to zero. This is because the core flow recovery is calculated to occur earlier than in the experiment. As mentioned in Subsec 4.1, the valve is calculated to be closed earlier than in the experiment. Then, the core flow recovery comes on before the core flow stagnation in the calculation. This is one of the reasons why the initial dryout is not calculated to occur.

After the relief valve, spray valve and feed water valve being closed, the core inlet flow slowly decreases according to the flow coastdown in pump P2, which is shown in Fig. 4.3.3. The calculated mass flow rate through pump P2 is in good agreement with the experimental data.

The core inlet flow suddenly decreases and the flow reversal occurs at about 12 s in the calculatlion and 15 s in the experiment. These timings are corresponding to when the cavitation starts in pump Pl, as shown in Fig. 4.3.4. These timings are also corresponding to the timings of downcomer dryout as will be shown in the next section. The core flow reversal will also be discussed in conjunction with the break flow transient. Relatively high enthalpy coolant flows into the lower plenum due to the core flow reversal and flashing starts. The core inlet flow again returns to be positive due to the lower plenum flashing.

The calculated mass flow rates at the inlet and outlet of the lower plenum and at the core inlet are shown in Fig.4.3.5. Althought the lower plenum inlet flow is downward, the core inlet flow is forced to be upward due to the flashing. The difference in the mass flow rates between the lower plenum outlet and the core inlet shows the mass flow rate from the core bypass to the bottom of the test section. It can be concluded from this figure that the effects of the core bypass and the guide tube volume to the core hydraulics are small in the calcultion.

Figure 4.3.6(a) and (b) show the calculated void fractions in the lower part and upper part of the core, respectively. These figures are helpful to understand the discussions stated above. The void fractions start to increase just after the break but soon start to decrease before reaching 1.0 s due to the closure of the relief valve. Sudden increase in the void fraction at about 15 s is brought about by the core flow reversal. The effect of the lower plenum flashing is again clearly shown after about 20 s. After about 36 s, the upper part of the core is filled with only steam but at the lower part two-phase mixture still remains.

4.4 Downcomer behavior

The calculated differential pressure through the downcomer is shown in Fig. 4.4.1 along with the experimental data. A good agreement is obtained. This figure shows that the downcomer becomes almost empty at about 12 s in the calculation and at about 15 s in the experiment. This downcomer dryout causes the pump degradation of pump P2. The fluid temperature at the downcomer inlet is shown in Fig. 4.4.2 along with the experimental data. After the feedwater valve and the spray valve being closed, the saturated fluid at the bottom of the steam dome is drained through the downcomer. Therefore the fluid temperature increases. The flashing of the downcomer starts earlier in the calculation than in the experiment. After the flashing, the fluid temperature stays at the saturation temperature. The descrepancy of the temperature between the calculation and the experiment after about 30 s is corresponding to the underprediction of the pressure.

4.5 Break Flow Transient

The calculated break flow is shown in Fig.4.5.1 along with the experimental data. The experimental data just after the break are not available. The calculation underpredicts the break flow until about 60 s. Figure 4.5.2 shows the integrated break mass flow rates. This figure also shows that the break flow is underestimated especially until 30 s.

The calculated mass flow rates at the break, and both the pump side and the vessel side of the broken recirculation line are shown in Fig.4.5.3. A local minimum of the break flow is calculated to occur at about 14 s. This behavior is caused by the change in the ratio of the contribution to the break flow from the pump P2 side to that from the vessel side. At about 14 s, the pump cavitation is calculated to occur at pump p2 caused by the downcomer dryout and the mass flow rate from pump P2 side suddenly decreases. Even when it suddenly decreases, the break flow stays unchanged since the other side flow, i.e. the flow from the vessel side, compensates it. But the change in the mixing ratio changes the enthalpy upstream of the break and therefore it changes the break flow behavior. This is one of the characteristic behaviors in the split type break.

Figure 4.5.4 shows the calculated mass flow rates through the flow paths connected to the lower plenum. Although the pump P2 flow suddenly decreases, the break flow slowly decrease and therefore the mass flow rate from the lower plenum to the break suddenly increases as stated above. As the result of this sudden increase in the flow rate, the core flow reversal is calculated to occur as clearly shown in this figure. The flow from pump P1 to the lower plenum also once increases accompanied by the sudden increase in the flow from the lower plenum to the break.

4.6 Bypass Hydraulics

Figures 4.6.1(a) and (b) show the calculated and measured differential pressures through the bypass, respectively. The sum of

the experimental curves for DPT20, DPT21 and DPT22 in Fig. 4.6.1(a) is corresponding to the predicted curve in Fig. 4.6.1(b). Both in the experiment and calclation, flashing starts at the bypass from 10 to 20 s and at the guide tube volume from 20 to 30 s. The two-phase mixture is forced into both the top of core and the bottom of core due to the flashing of the guide tube volume. As already shown in Fig. 4.3.5, the core inlet flow rate is not very different from the lower plenum outlet flow. Therefore the effect of the bypass to the core hydraulics is considered to be small.

5. Concluding Remarks

The present calculation has been performed based on the data provided for the blind calculation for ISP No. 15(12), which contain the system geometrical data and the planned initial conditions and boundary conditions, being different from those measured in the experiment. In addition, the system characteristics is unknown before the calculation starts, because the experiment is the first LOCA experiment in the FIX II test facility. In these sense, the present pre-test prediction calculation can be categorized as what is called a double-blind calculation. In spite of the fact, the physical phenomena observed in the experiment are adequately predicted in the present calculation. The major concluding remarks derived from the present calculation are:

(1) The pressure transient is well predicted. In detail, it is overestimated in the early stage and is underestimated estimated in the late portion. One of the reasons for the overestimation is that the steam relief valve is closed earlier in the calculation than in the experiment. The planned valve actions are meaningfully different from the those actually performed in the experiment.

(2) Ambient heat loss is considered to be one of the reasons for both overestimation and underestimation of pressure in the early stage and late stage, respectively.

(3) The early dryout observed just after the break is not predicted to occur because the relief valve is closed earlier in the calculation. The core wide dryout is predicted to occur early in the upper part of the core and late in the upper part of the bundle in comparison with the experimental data. This means the phase separation in the test tection is not correctly predicted.

(4) Most of the key phenomena observed in the experiment such as the downcomer dryout, core flow reversal and lower plenum flashing are adequately predicted to occur in the present pre-test prediction calculation. Especially the effect of the lower plenum flashing is in good agreement with the experimental data, and

(5) THYDE-P1 is applicable to BWR. Improvement should be performed with special attention to the drift flux model.

REFERENCES

(1) ASAHI, Y.: Description of THYDE-P code (Preliminary report of methods and models, JAERI-M7751, (1978).

(2) ASAHI, Y., HIRANO, M. : Verification study of LOCA analysis code THYDE-P (Sample calculation run 10), JAERI-M8560, (1979).

(3) HIRANO, M., ASAHI, Y.: Through analysis of LOFT L2-2 by THYDE-P code 1 (Sample calculation run 30), JAERI-M9535, (1981).

(4) HIRANO, M.: Through analysis of LOFT L2-3 by THYDE-P code (Sample calculation run 40), JAERI-M9765, (1981).

(5) SHIMIZU, T., ASAHI, Y.: Through calculation of 1.100MWe PWR large break LOCA by THYDE-P (Sample calculation run 20), JAERI-M9818, (1981).

(6) HIRANO, M.: Analysis of LOFT small break experiment L3-1 with THYDE-P code (CSNI international standard problem No. 9 and THYDE-P sample calculation run 50), JAERI-M82-008, (1982).

(7) HIRANO, M.: Analysis of LOFT L3-6/L8-1 with THYDE-P (CSNI international standard problem No. 11 and THYDE-P sample calculation run 60), JAERI-M82-028, (1982).

(8) KOSUGI, S. et al.: Analysis of PKL test K9 by THYDE-P code (CSNI ISP No. 10 and THYDE-P sample calculation run 70), JAERI-M82-115, (1982).

(9) ASAHI, Y.: User's manual for THYDE-P1, JAERI-M 82-38, (1982).

(10) KANAZAWA, M. et al.: A through calculation of 1,100 MWe PWR large break LOCA by THYDE-P1 EM model, JAERI-M 84-132, (1984).

(11) REEDER, D. L.: LOFT system and test description (5.5ft corel LOCES), NUREG/CR-0247, (1978).

(12) SANDERVAAG, O.: Basis of a split break LOCA in the FIX II facility, sweden, STUDSVIK/NR-83/293, (1983)

(13) SANDERVAAG, et al.; Minutes from the ISP-15 preliminary meeting at STUDSVIK, Sweden held on 7th March, 1983, STDUSVIK/NR-83/247, (1983).

(14) SANDERVAAG, et al.; FIX II experimental results of test 3025 (ISP15), STDUSVIK/NR-83/283, (1983)

(15) MOODY, F. J.: Maximum flow rate of single phase and two-phase mixture, Heat Trans.-Trans. ASME, 87nl, pp134-142, (1965)

(16) ZALOUDEK, F. R.: Steam water critical flow from high pressure system, HW-63936, Hanford work, (1967).

(17) ZUBER, N., FINDLAY, J.A.: Averagevolumetric concentrations in two-phase flow systems, J. Heat Trans. 87, 453, (1965).

(18) DITTUS, F. W, BOELTER, L. M. K.: Heat transfer in automobile Radiators of the tubelar tube, 2, No. 13, pp.334-461, (1930).

(19) THOM, J. R. S., et al.: Biling in subcooled water during flow up heated tube or annuli, Proc. Instn. Mech. Engrs., Vol 1801 Part 3C, pp 226-246, (1966).

(20) BROMLEY, L.A., et al.: Heat transfer in forced convection film boiling, Ind. Eng. Chem, 45, 2619, (1953).

(21) POMERALTZE: Film boiling on a horizontal tube in increased gravity fields, J of Heat Transfer, 86, pp 213-219, (1964).

(22) GROENEVELT, D. C.: An invesigation of heat transfer in the liquid deficient regime, Report AECL-3281, Chalk Rever, Ontario, (1968).

(23) DOUGAL, R. L., ROHSENOW, W. M.: Film boiling on the inside of vertical tubes with flow of the fluid at low qualities, MIT-TR-9079-26, (1963).

(24) MCELIGOT, D. M., et al., J. Trans. Amer. Soc. Mech. Engrs., 88, Series C, pp 239-245, (1966).

(25) BIASI, L., etal.: Studies onburnout: Part 3, Energia Nucleare, (1967).

(26) ZUBER, N., et al.: The hydrodynamic crisis in pool boiling of saturated and subcooled liquids, International Developments in Heat Transfer, Part II, pp 230-236, (1961).

Table 2.2.1 Planned performance chronology

Start opening of the break valve (V120)	0.	s
Break valve fully open (Area 1.13 cm^2)	0.2	s
Steam relief valve starts to open (V112)	0.2	s
Steam relief value fully open	0.5	s
Steam relief valve starts to close	1.35	s
Spray flow, feed water flow and cooler flow valves start to close (V104, V106, V107)	1.4	s
Steam relief valve closed	1.65	s
Spray flow, feed water flow, cooler flow valves closed	1.8	s
Steam relief valve starts to open	11.8	s
Steam relief valve fully open	12.1	s

The test is terminated on the first occurence of one of the following conditions:

a) 120 s
b) Clad temperature exceeds 700 ^{o}C
c) Pressure drops below 2 MPa

Table 2.2.2 Measured performance chronology

Break valve starts to open	0 s
Break valve fully open	0.08 s
Steam relief valve (SRV) starts to open	0.4 s
SRV open *	1.0 s
SRV starts to close	1.6 s
Spray flow valve starts to close	1.65 s
Valve V104 (to cooler) starts to close,	1.78 s
Spray flow closed	1.9 s
Feed water valve starts to close	1.9 s
Valve V104 closed	2.0 s
Feed water closed	2.0 s
SRV closed	2.3 s
SRV starts to open	12.05 s
SRV open *	12.65 s
Test termination	76 s

Table 2.3.1 Planned initial conditions

Steam dome pressure	7.0	MPa
Core inlet flow	5.34	kg/s
Core power	3.5	MW
Core inlet subcooling relative to steam dome temperature	19	°C
Bypass flow	0.66	kg/s
Bypass power	62.5	kW
Flow through pump P1	4.5	kg/s*
Flow through pump P2	1.5	kg/s*
Water spray to the steam dome	5.905	kg/s
Water spray subcooling relative to steam dome conditions	106	°C
Feed water flow	2.95	kg/s
Feed water subcooling relative to steam dome conditions	106	°C
Mass flow rate through the cooler	8.855	kg/s

Table 2.3.2 Planned initial conditions and rated values for recirculation pumps

Pump P1:		
Rated pump speed	303.69	rad/s
Initial pump speed ratio	0.5399*	
Rated pump flow	0.0383	m^3/s
Rated pump head	50	m
Rated pump torque	81.7	Nm
Pump rated density	1000	kg/m^3
Pump P2:		
Rated pump speed	303.69	rad/s
Initial pump speed ratio	0.7018*	
Rated pump flow	0.01056	m^3/s
Rated pump head	25	m
Rated pump torque	13.2	Nm
Pump rated density	1000	kg/m^3

Table 2.3.3 Measured initial conditions

Steam dome pressure	6.997 MP
Bundle inlet flow	5.51 kg/s
Bundle power	3.385 MW
Bundle inlet temperature	542.0 K
Bypass flow	0.6 kg/s
Bypass power	57.4 KW
Flow through pump P1	4.56 kg/s
Flow through pump P2	1.55 kg/s
Spray flow	5.36 kg/s
Feedwater flow	2.49 kg/s
Feedwater and spray temperature	454.0 K
Mass flow through cooler	7.85 kg/s
Water level in steam dome above loop reference plane	6.34 m
Pump speed, P1	160 rad/s
Pump speed, P2	210 rad/s
Steam dome TE21	Saturated
Steam dome bottom TE25	542.5 K
Downcomer inlet TE26	541.8
Downcomer bottom TE31	541.6
Intact recirculation line TE32	541.0 K
Lower plenum TE2	542.0 K
Upstream break TE34	539.1 K
Bypass bottom TE17	541.5 K
Guide tube volume TE16	540.6 K
Bypass outlet TE20	556.4 K

Table 3.1.1 Discription of nodes and heat slabs

Node No.	Description
1	Lower plenum
2	Lower plenum buffle inlet
3-12	Test section
13	Upper plenum lower part and upper part
14	Steam separator
15	Lower part of spray condensor
16-20	Downcomer, upper horizontal part
21-26	Downcomer, upper vertical part
27	Downcomer, vertical part to pump P1
28	Pump P1
29	Intact recirculation line pressure vessel side
30	Pump 2 suction line to pump P2
31	Pump P2
32	Broken recirculation line, pump P2 to split break T-connection
33	Broken recirculation line, split break T-connection to break from lower plenum
34	Broken recirculation line back to lower plenum
35	Bypass channel lower horizontal part
36-40	Bypass channel vertical part
41	Bypass channel upper horizontal part
42	Coolant flow line from downcomer to pump P3
43	Pump P3
44	From pump P3 to evaporation cooler
45	Evaporation cooler
46	From outlet of evaporation cooler to feed water line
47-48	Spray line
49	Feed water line
50	Spray condensor (Steam dome)
51	Relief valve line
52	Guide tube simulator volume
53-54	Split break line, from T-connection to break flow restrictor K12

Slab No.	Description
1	Non-heated part of average heater rod
2-11	Average heater rod
12	Non-heated part of average heater rod
13	Non-heated part of hottest heater rod
14-23	Hottest heater rod
24	Non-heated part of hottest heater rod
25-29	Bypass heater rod
30	Evaporation cooler

Table 3.6.1 Loss coefficients in loop

Item no	Description	Minimum flow area (cm^2)	Loss coefficient*	Reference flow area*** (cm^2)
1	Bundle inlet orifice**	4.73	72	60.34
2	Spacer		0.65	60.34
3	Upper tie plate	76	0.2	60.34
4	Steam separator flow restrictor	27.3	21	78.5
5	Pump P1 exit flow restriction	9.08	400	112.5
6	Measuring orifice, K1 (see figure 2:1)	13.9	14	42.7
7	Pump P2 exit flow restriction	3.80	230	34.3
8	Measuring orifice, K2	7.02	9.4	19.0
9	Bypass inlet , incl measuring orifice, K7 and valve V114	1.54	102	5.7
10	Split break line flow restriction, K12**	1.131	-	42.7
11	Guillotine break line from lower plenum flow restriction, K13**	3.664	-	34.3
12	Guillotine break line from downcomer flow restriction K11**	2.011-3.664	-	34.3
13	Steam line measuring orifice K6	14.3	8.4	42.6

*) Loss coefficient is defined as : $\xi = \frac{2 \cdot \Delta p}{\rho \cdot u^2}$

referred to the reference flow area. From preliminary, measured pressure drop; variation with Re has to be taken into consideration.

**) Variable parameter that will be subject to change between different experiments

***) Area to be used for sudden area change

Table 3.7.1 Ambient heat losses evaluated before experiment conducted

Steam condenser	13 KW
Upper plenum	12 KW
Test section	4 KW
Lower plenum	14 KW
Bypass channel	7 KW
Downcomer and recirculation lines	20 KW
Pump P1	5 KW
Pump P2	6 KW
Pump P3	5 KW
Spray and feedwater lines	22 KW
Total	108 KW

Table 3.7.2 Measured ambient heat losses

Cooling flow between teflon filler and vessel:	
Inlet temperature	403 K
Outlet temperature	493 K
Mass flow	0.565 kg/s
Total loss	204 kW

Table 4.1 Chronology of key events

Key Event	Time (s) Experiment	Prediction
Spray condensor emptied	6.5	5.5
Maximum steamdome pressure	7.6	7.0
Bypass inlet flow reversal	10	8.8
Start of flashing in bypass	12	11
Start of flashing in broken loop recirculation line (downcomer side)	16	12
Start of flashing in intact loop recirculation line	21	14
Start of flashing in broken loop recirculation line (lower plenum side)	22	20
Start of flashing in broken loop recirculation line (lower plenum side)	22	20
Start of flashing in lower plenum	22	19
Start of flashing in control rod guide tube volume	25	26
Core uncovery	50-64	38
Transient terminated	76	120

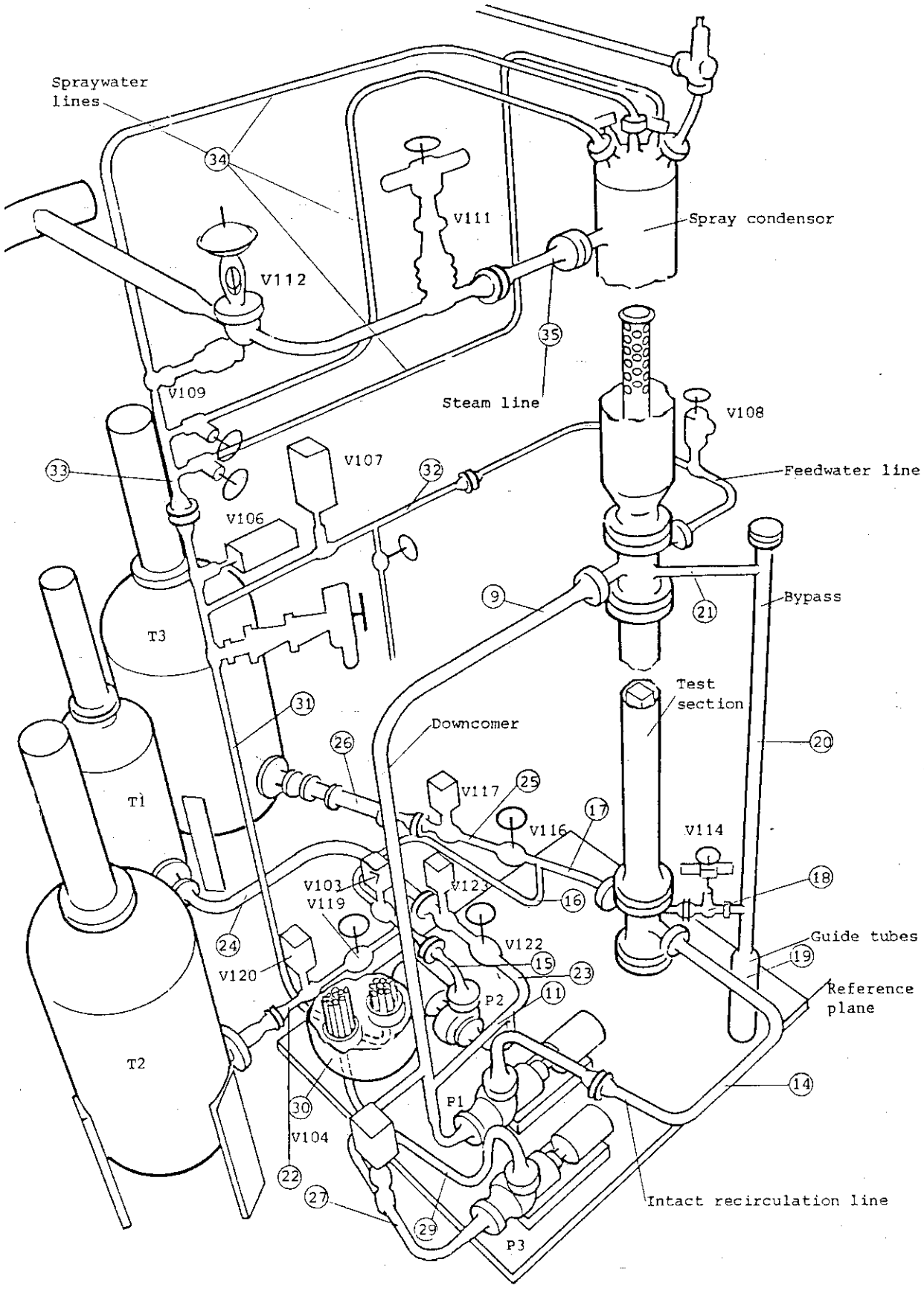

Fig. 2.1.1 Lay-out of FIX II loop

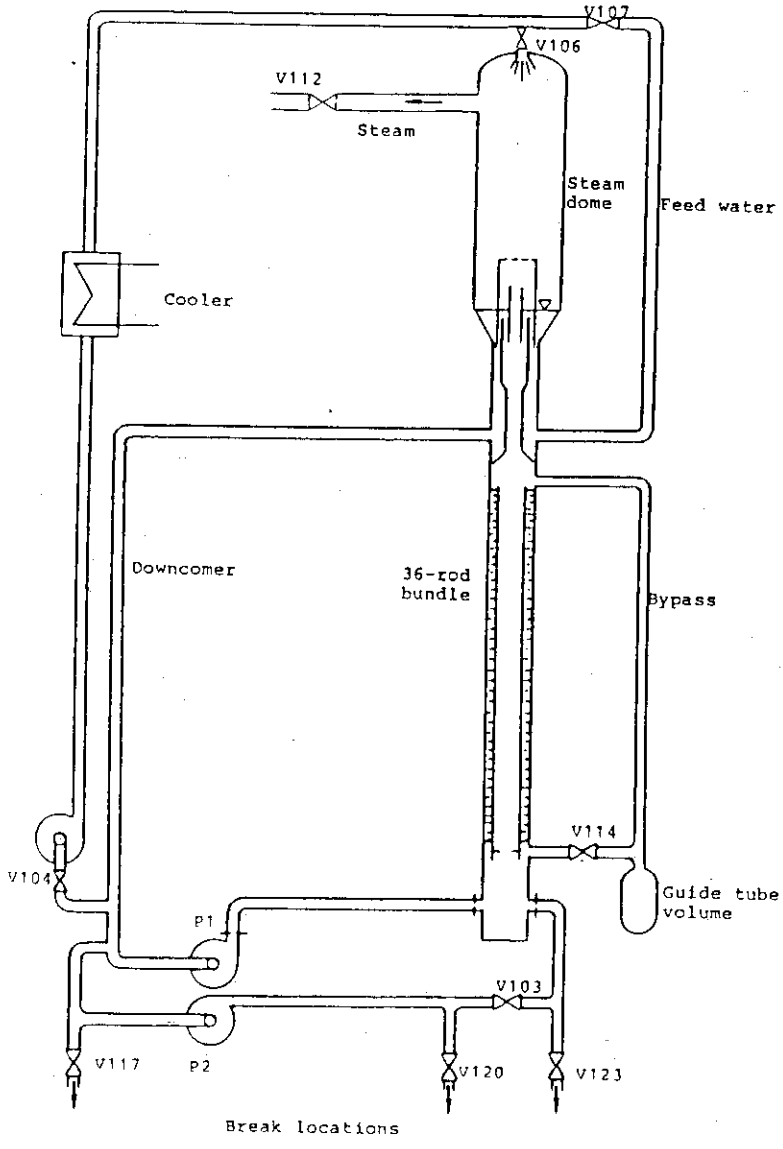

Fig. 2.1.2 Schematic diagram of central loop section

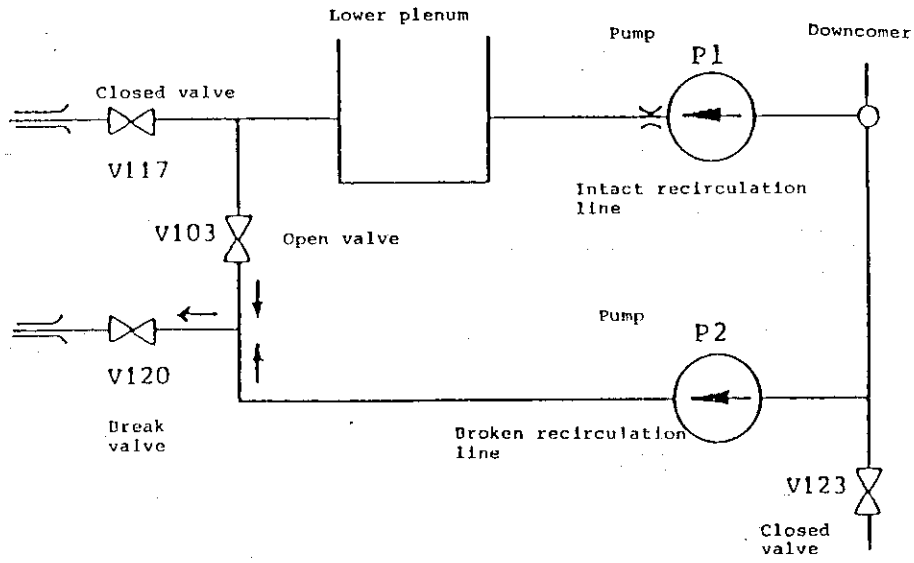

Fig. 2.1.3 Split break simulation

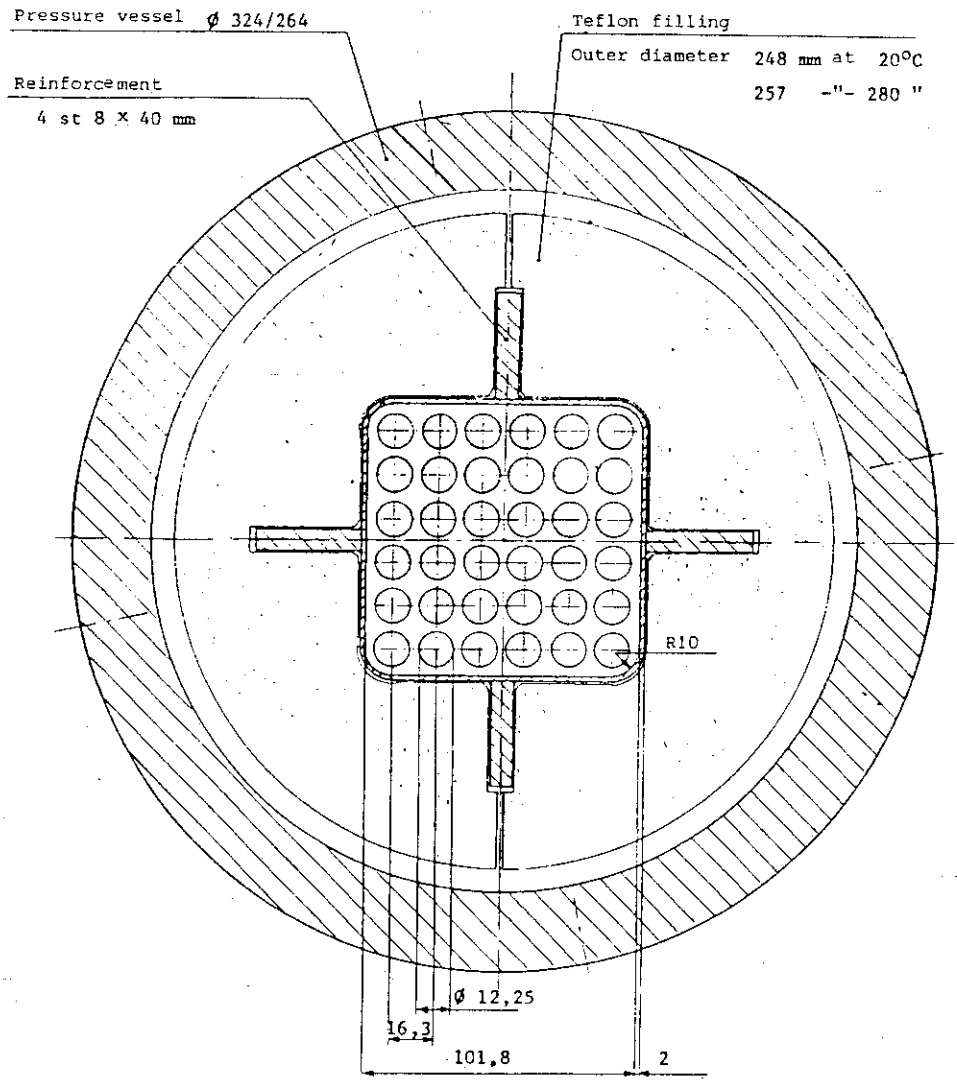

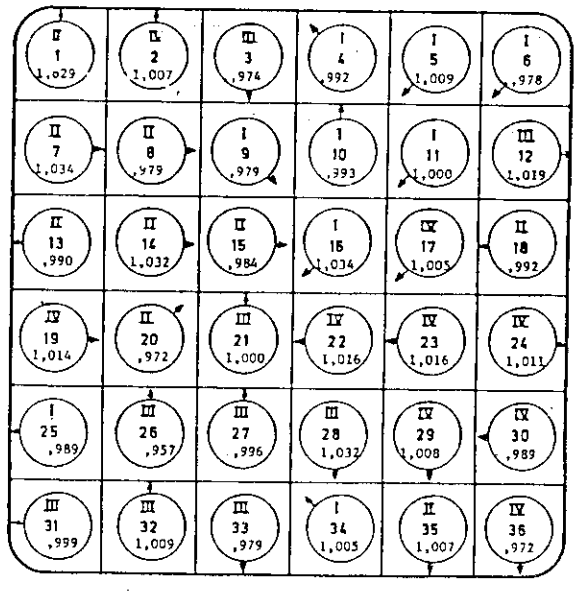

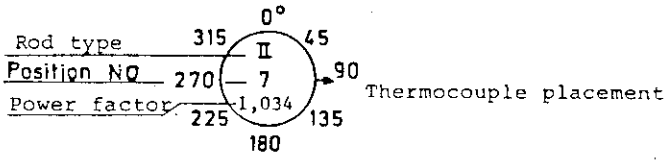

Fig. 2.1.4 Horizontal cut view of test section and radial power distribution

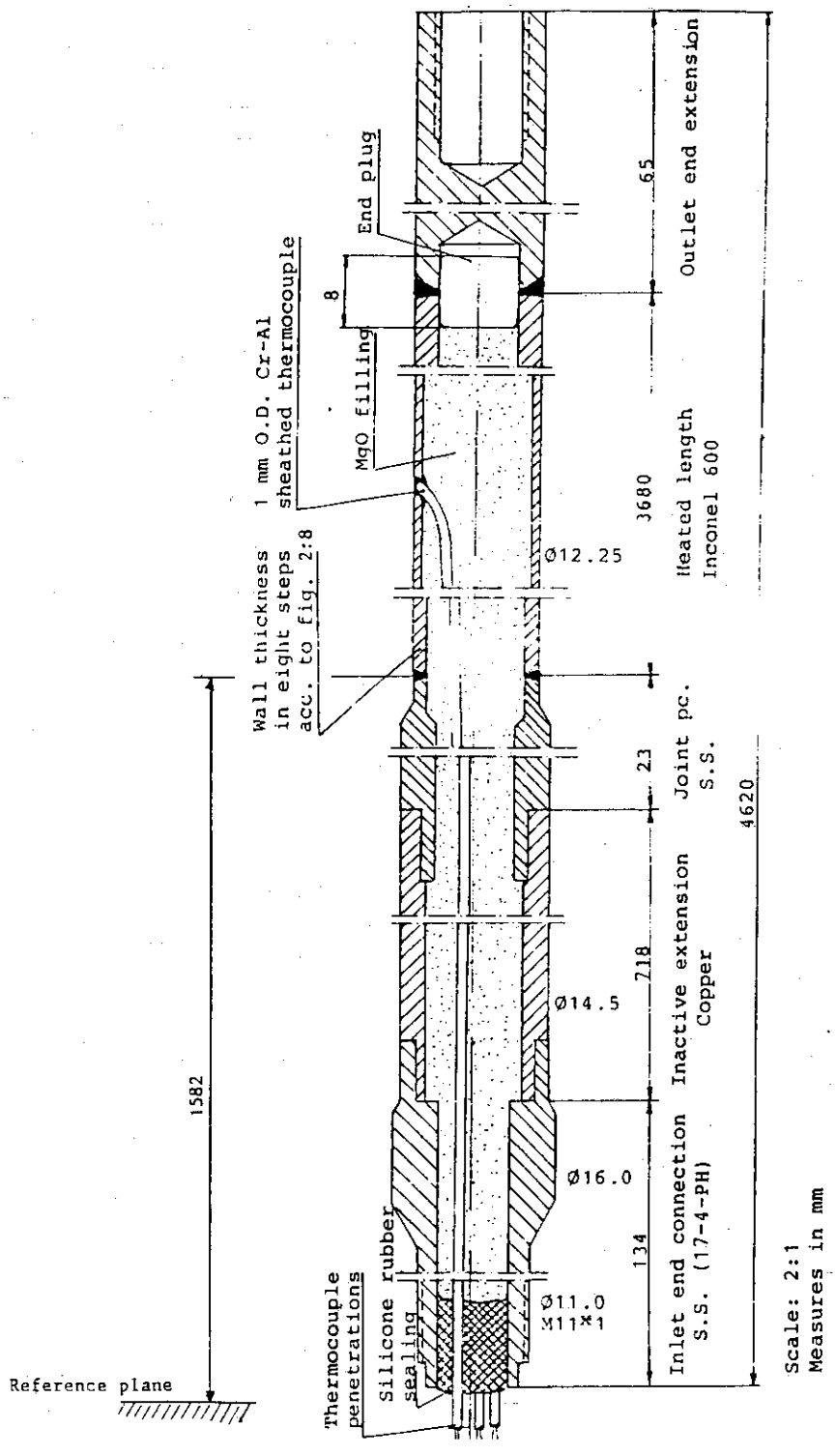

Fig. 2.1.5 Structure of fuel rod simulator

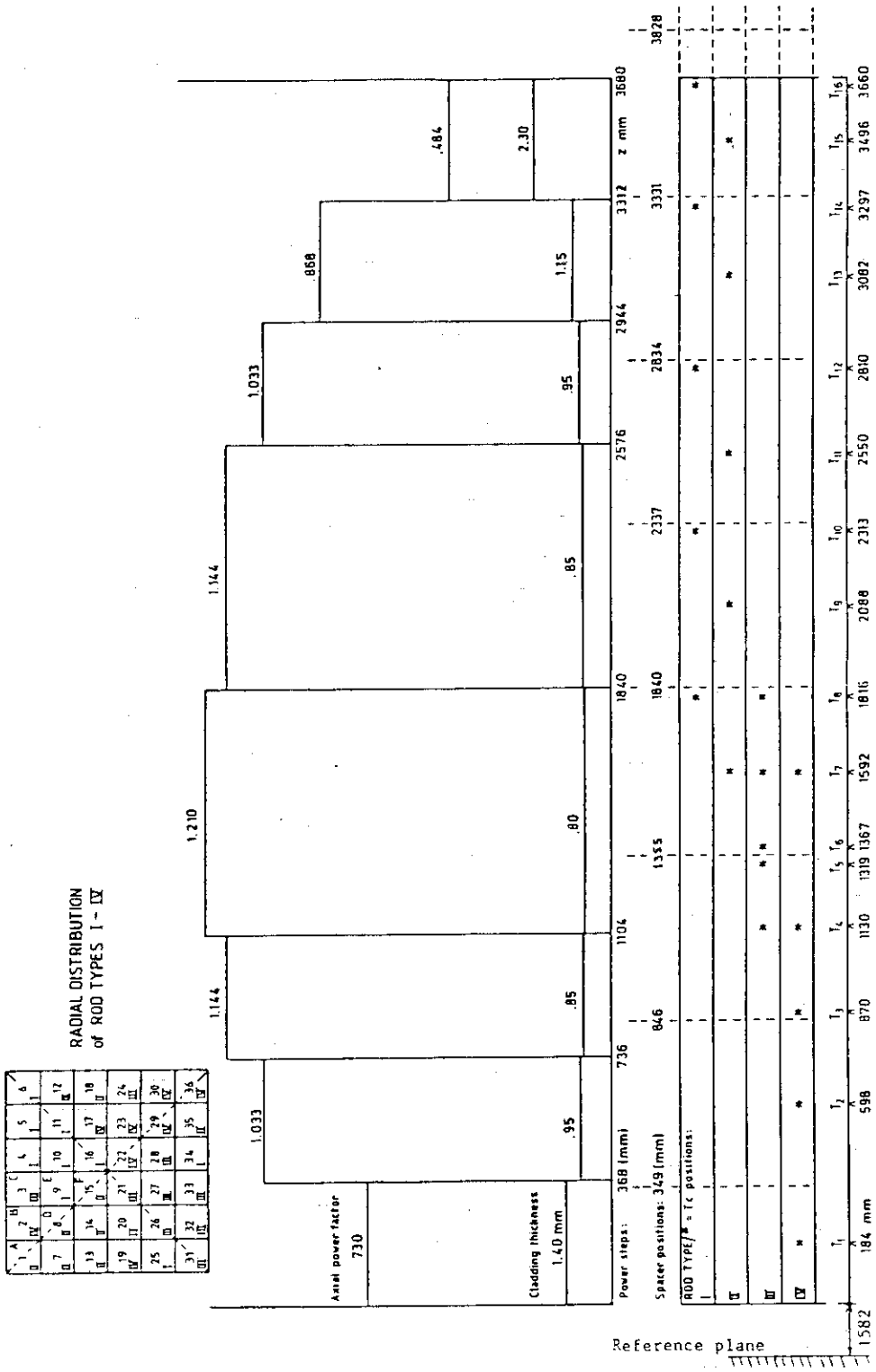

Fig. 2.1.6 Axial power distribution and instrumentation location

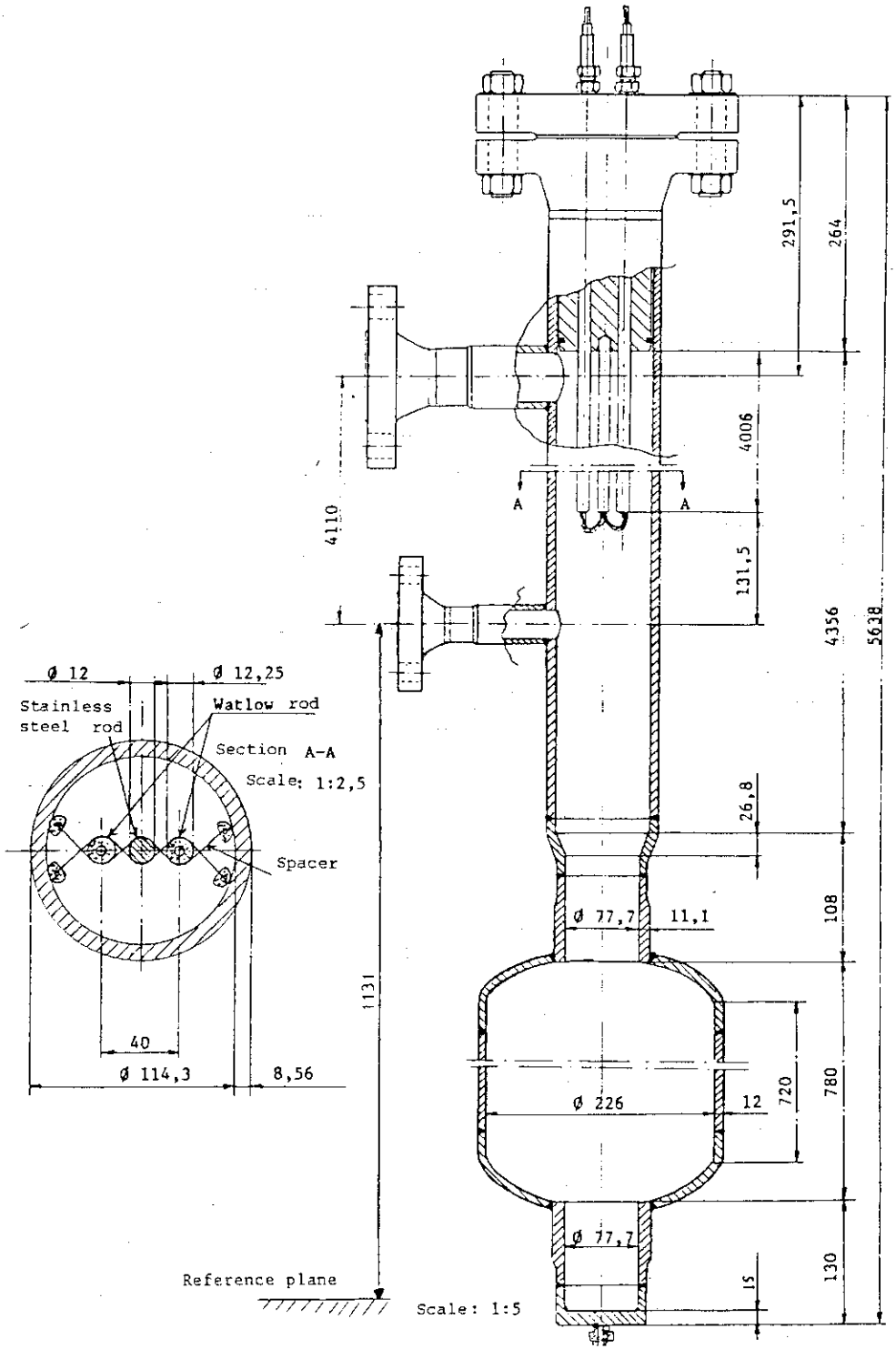

Fig. 2.1.7 Structure of bypass and control rod guide tube volume

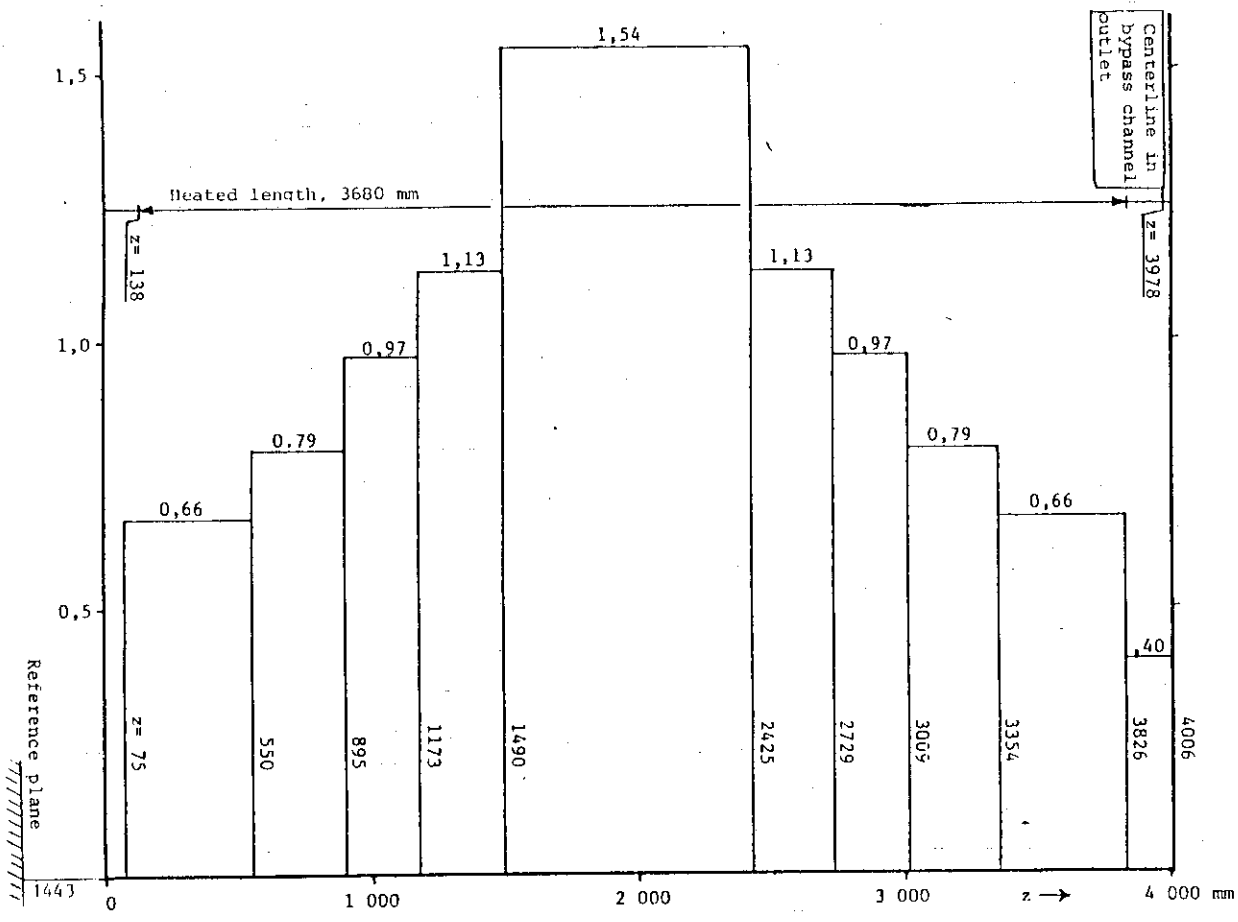

Fig. 2.1.8 Axial power distribution of bypass channel

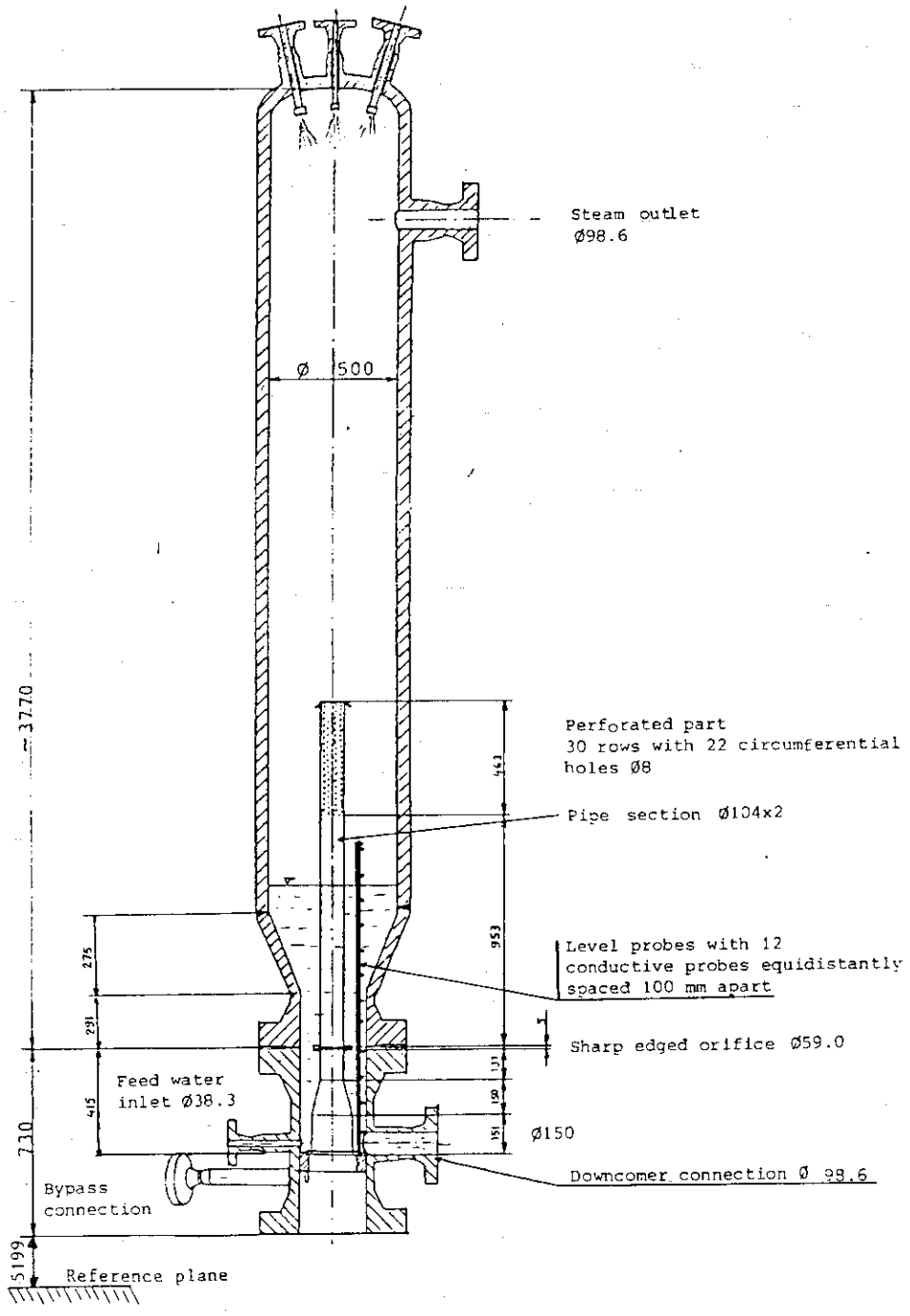

Fig. 2.1.9 Structure above test section

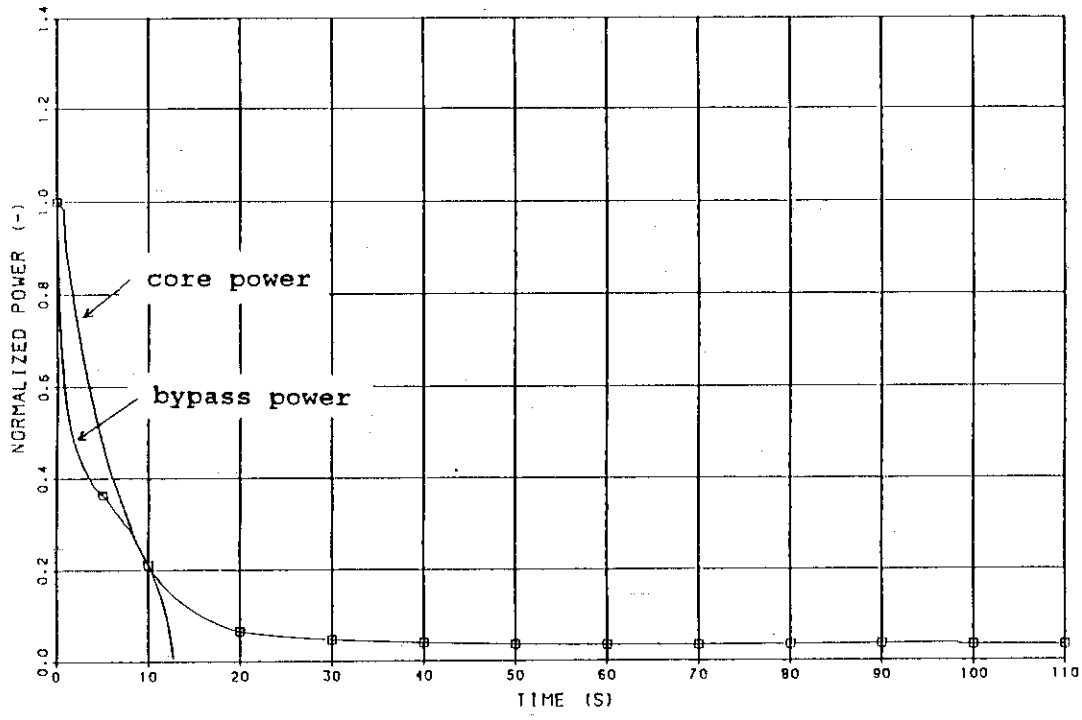

Fig. 2.3.1 Planned core and bypass power histories

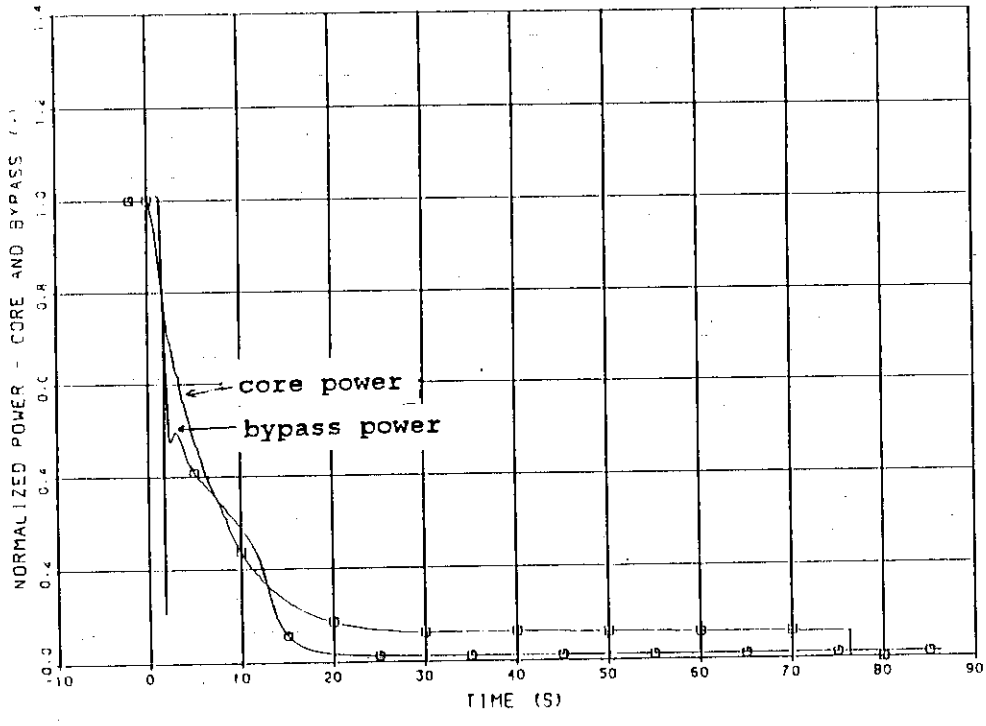

Fig. 2.3.2 Measured core and bypass power histories

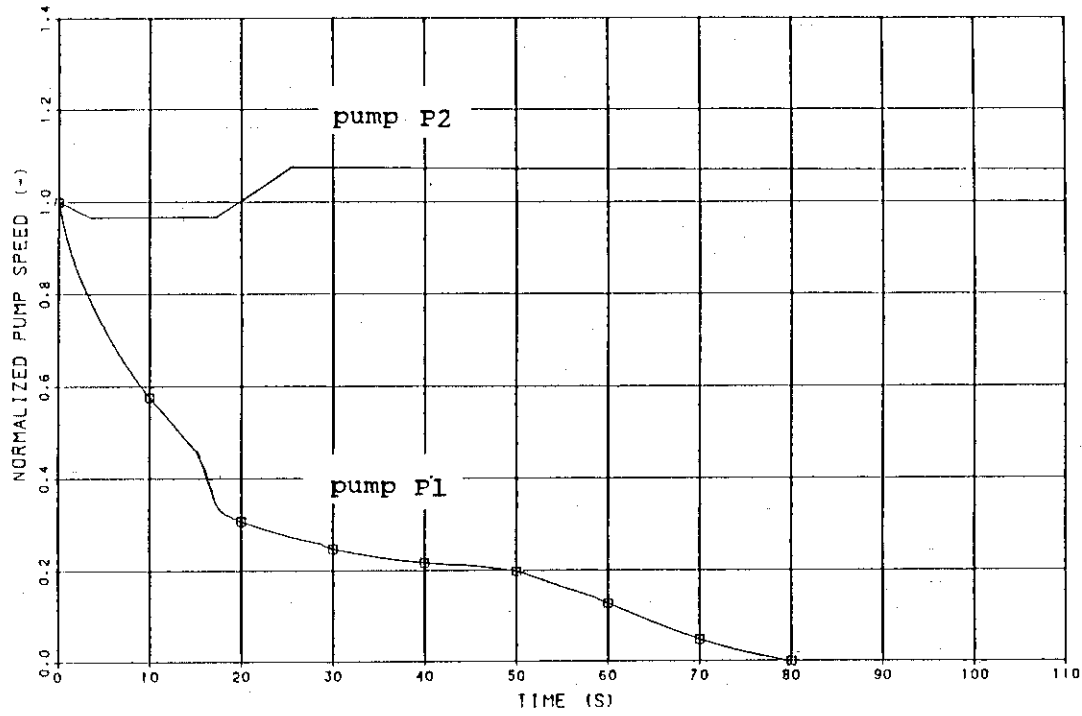

Fig. 2.3.3 Planned pump speed histories

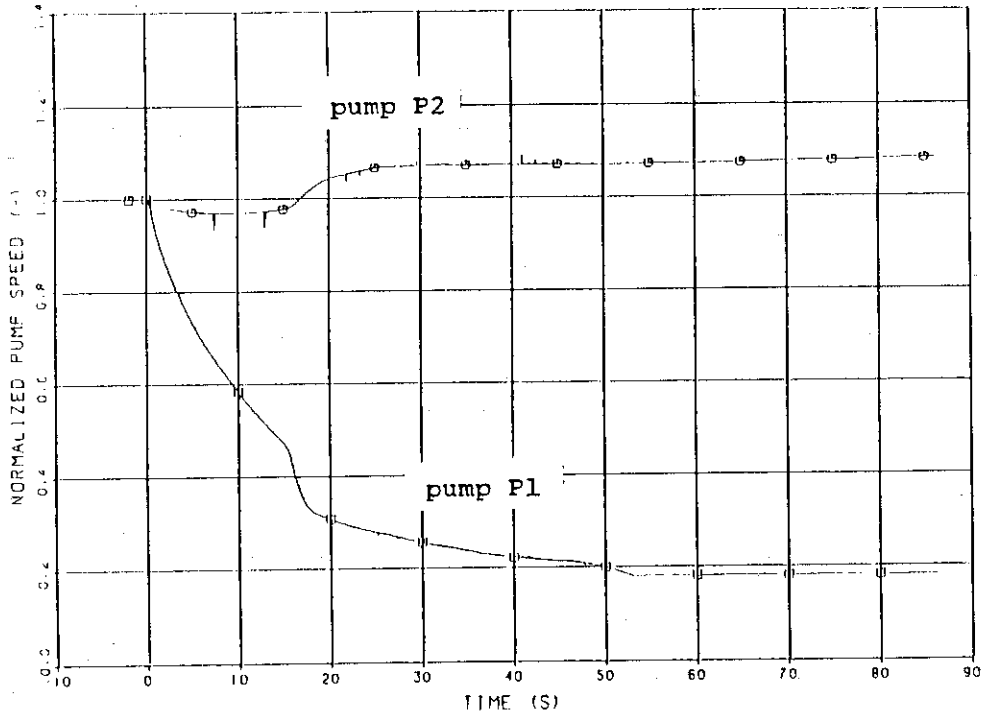

Fig. 2.3.4 Measured pump speed histories

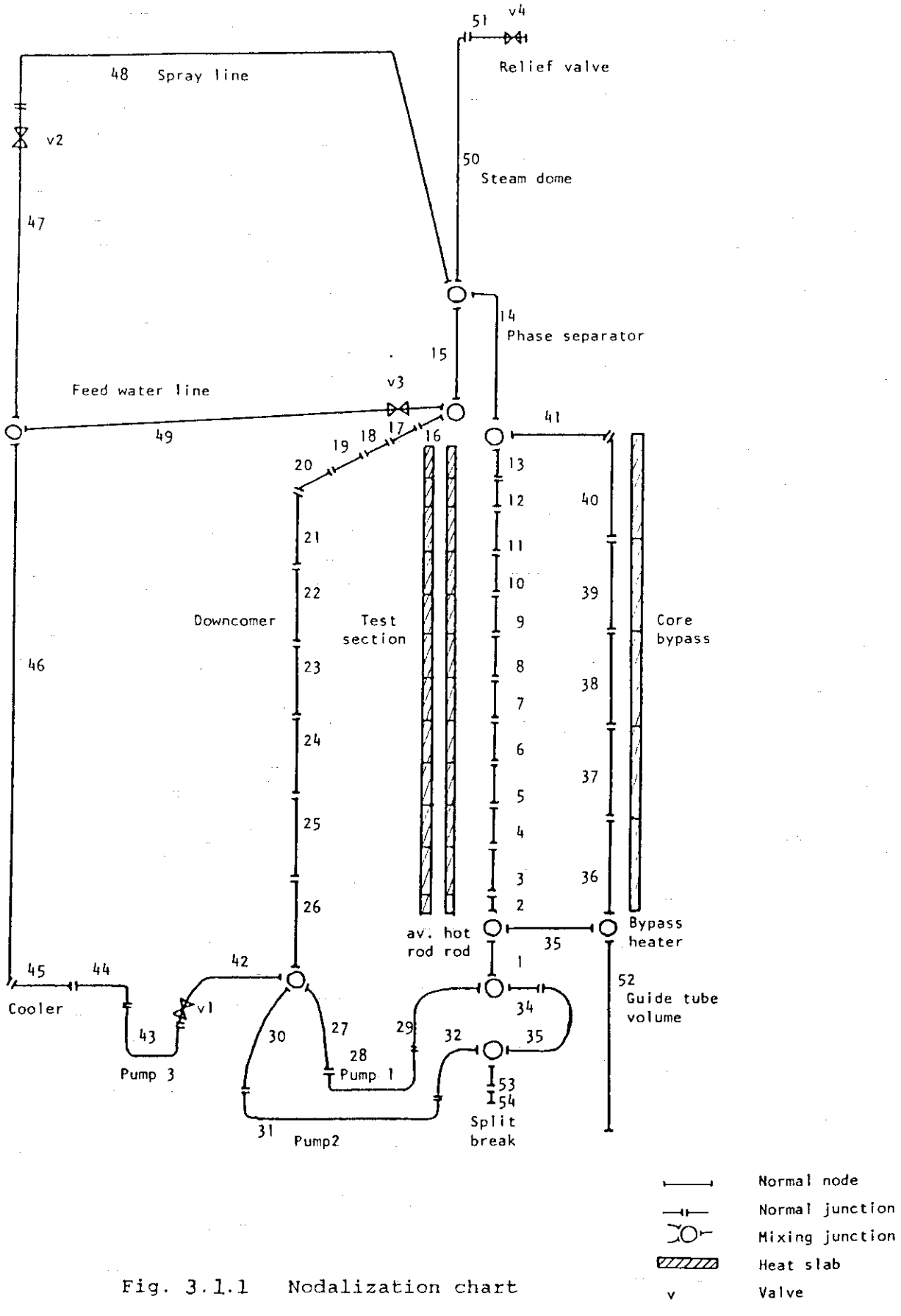

Fig. 3.1.1 Nodalization chart

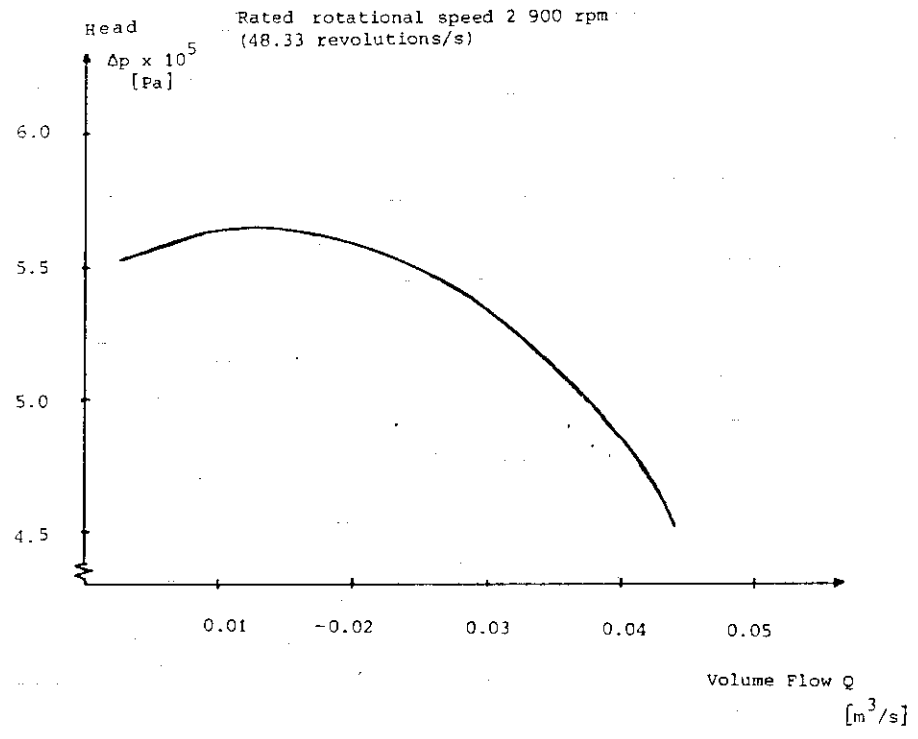

Fig. 3.5.1 Pump characteristic curve for pump P1

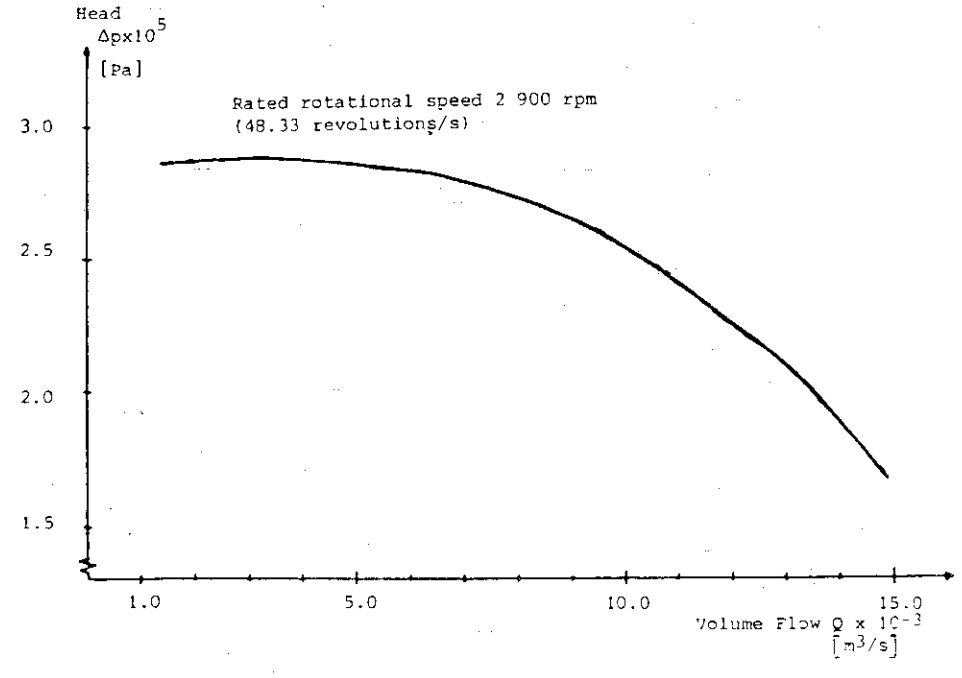

Fig. 3.5.2 Pump characteristic curve for pump P2

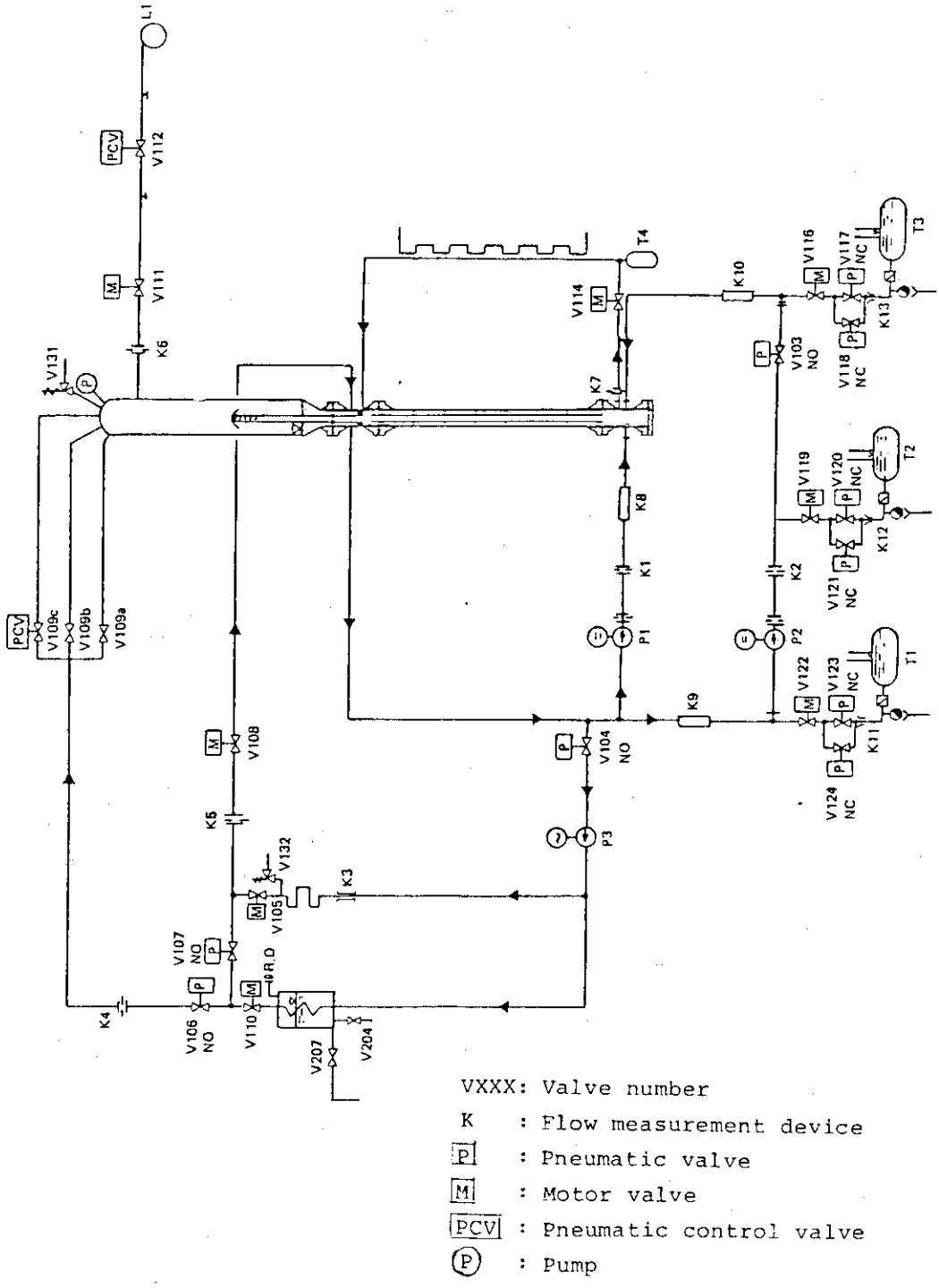

Fig. 3.6.1 Flow diagram of FIX II loop

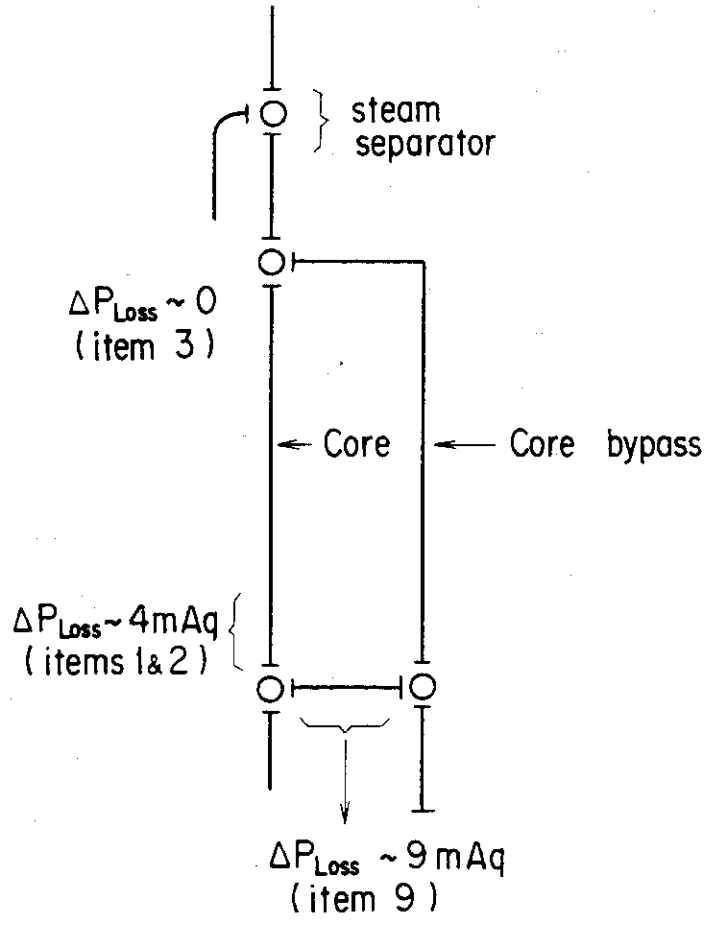

Remarks

1) See Table 3.6.1 for item numbers
2) ΔP_{Loss}: pressure drop (m of water head)

Fig. 3.6.2 Pressure losses at core and bypass

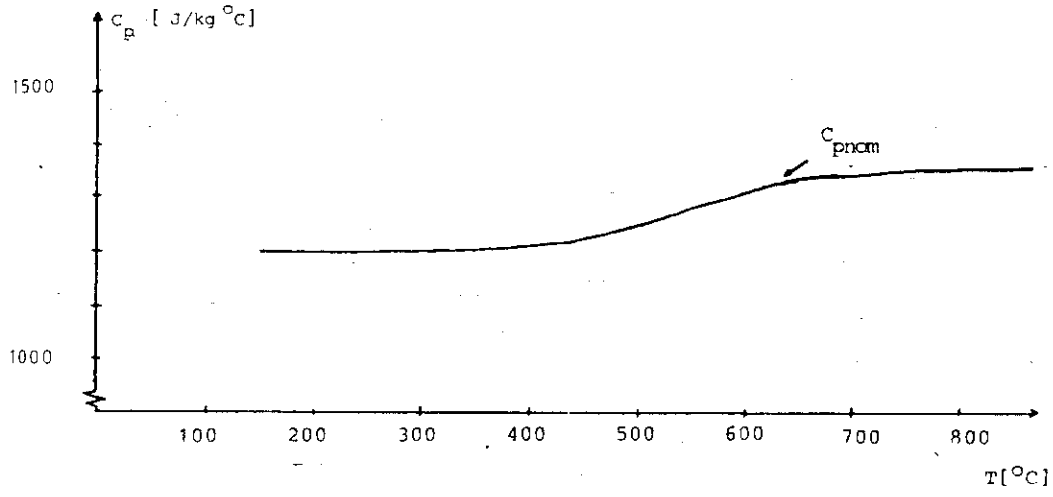

Fig. 3.8.1 Specific heat of fuel rod simulator filler material

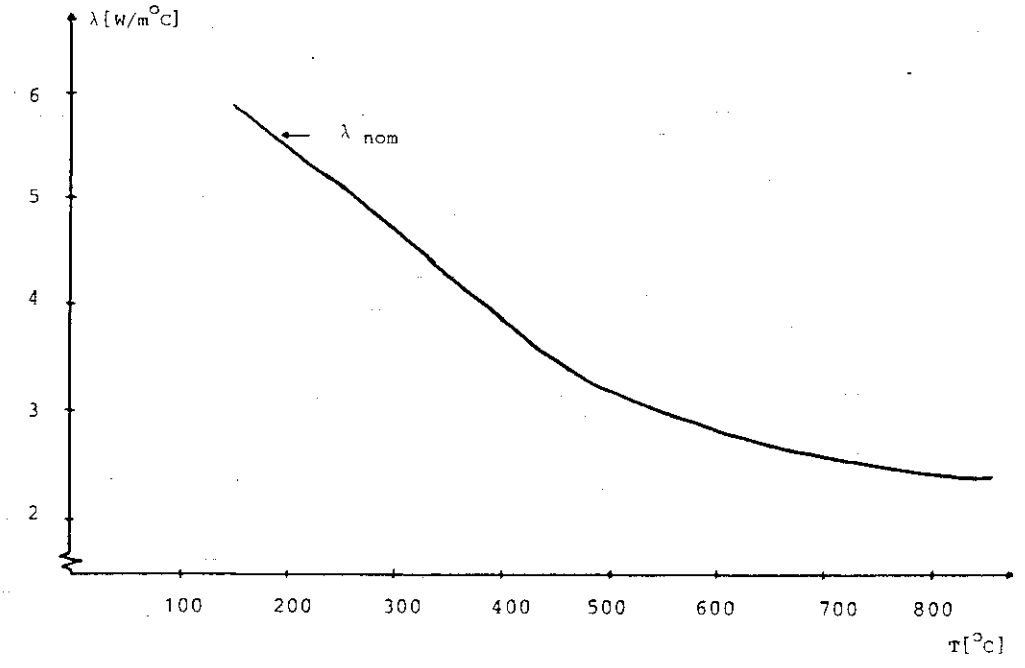

Fig. 3.8.2 Thermal conductivity of fuel rod simulator filler material

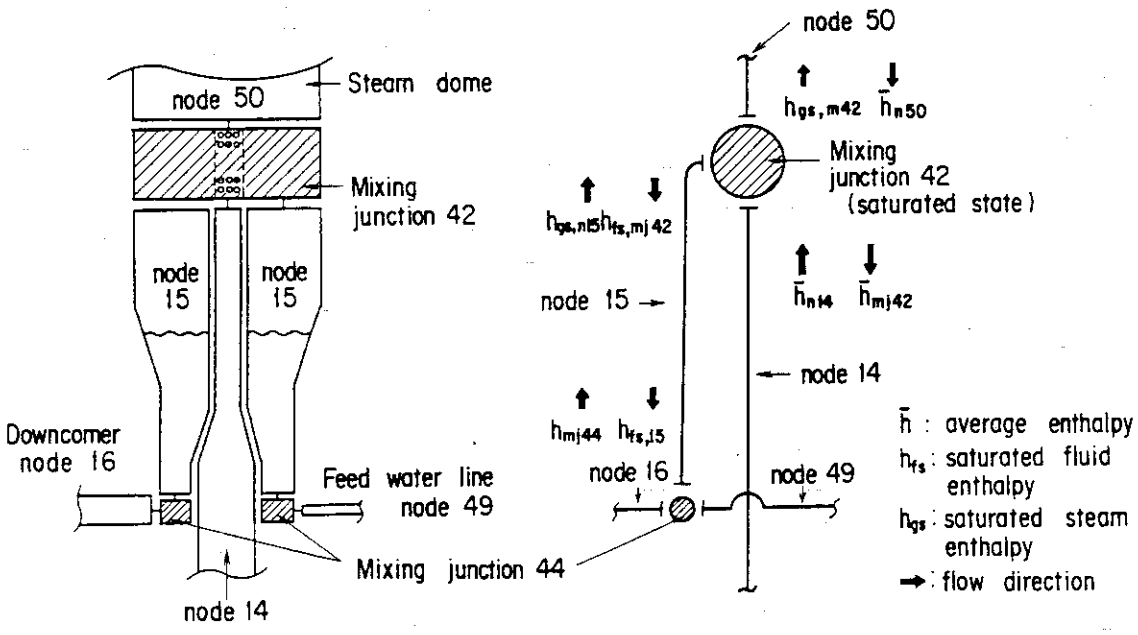

Fig. 3.9.1 Schematic diagram of phase separation

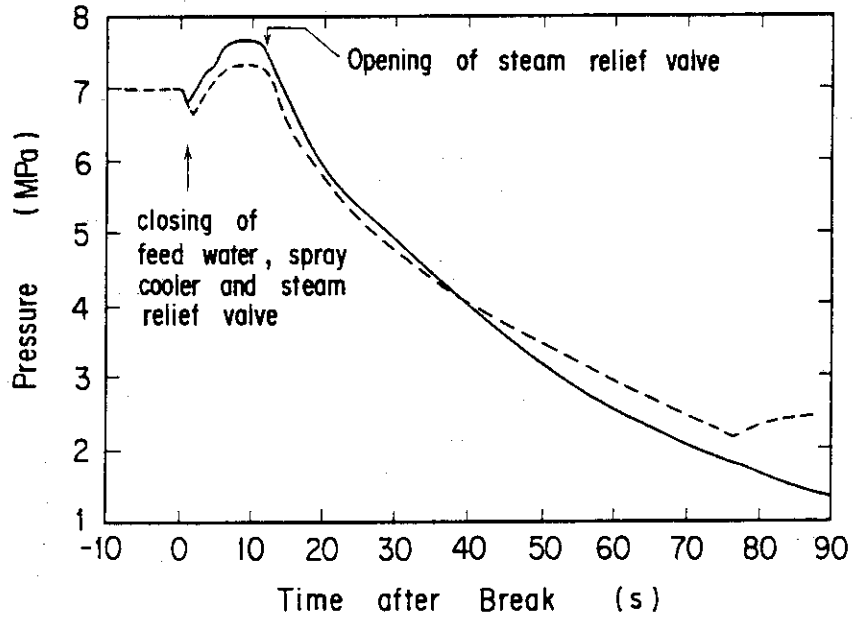

Fig. 4.1.1 Pressure at steam dome

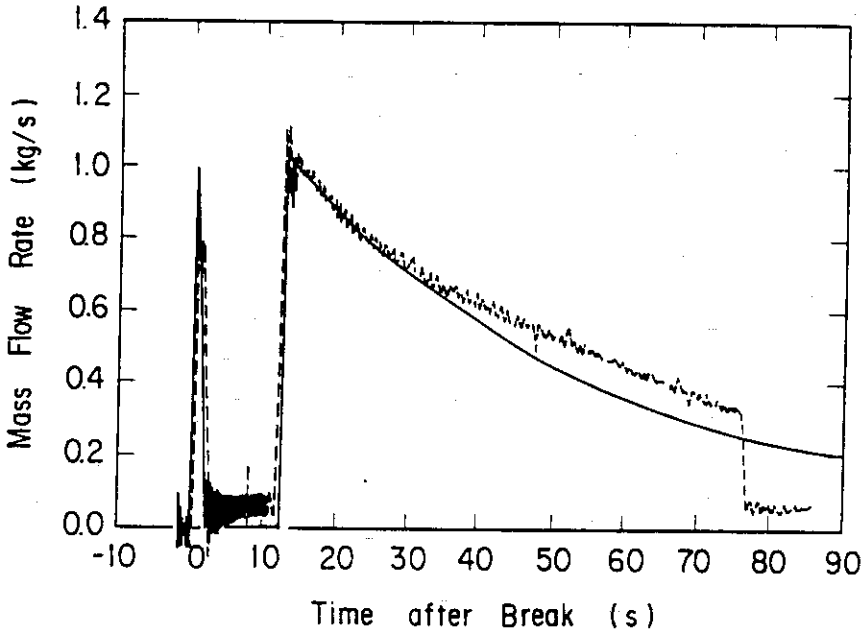

Fig. 4.1.2 Mass flow rate through steam relief valve

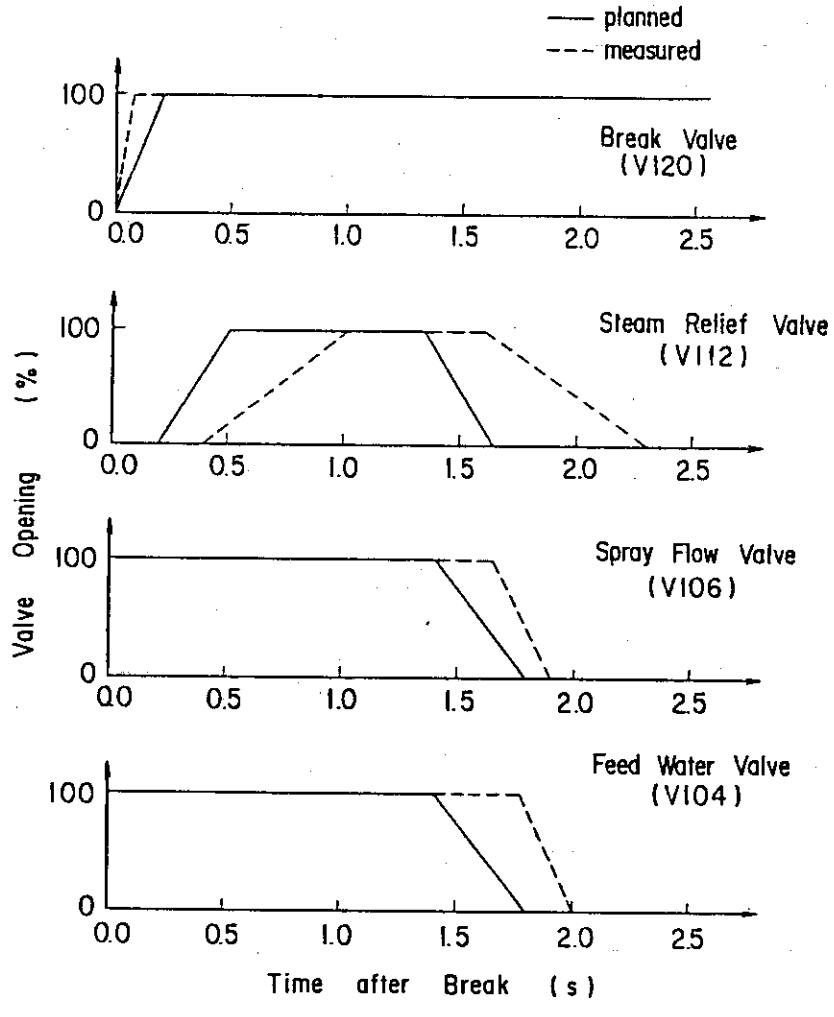

Fig. 4.1.3 Schematic diagram of valve actions

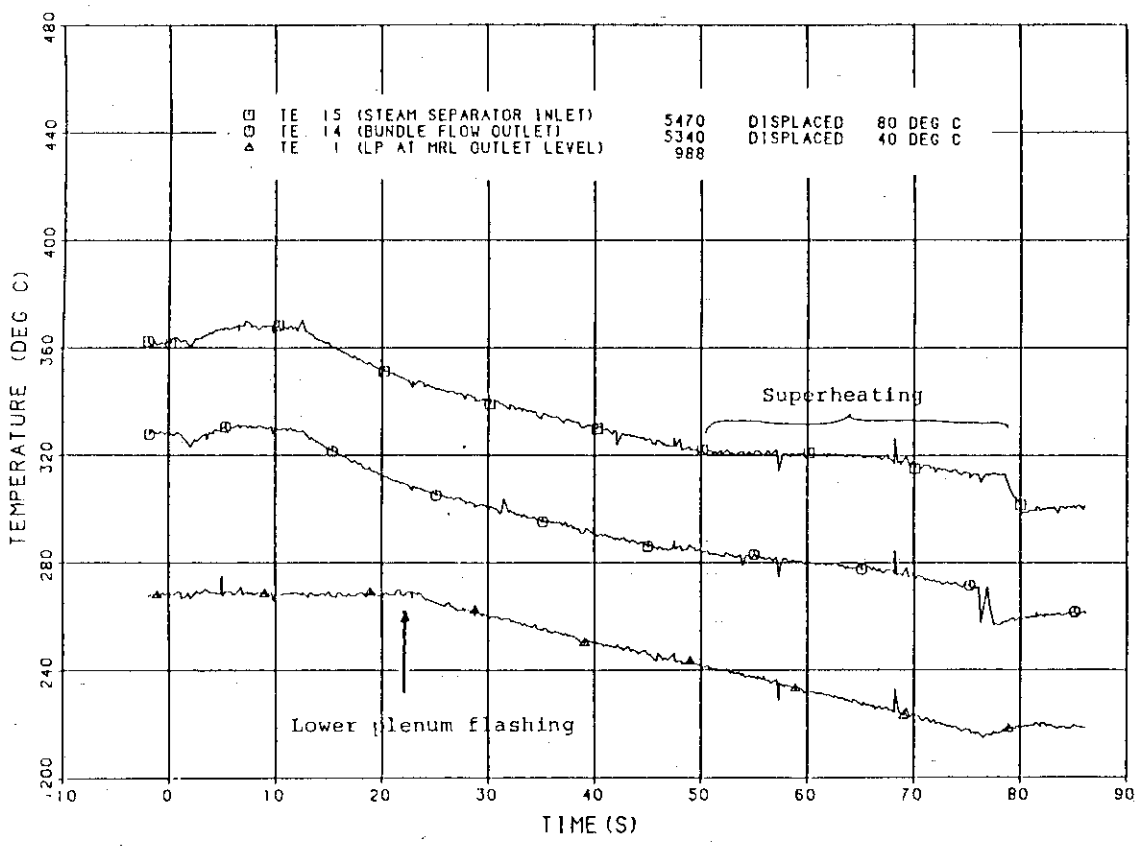

Fig. 4.1.4 Measured fluid temperatures at loer plenum and upper plenum

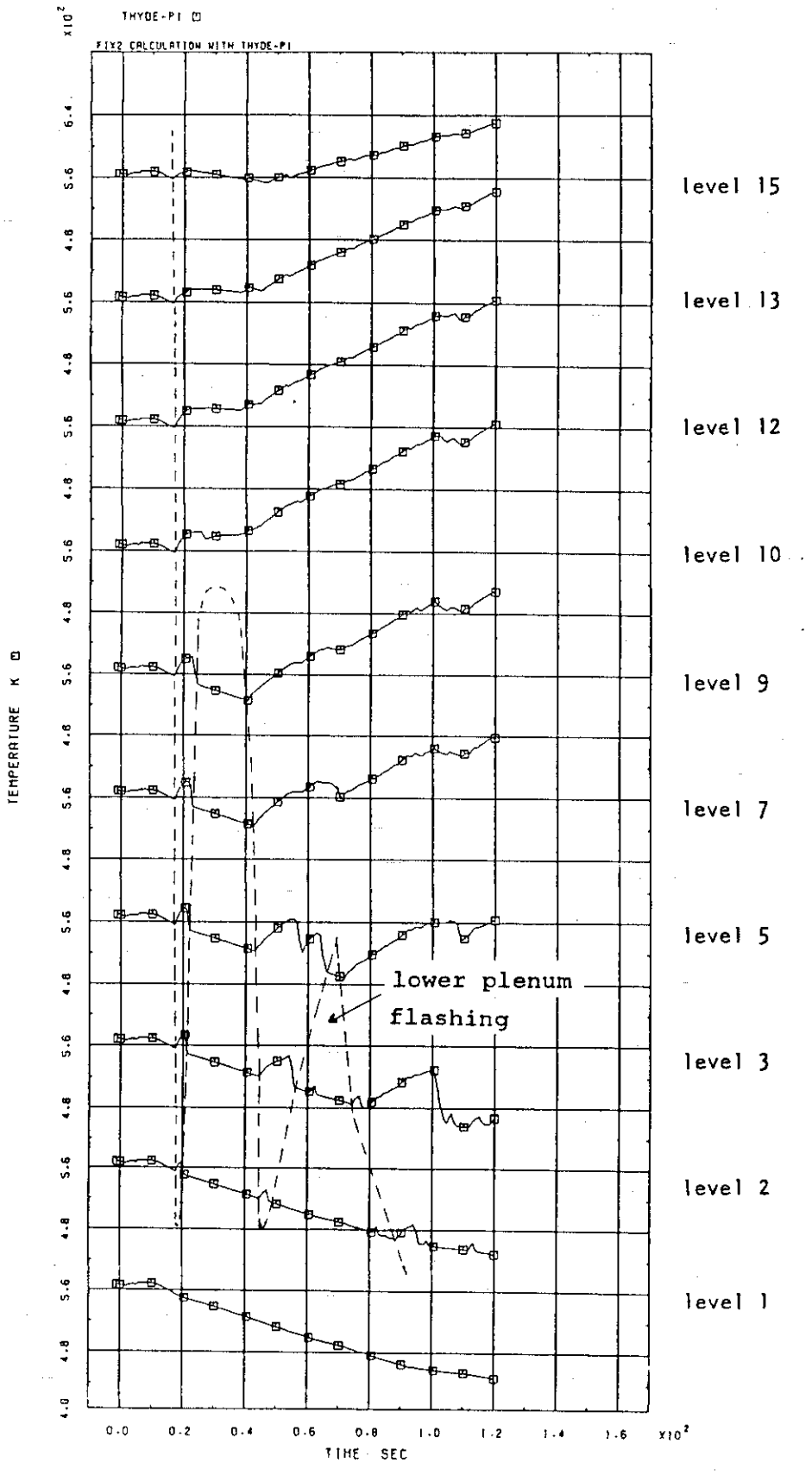

Fig. 4.2.1 Vertical distribution of calculated cladding surface temperature

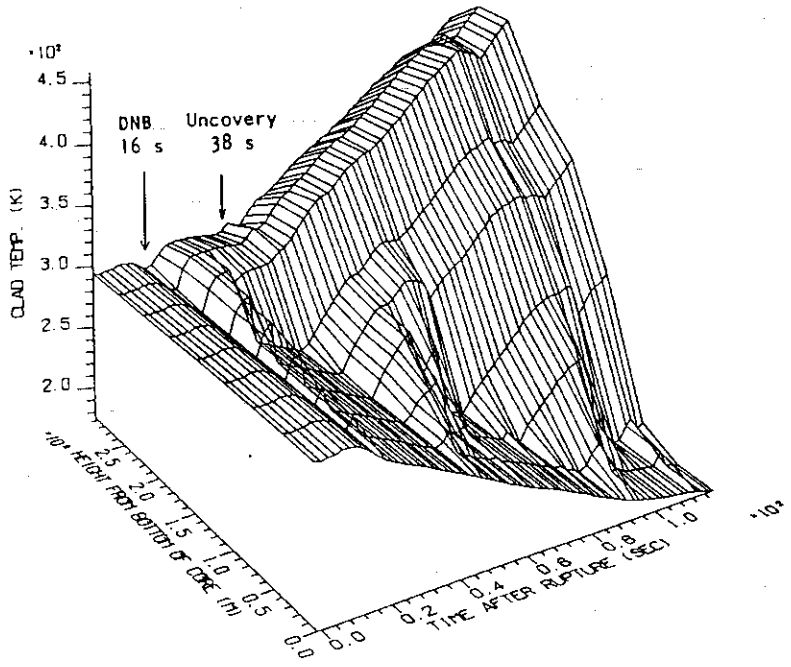

Fig. 4.2.2 Three-Dimensional view of calculated cladding surface temperature

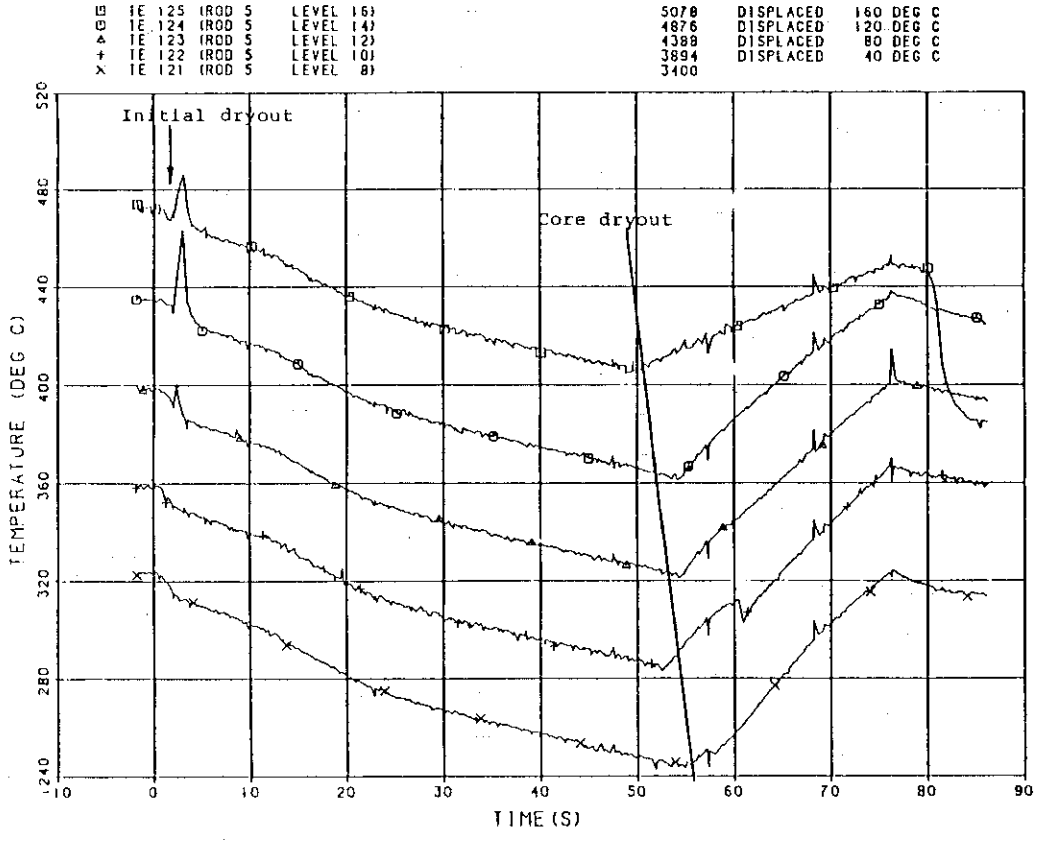

Fig. 4.2.3 Experimental cladding surface temperatures in upper part part of core

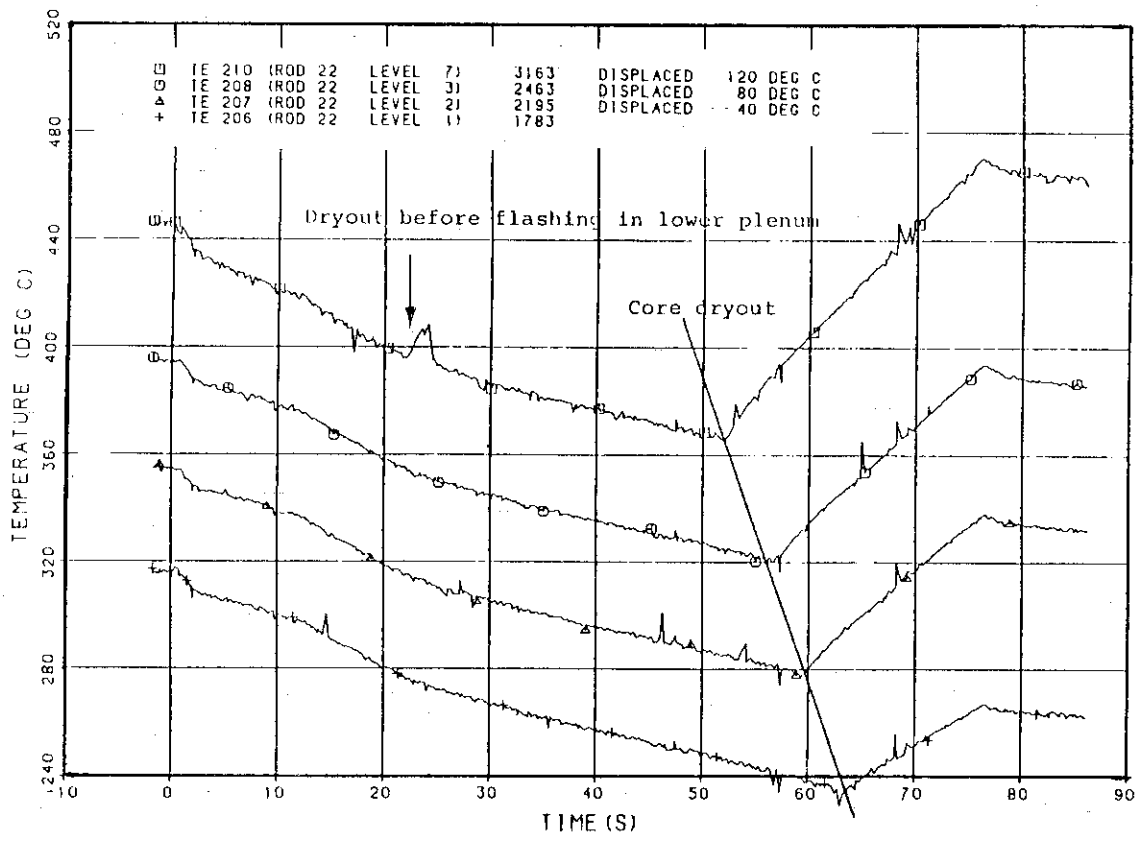

Fig. 4.2.4 Experimental cladding surface temperatures in lower part part of core

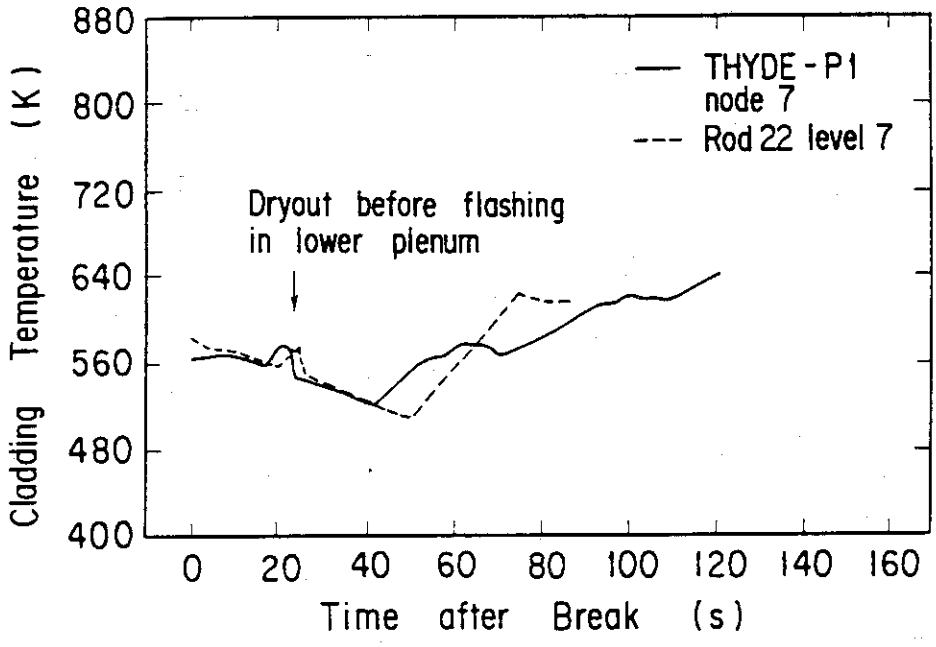

Fig. 4.2.5 Effect of lower plenum flashing on cladding surface temperature

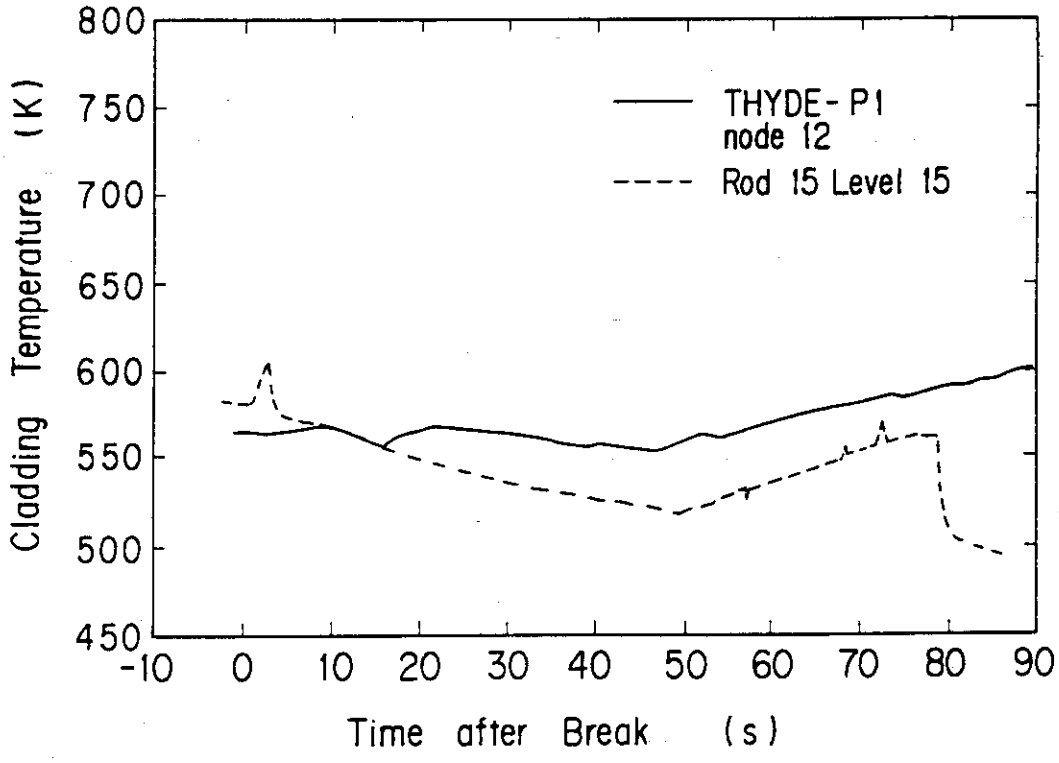

Fig. 4.2.6 Cladding surface temperature at level 1

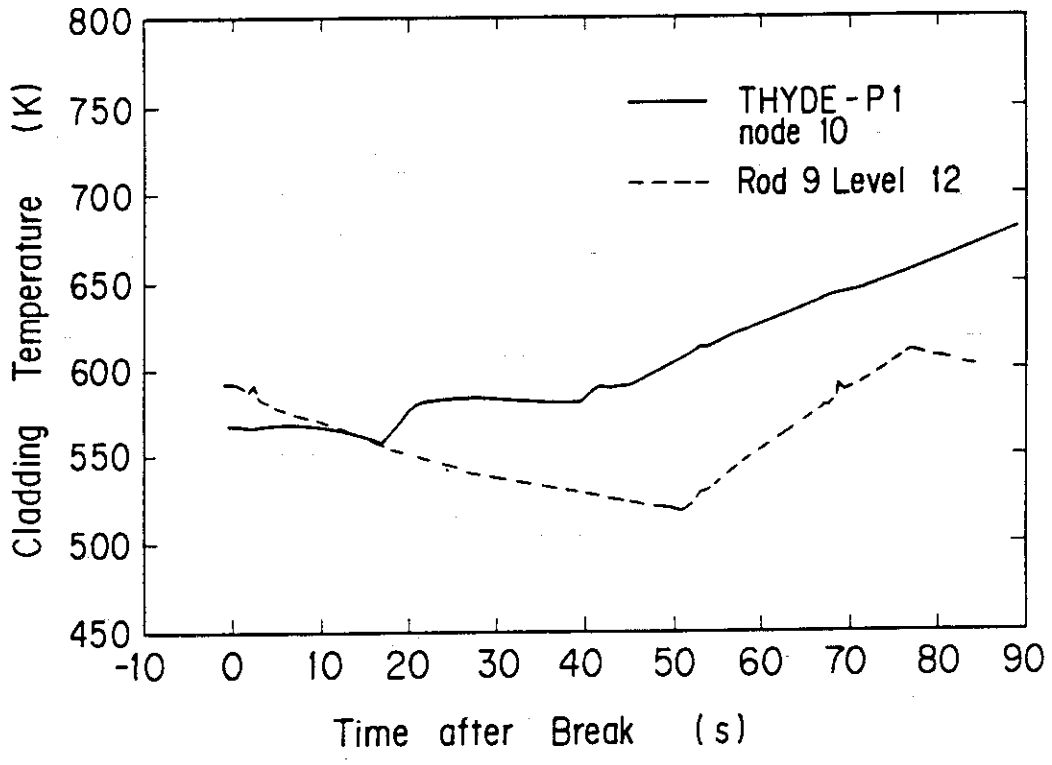

Fig. 4.2.7 Cladding surface temperature at level 3

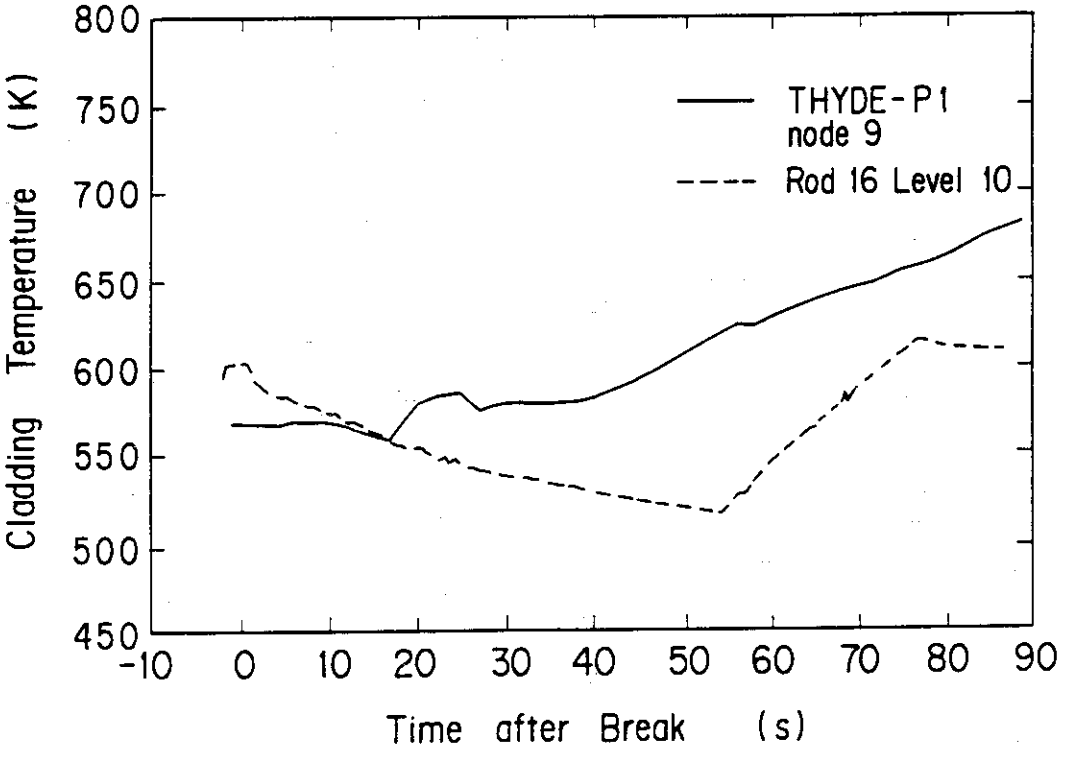

Fig. 4.2.8 Cladding surface temperature at level 5

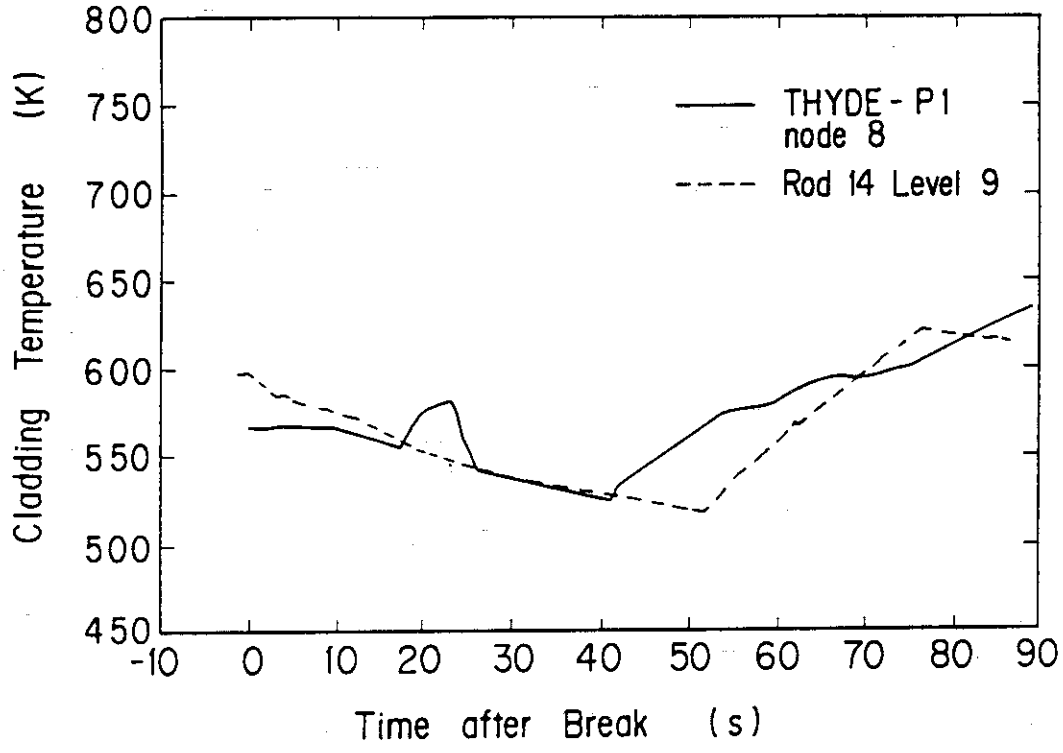

Fig. 4.2.9 Cladding surface temperature at level 7

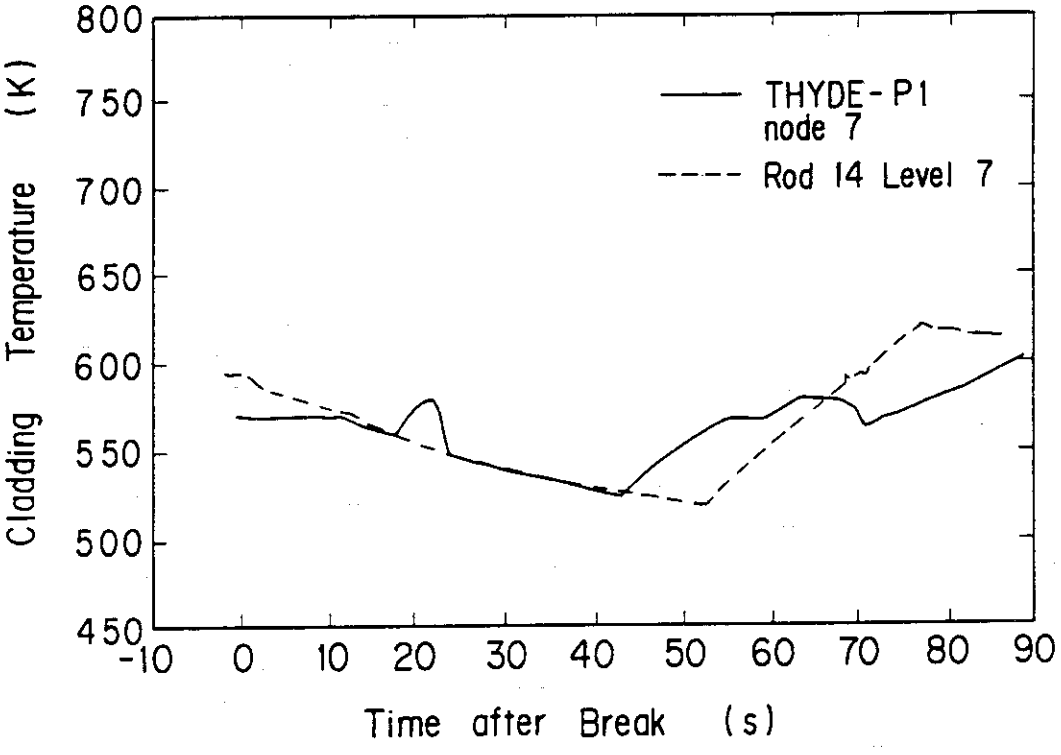

Fig. 4.2.10 Cladding surface temperature at level 9

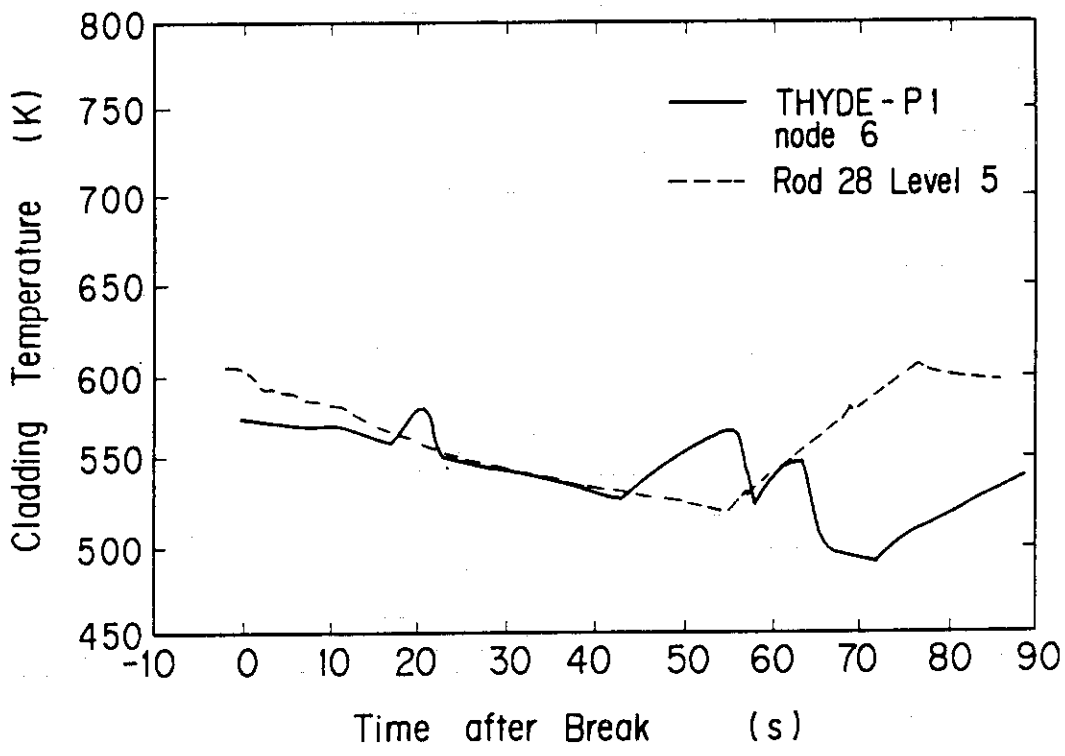

Fig. 4.2.11 Cladding surface temperature at level 10

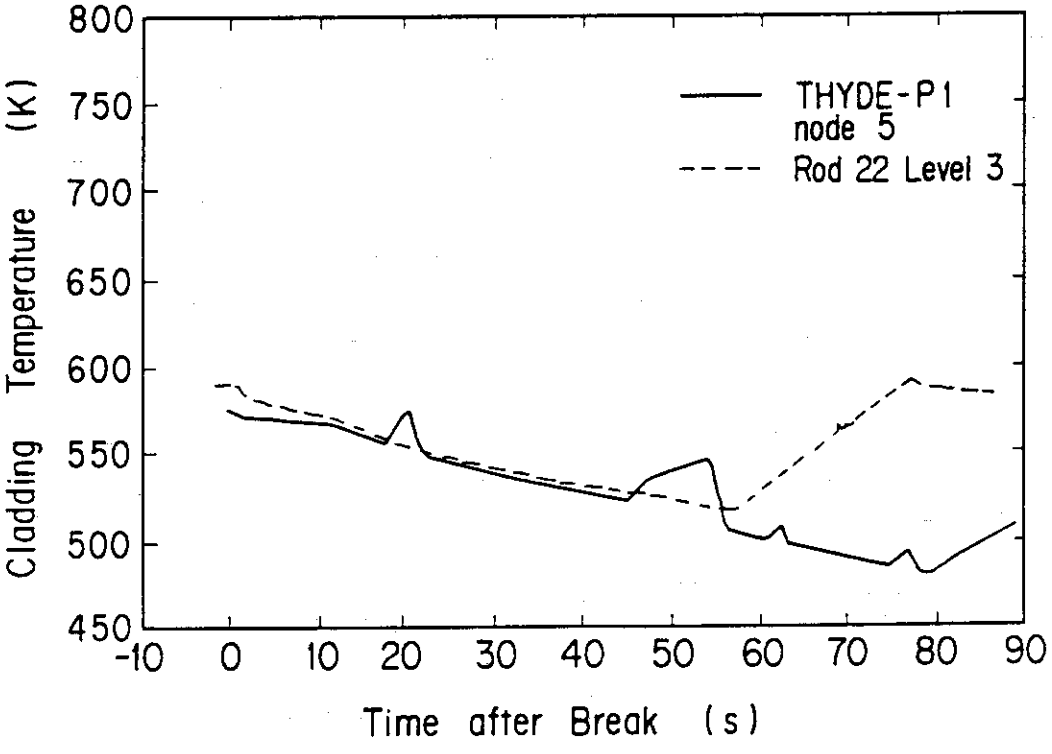

Fig. 4.2.12 Cladding surface temperature at level 12

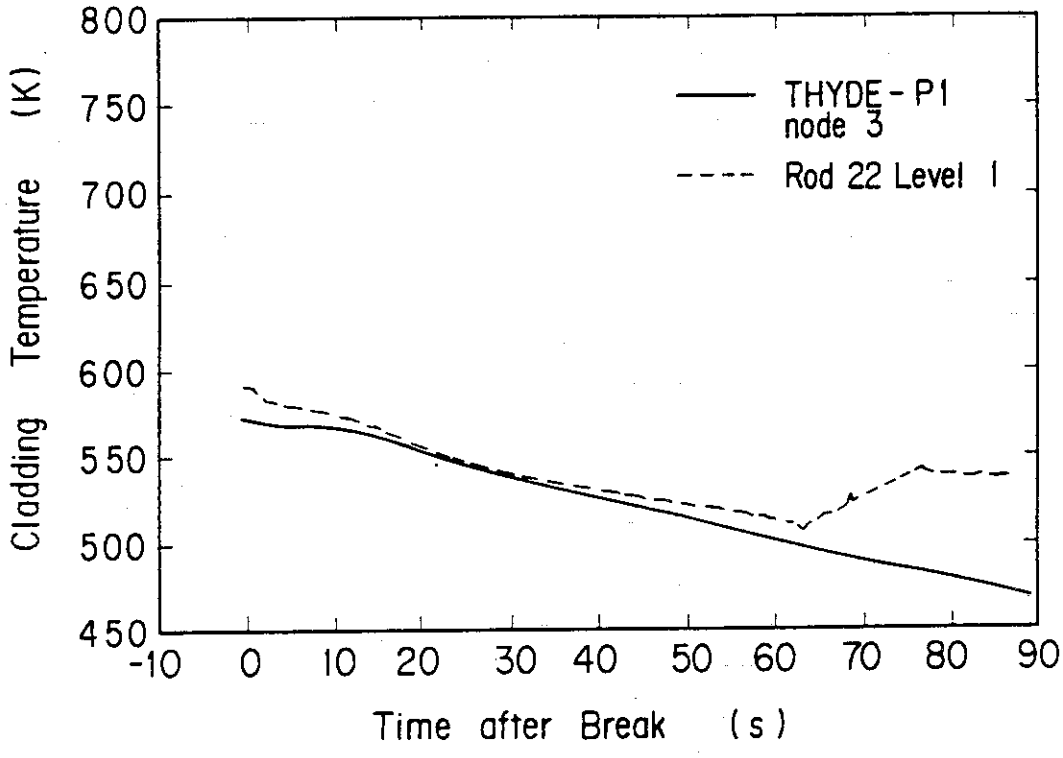

Fig. 4.2.13 Cladding surface temperature at level 15

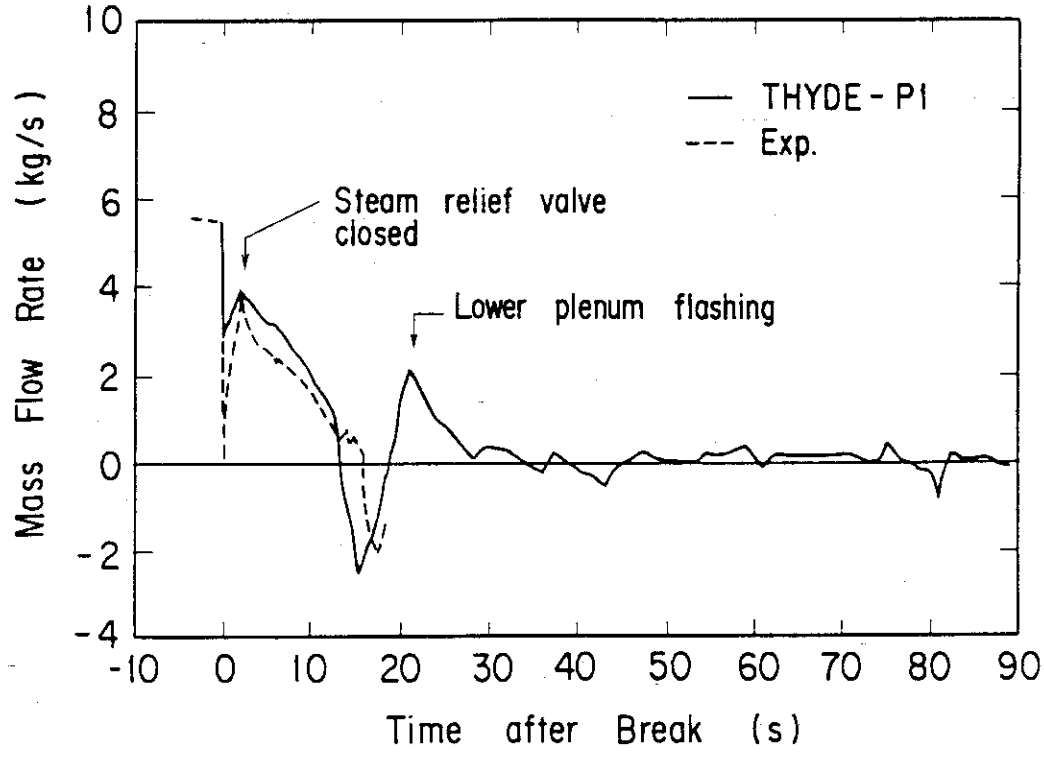

Fig. 4.3.1 Bundle inlet mass flow rate

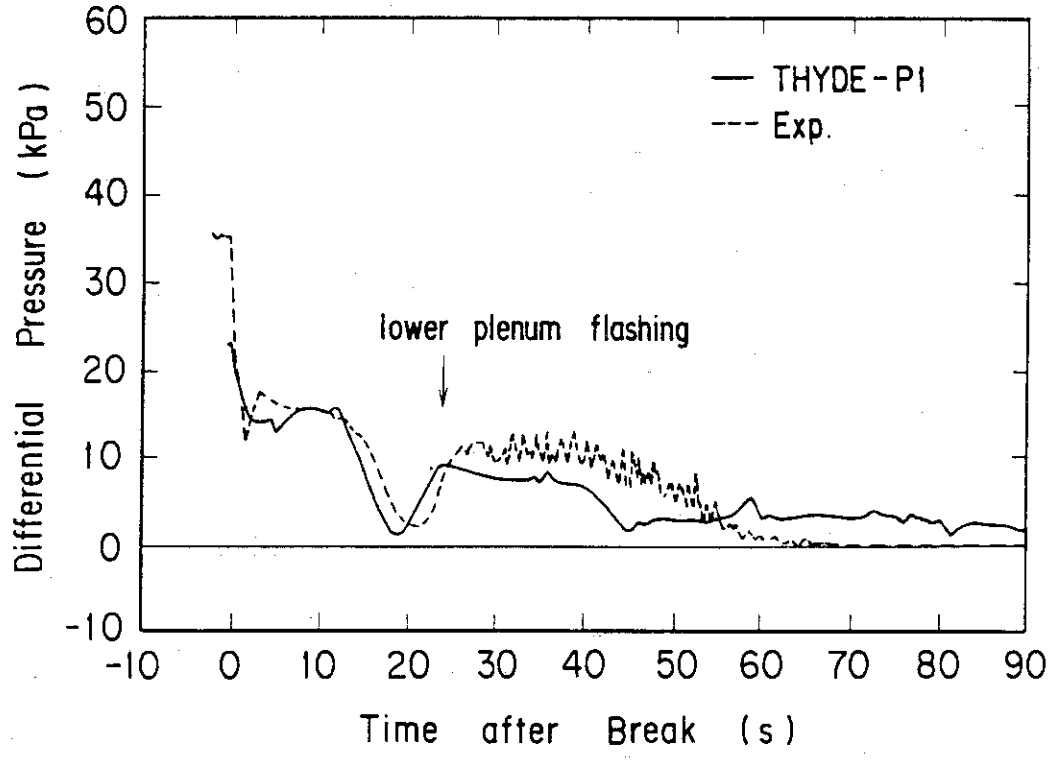

Fig. 4.3.2 Differential pressure through core

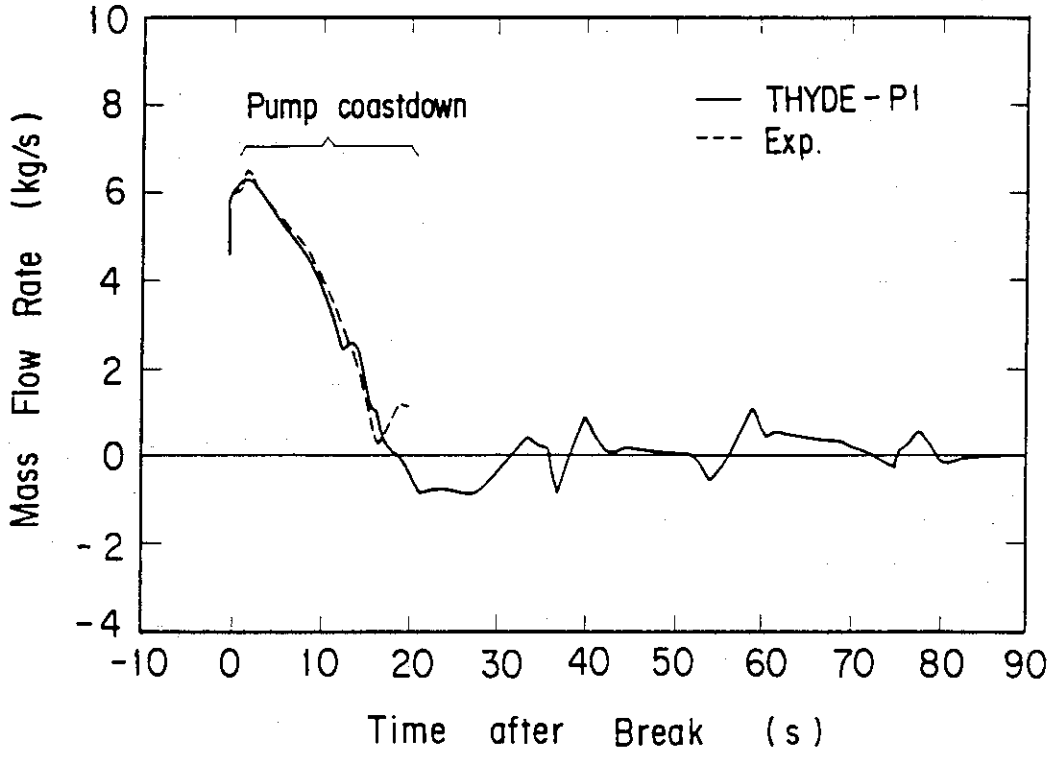

Fig. 4.3.3 Mass flow rate through pump P1

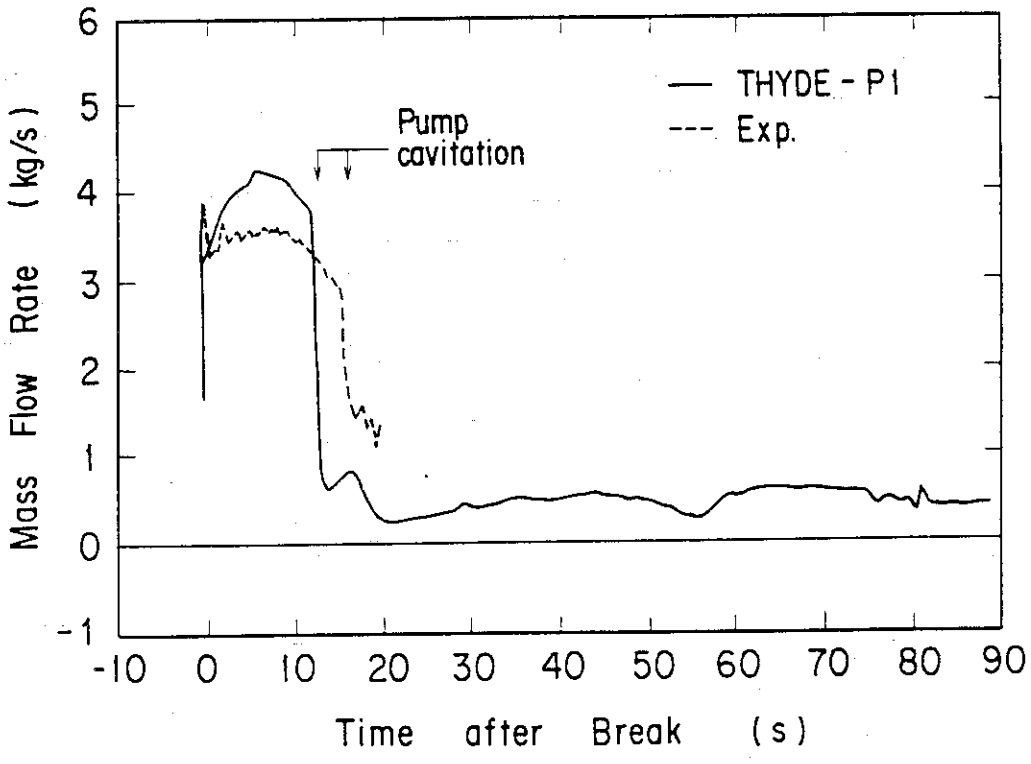

Fig. 4.3.4 Mass flow rate through pump P2

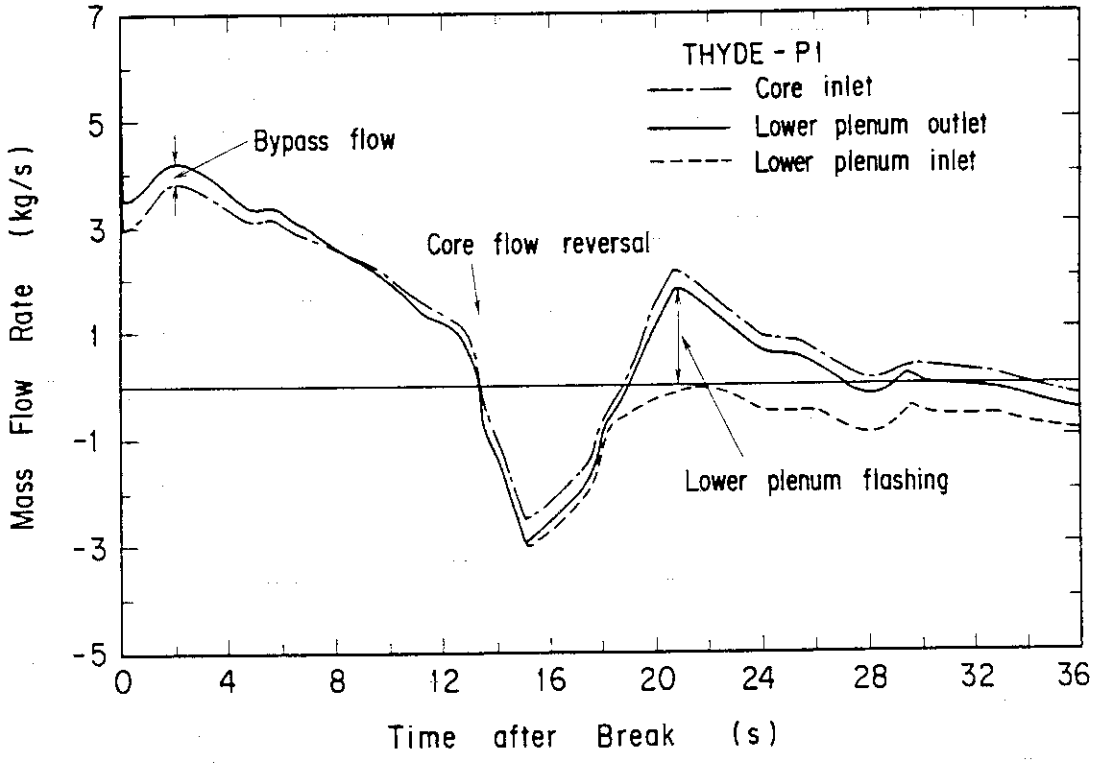

Fig. 4.3.5 Calculated mass flow rates at core inlet and both inlet and outlet of lower plenum

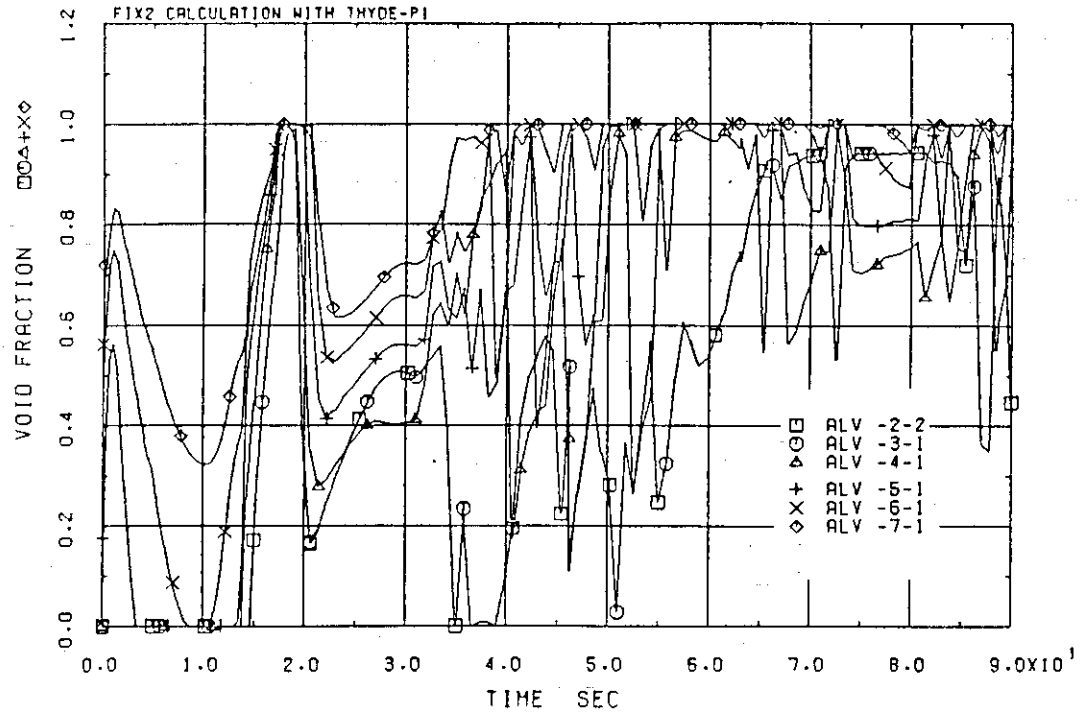

(a) Lower part of core

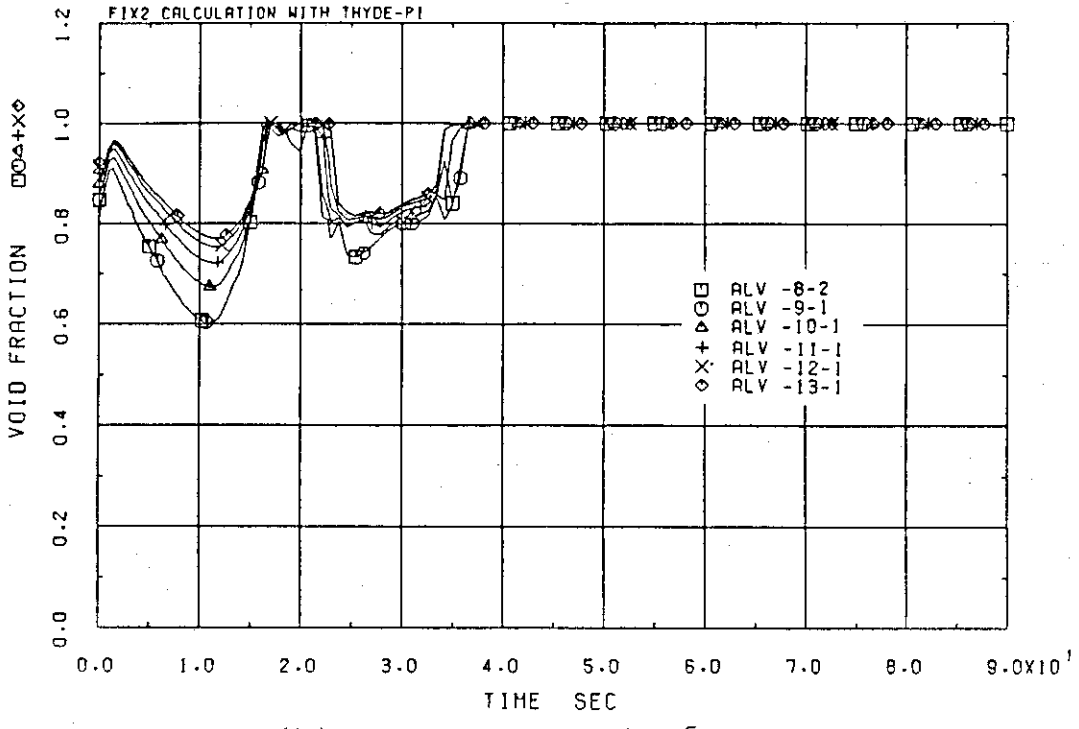

(b) Upper part of core

Fig. 4.3.6 Calculated void fractions at core

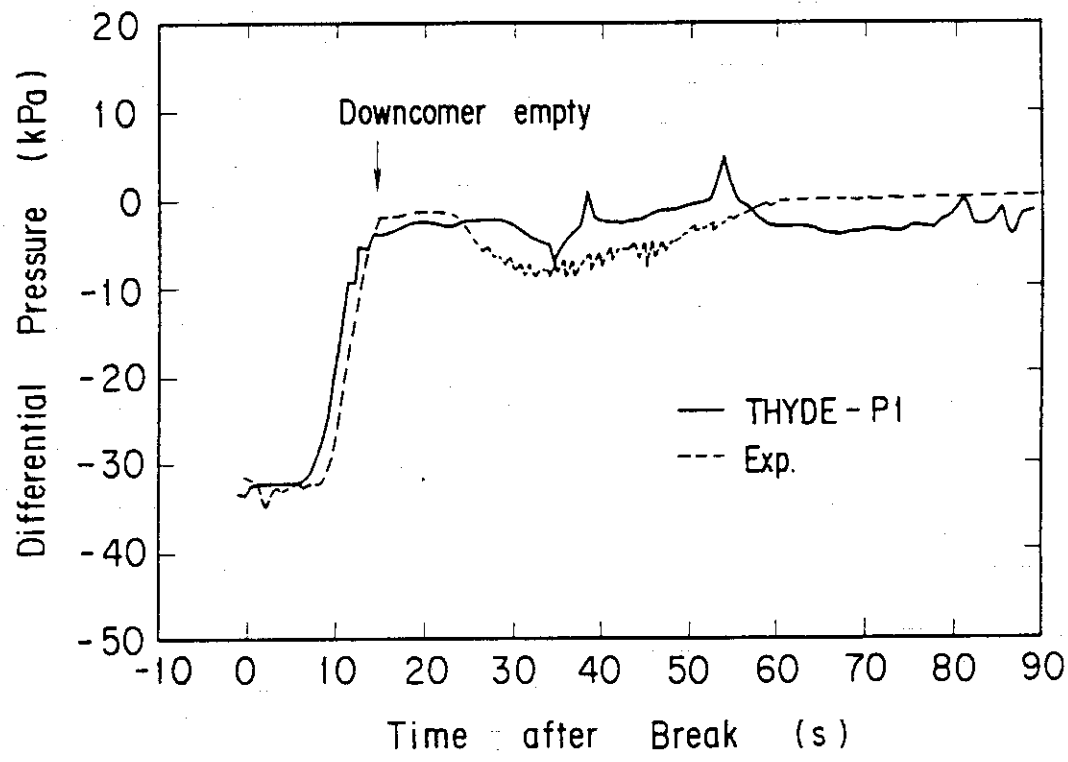

Fig. 4.4.1 Differential pressure through downcomer

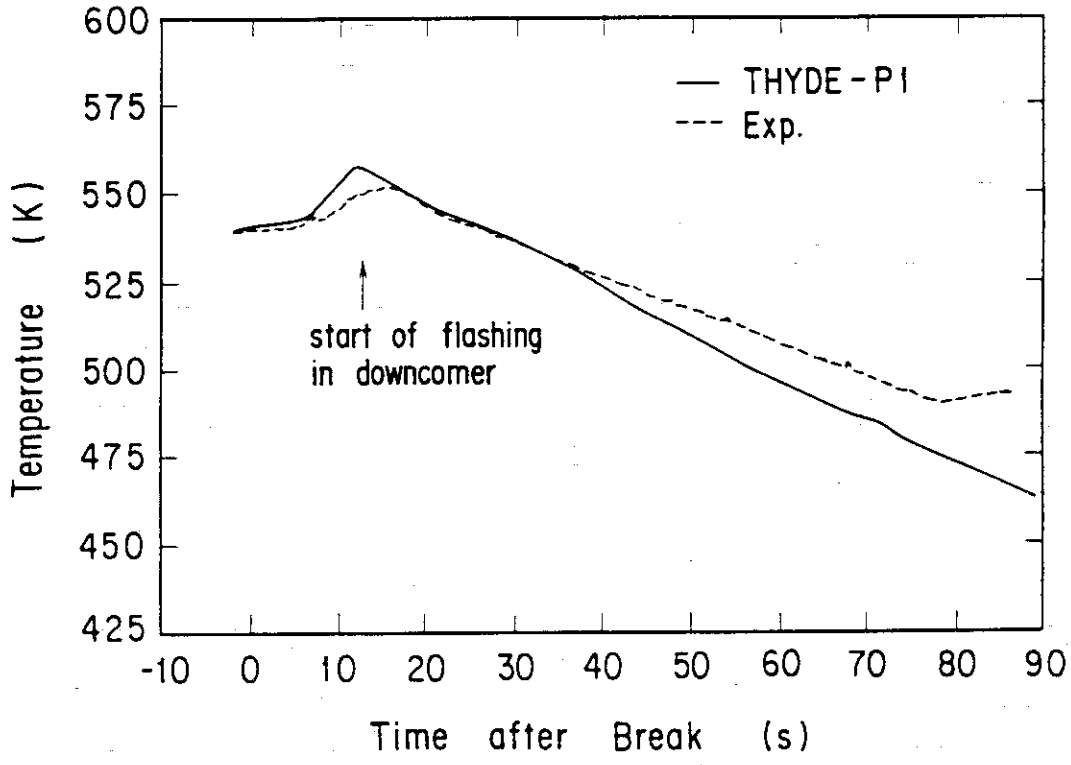

Fig. 4.4.2 Fluid temperature at downcomer inlet

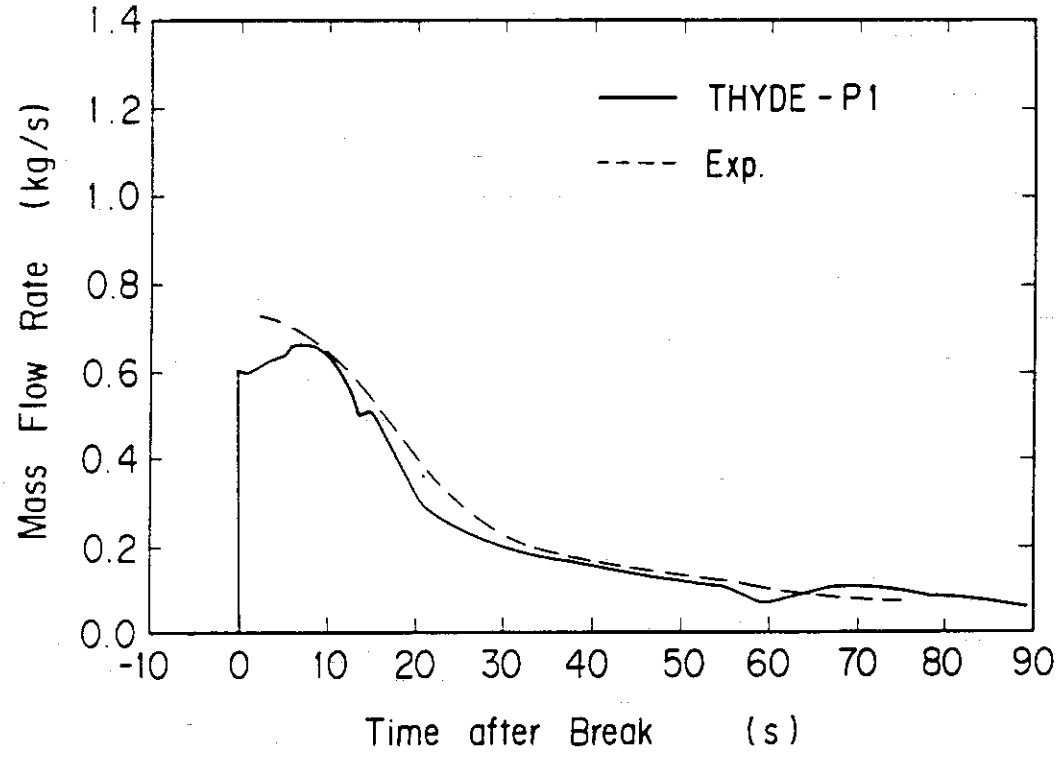

Fig. 4.5.1 Break flow

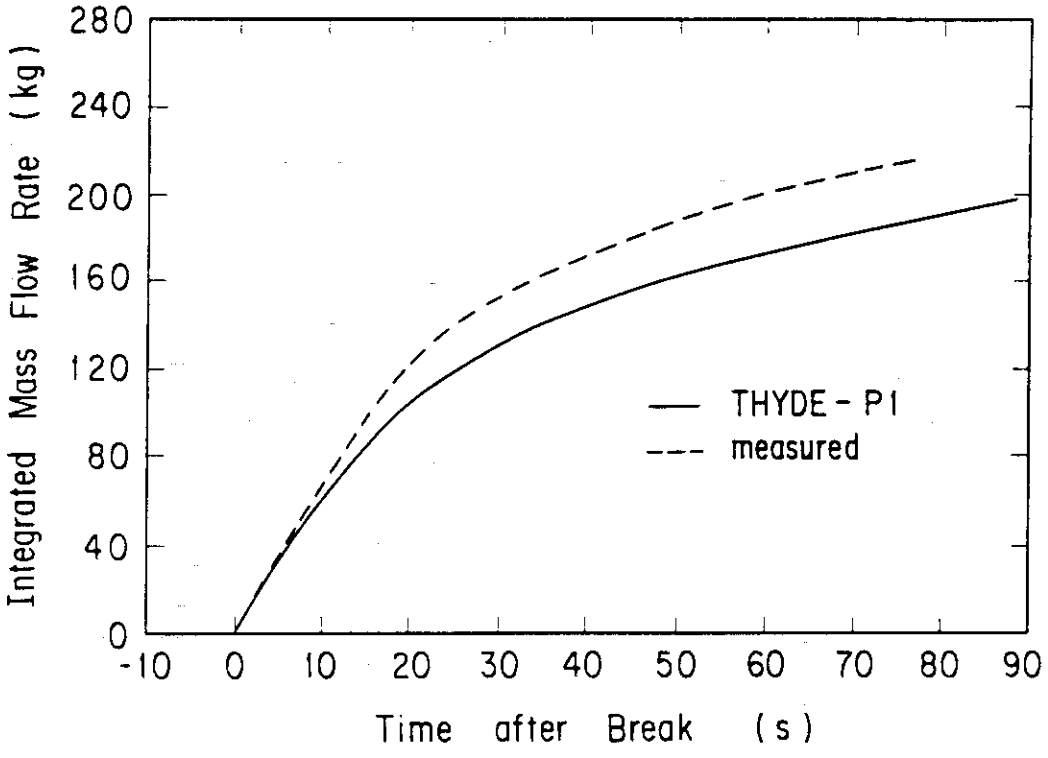

Fig. 4.5.2 Integrated break mass flow

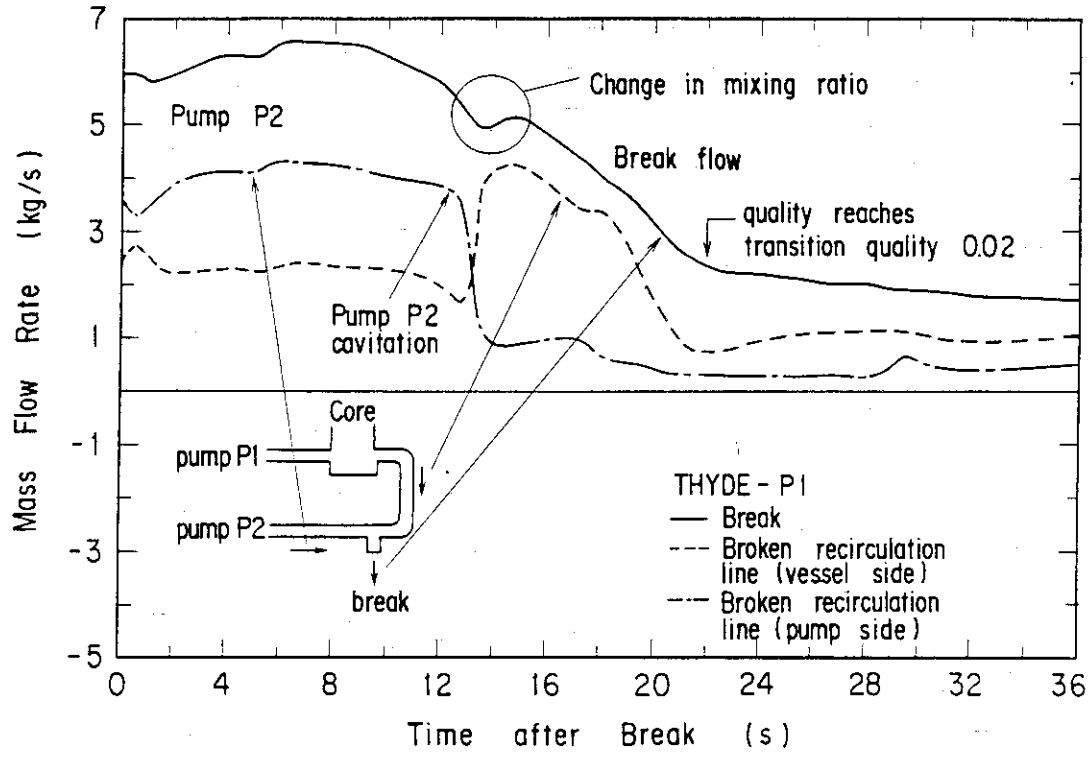

Fig. 4.5.3 Calculated mass flow rates at break, vessel side and pump side of broken recirculation line

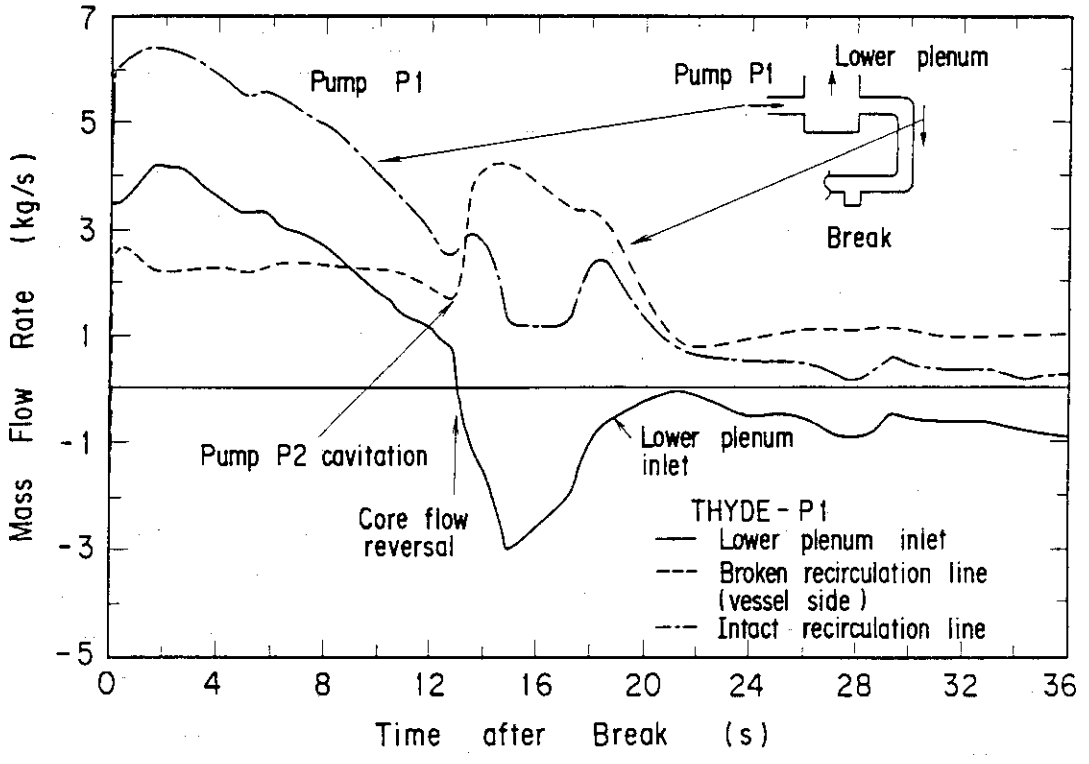

Fig. 4.5.4 Calculated mass flow rates at lower plenum inlet, vessel side of broken recirculation line and intact recirculation line

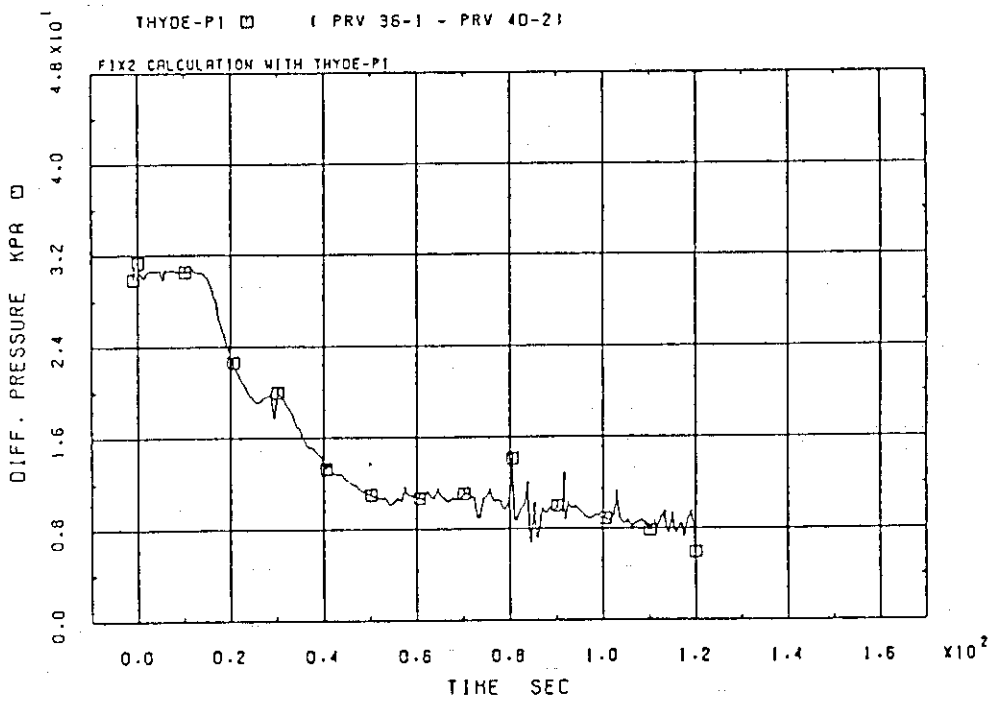

(a) Calculated

⊡ DPT 23 (BYPASS CHANNEL LEVEL 3 -UPPER PLENUM) DISPLACED 30 KPA
△ DPT 22 (BYPASS CHANNEL LEVEL 2 -BYPASS CHANNEL LEVEL 3) DISPLACED 20 KPA
DPT 21 (BYPASS CHANNEL LEVEL 1 -BYPASS CHANNEL LEVEL 2) DISPLACED 10 KPA
+ DPT 20 (BYPASS CHANNEL BOTTOM -BYPASS CHANNEL LEVEL 1)

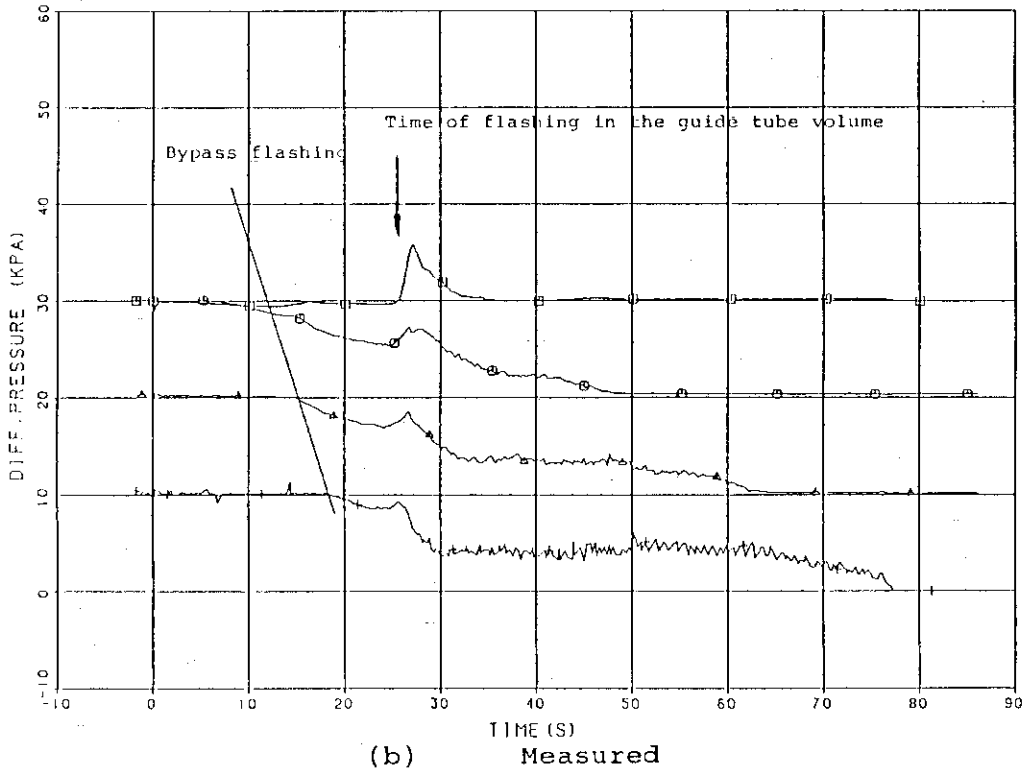

(b) Measured

Fig. 4.6.1 Differential pressure through bypass

Appendix A List of input data

```
***** THYDE-P  INPUT   DATA *****          PAGE     1

      --- FIX-II CALCULATION WITH THYDE-P1 ---  FIX2.DATA(FIX2)     83/04/22000001CC
     /                                                                00000200
     / PROBLEM DIMENSION DATA                                         00000300
     BB01                                                             00000400
       0  0  9  4   6  55  50  9  0  3  0  1  1 12  5  3  1  1  1     00000500
       5  1  5  4   0  24   2                                         00000600
     /                                                                00000700
     / MINOR EDIT DATA                                                00000800
     BB02                                                             00000900
     GLE-51  GLE-49  GLE-54  GLA-02  GLA-36  GLE-15  GLE-13  GLE-35  PRA-50  00001000
     /                                                                00001100
     / TIME STEP CONTROL DATA                                         00001200
     BB03                                                             00001300
     SB0301                                                           00001400
         0.2  0.2  100.                                              00001500
     SB0302                                                           00001600
         20  20  50   0  8.0E-3  1.0E-6   0.99  0.1                  00001700
     SB0303                                                           00001800
         20  20  50   0  4.0E-3  1.0E-6   1.2   0.1                  00001900
     SB0304                                                           00002000
         25  30  50   0 16.0E-3  1.0E-6  20.0   0.1                  00002140
     SB0305                                                           00002200
         25  30  50   0 32.0E-3  1.E-6 1000.0   0.1                  00002300
     /                                                                00002400
     / TRIP CONTROLL DATA                                             00002500
     BB04                                                             00002600
     SB0401                                                           00002700
       1    0  1  0   1.E4    0.0    / END OF PROBLEM                 00002800
     SB0402                                                           00002900
       2   28  1  0   1.0     0.0    / PUMP 1 TRIP                    00003000
     SB0403                                                           00003100
       2   31  1  0   1.      0.0    / PUMP 2 TRIP                    00003200
     SB0404                                                           00003300
       2   43  1  0   1.      0.0    / PUMP 3 TRIP                    00003400
     SB0405                                                           00003500
       3    0  1  0   1.E4    0.0    / SCRAM                          00003600
     SB0406                                                           00003700
       5   55  1  0   5.      0.0    / SG ISOLATION                   00003800
     /                                                                00003900
     / STEADY STATE MASS FLUX AND ENTHALPY                            00004000
     BB05                                                             00004100
       1   150.63 280.                                                00004200
     /                                                                00004300
     / CONTROL VOLUME DATA                                            00004400
     BB06                                                             00004500
     SB0601                                                           00004600
     /1  1 39 40   0  1 70.4303    0.2252  0.      0.3840  0.3000     00004700
      1  1 39 40   0  1 70.3303    0.2252  0.      0.7680  0.3000     00004710
                                   0.      0.      0.      0.      0.  00004800
     SB0602                                                           00004900
      2  2 40  1   0 36 70.1970    1.      1.      0.1260  0.0810     00005000
                                   0.      0.     56.     56.      0.  00005100
     SB0603                                                           00005200
      3  2  1  2   1 36 70.0101    1.      1.      0.3680  0.3680     00005300
                                   0.      0.      0.      0.      0.  00005400
     SB0604                                                           00005500
      4  2  2  3   1 36 69.9802    1.      1.      0.3680  0.3680     00005600
                                   0.      0.      0.      0.      0.  00005700
     SB0605                                                           00005800
      5  2  3  4   1 36 69.9513    1.      1.      0.3680  0.3680     00005900
                                   0.      0.      0.      0.      0.  00006000
     SB0606                                                           00006100
      6  2  4  5   1 36 69.9214    1.      1.      0.3680  0.3680     00006200
                                   0.      0.      0.      0.      0.  00006300
     SB0607                                                           00006400
```

```
 7  2  5  6  1 36 69.8935    1.       1.       0.3680   0.3680              00006500
                              0.       0.       0.       0.        0.       00006600
SB0608                                                                      00006700
 8  2  6  7  1 36 69.8671    1.       1.       0.3680   0.3680              00006800
                              0.       0.       0.       0.        0.       00006900
SB0609                                                                      00007000
 9  2  7  8  1 36 69.8402    1.       1.       0.3680   0.3680              00007100
                              0.       0.       0.       0.        0.       00007200
SB0610                                                                      00007300
10  2  8  9  1 36 69.8126    1.       1.       0.3680   0.3680              00007400
                              0.       0.       0.       0.        0.       00007500
SB0611                                                                      00007600
11  2  9 10  1 36 69.7853    1.       1.       0.3680   0.3680              00007700
                              0.       0.       0.       0.        0.       00007800
SB0612                                                                      00007900
12  2 10 11  1 36 69.7585    1.       1.       0.3680   0.3680              00008000
                              0.       0.       0.       0.        0.       00008100
SB0613                                                                      00008200
13  2 11 41  0 36 69.7357    1.       1.       0.4970   0.1820              00008300
/                             0.       0.       0.85     0.85      0.       00008400
                              0.       0.       0.       0.        0.       00008500
SB0614                                                                      00008600
14  1 41 42  0  1 69.6717    0.1132   0.       1.4570   1.457               00008700
                              0.       0.      34.5     34.5       0.       00008800
SB0615                                                                      00008900
/15  1 42 43  0  1 69.1776    0.3423   0.       1.3900  -1.519               00009000
 15  1 42 43  0  1 69.0766    0.3423   0.       1.3900  -1.338               00009010
                              0.       0.       0.       0.        0.6      00009100
SB0616                                                                      00009200
16  1 43 12  0  1 69.1011    0.1081   0.       0.6840  -0.094               00009300
                              0.       0.       0.       0.        0.       00009400
SB0617                                                                      00009500
17  1 12 13  0  1 69.1068    0.1081   0.       0.6840  -0.094               00009600
                              0.       0.       0.       0.        0.       00009700
SB0618                                                                      00009800
18  1 13 14  0  1 69.1125    0.1081   0.       0.6840  -0.094               00009900
                              0.       0.       0.       0.        0.       00010000
SB0619                                                                      00010100
19  1 14 15  0  1 69.1182    0.1081   0.       0.6840  -0.094               00010200
                              0.       0.       0.       0.        0.       00010300
SB0620                                                                      00010400
20  1 15 16  0  1 69.1239    0.1081   0.       0.6840  -0.094               00010500
                              0.       0.       0.       0.        0.       00010600
SB0621                                                                      00010700
21  1 16 17  0  1 69.1302    0.1090   0.       0.6630  -0.6630              00010800
                              0.       0.       0.       0.        0.       00010900
SB0622                                                                      00011000
22  1 17 18  0  1 69.1787    0.1090   0.       0.6630  -0.6630              00011100
                              0.       0.       0.       0.        0.       00011200
SB0623                                                                      00011300
23  1 18 19  0  1 69.2272    0.1090   0.       0.6630  -0.6630              00011400
                              0.       0.       0.       0.        0.       00011500
SB0624                                                                      00011600
24  1 19 20  0  1 69.2759    0.1090   0.       0.6630  -0.6630              00011700
                              0.       0.       0.       0.        0.       00011800
SB0625                                                                      00011900
25  1 20 21  0  1 69.3244    0.1090   0.       0.6630  -0.6630              00012000
                              0.       0.       0.       0.        0.       00012100
SB0626                                                                      00012200
26  1 21 44  0  1 69.3729    0.1090   0.       0.6630  -0.6630              00012300
                              0.       0.       0.       0.        0.       00012400
SB0627                                                                      00012500
27  1 44 22  0  1 69.4301    0.1090   0.       0.9240  -0.7500              00012600
                              0.       0.       0.       0.        0.       00012700
SB0628                                                                      00012800
28  8 22 23  0  1 69.4925    0.1197   0.       0.8980   0.2830              00012900
                              0.       0.     130.     130.        0.       00013000
SB0629                                                                      00013100
29  1 23 39  0  1 70.4701    0.0772   0.       6.1500   0.5530              00013200
                              0.       0.      16.8     16.8       0.       00013300
SB0630                                                                      00013400
```

```
30  1 44 24  0  1 69.4301     0.0654  0.      2.2900 -0.8200                00013500
                              0.      0.      0.      0.           0.       00013600
SB0631                                                                      00013700
31  8 24 25  0  1 69.4971     0.0661  0.      1.4570  0.2280                00013800
                              0.      0.     64.4    64.4          0.       00013900
SB0632                                                                      00014000
32  1 25 45  0  1 70.4198     0.0503  0.      1.4100  0.4170                00014100
                              0.      0.     10.3    10.3          0.       00014200
SB0633                                                                      00014300
33  1 45 26  0  1 70.3495     0.0492  0.      3.0600  0.2610                00014400
                              0.      0.      0.      0.           0.       00014500
SB0634                                                                      00014600
34  1 26 39  0  1 70.3302     0.0824  0.      1.4200  0.001                 00014700
                              0.      0.      0.      0.           0.       00014800
SB0635                                                                      00014900
35  1 40 46  0  1 70.410793   0.0392  0.      1.1600  0.001                 00015000
                              0.      0.    167.    167.           0.       00015100
SB0636                                                                      00015200
36  1 46 27  0  1 69.991365   0.0949  0.      0.6840  0.6840                00015300
                              0.      0.      0.      0.           0.       00015400
SB0637                                                                      00015500
37  1 27 28  0  1 69.940307   0.0949  0.      0.9400  0.9400                00015600
                              0.      0.      0.      0.           0.       00015700
SB0638                                                                      00015800
38  1 28 29  0  1 69.870840   0.0949  0.      0.9350  0.9350                00015900
                              0.      0.      0.      0.           0.       00016000
SB0639                                                                      00016100
39  1 29 30  0  1 69.802854   0.0949  0.      0.9290  0.9290                00016200
                              0.      0.      0.      0.           0.       00016300
SB0640                                                                      00016400
40  1 30 31  0  1 69.735975   0.0949  0.      0.6520  0.6520                00016500
                              0.      0.      0.      0.           0.       00016600
SB0641                                                                      00016700
41  1 31 41  0  1 69.666476   0.0485  0.      1.1600  0.0                   00016800
                              0.      0.      0.      0.           0.       00016900
SB0642                                                                      00017000
42  1 44 32  0  1 69.4301     0.0802  0.      3.0700  0.                    00017100
                              0.      0.      0.      0.           0.       00017200
SB0643                                                                      00017300
43  8 32 33  0  1 69.3947     0.1     0.      0.75   -0.7500                00017400
                              0.      0.      0.      0.           0.       00017500
SB0644                                                                      00017600
44  1 33 34  0  1 70.4520     0.0722  0.      2.4600  0.0580                00017700
                              0.      0.      0.      0.           0.       00017800
SB0645                                                                      00017900
45  7 34 35  1 139 70.4576    0.0080  0.      6.8140  4.000                 00018000
                              0.      0.      0.      0.           0.       00018100
SB0646                                                                      00018200
46  1 35 47  0  1 69.9494     0.0718  0.      6.9000  4.7020                00018300
                              0.      0.      0.      0.           0.       00018400
SB0647                                                                      00018500
47  1 47 36  0  1 69.5548     0.0590  0.      2.4900  2.4920                00018600
                              0.      0.      0.      0.           0.       00018700
SB0648                                                                      00018800
48  1 36 42  0  2 69.2898     0.0427  0.      7.3500  1.8350                00018900
                              0.      0.      0.      0.           0.       00019000
SB0649                                                                      00019100
49  1 47 43  0  1 69.4936     0.0467  0.      6.2700  0.1560                00019200
                              0.      0.      0.      0.           0.       00019300
SB0650                                                                      00019400
50 13 42 37  0  1       0.    0.5000  0.      2.3600  2.3480                00019500
                              0.      0.      0.      0.         658.00     00019600
SB0651                                                                      00019700
51 13 37 49  0  1       0.    0.0809  0.      1.8900  0.                    00019800
                              0.      0.     12.2    12.2        658.00     00019900
SB0652                                                                      00020000
52 13 45 43  0  1       0.    0.1836  0.      1.2200 -1.2210                00020100
                              0.      0.      0.      0.           0.       00020200
SB0653                                                                      00020300
53 13 45 38  0  1       0.    0.07360 0.      1.4800  0.                    00020400
```

```
                                        0.      0.      0.      0.      0.      00020500
SB0654                                                                          00020600
/54 13 38 50  0  1       0.    0.0120  0.      0.2000  0.                      00020700
 54 13 38 50  0  1       0.    0.07360 0.      0.2000  0.                      00020710
                                        0.      0.      0.      0.      0.      00020800
/                                                                               00020900
/ JUNCTION DATA                                                                 00021000
8807                                                                            00021100
    1    1    0.0                                                              00021200
    2    1    0.0                                                              00021300
    3    1    0.0                                                              00021400
    4    1    0.0                                                              00021500
    5    1    0.0                                                              00021600
    6    1    0.0                                                              00021700
    7    1    0.0                                                              00021800
    8    1    0.0                                                              00021900
    9    1    0.0                                                              00022000
   10    1    0.0                                                              00022100
   11    1    0.0                                                              00022200
   12    1    0.0                                                              00022300
   13    1    0.0                                                              00022400
   14    1    0.0                                                              00022500
   15    1    0.0                                                              00022600
   16    1    0.0                                                              00022700
   17    1    0.0                                                              00022800
   18    1    0.0                                                              00022900
   19    1    0.0                                                              00023000
   20    1    0.0                                                              00023100
   21    1    0.0                                                              00023200
   22    1    0.0                                                              00023300
   23    1    0.0                                                              00023400
   24    1    0.0                                                              00023500
   25    1    0.0                                                              00023600
   26    1    0.0                                                              00023700
   27    1    0.0                                                              00023800
   28    1    0.0                                                              00023900
   29    1    0.0                                                              00024000
   30    1    0.0                                                              00024100
   31    1    0.0                                                              00024200
   32    1    0.0                                                              00024300
   33    1    0.0                                                              00024400
   34    1    0.0                                                              00024500
   35    1    0.0                                                              00024600
   36    1    0.0                                                              00024700
   37    1    0.0                                                              00024800
   38    1    0.0                                                              00024900
   39    4  0.0045                                                             00025000
/  40    4  0.0153                                                             00025100
   40    4  0.0010                                                             00025110
   41    4  0.0030                                                             00025200
   42    4  0.0909                                                             00025300
   43    4  0.0010                                                             00025400
   44    4  0.0028                                                             00025500
   45    4  0.0010                                                             00025600
   46    4  0.0010                                                             00025700
   47    4  0.0010                                                             00025800
   48    8  0.0                                                                00025900
   49    8  0.0                                                                00026000
   50    8  0.0                                                                00026100
/                                                                               00026200
/ MIXING JUNCTION DATA                                                          00026300
8803                                                                            00026400
SB0801                                                                          00026500
   39    1     1   0   0   0   1.      .0      .0      .0                       00026600
SB0802                                                                          00026700
   40    2     2  35   0   0    .89     .11     .0      .0                       00026800
SB0803                                                                          00026900
   41    1    14   0   0   0   1.      .0      .0      .0                       00027000
SB0804                                                                          00027100
```

```
   42   2   15  50   0   0   1.        .0      .0     .0                    00027200
SB0805                                                                      00027300
   43   1   16   0   0   0   1.        .0      .0     .0                    00027400
SB0807                                                                      00027500
   44   3   27  30  42   0    .303     .101    .596   .0                    00027600
SB0808                                                                      00027700
   45   2   33  53   0   0   1.        .0      .0     .0                    00027800
SB0809                                                                      00027900
   46   2   36  52   0   0   1.        .0      .0     .0                    00028000
SB0810                                                                      00028100
   47   2   47  49   0   0    .667     .333    .0     .0                    00028200
/                                                                           00028300
/ PUMP DATA                                                                 00028400
BB10                                                                        00028500
SB1001                                                                      00028600
 26  1 0 2900.  0.0383  81.7  50.0  1000.  1566.  1.E3  .0 .0     2.         00028700
SB1002                                                                      00028800
 31  2 0 2900.  0.0106  13.2  25.0  1000.  2035.  1.E3  .0 .0     2.         00028900
SB1003                                                                      00029000
 43  1 0 2900.  0.0106  13.2  30.0  1000.  2035.  1.E3  .0 .0     2.         00029100
/                                                                           00029200
/ PUMP CHARACTERISTIC CURVES                                                00029300
BB11                                                                        00029400
SB1101                                                                      00029500
 1    / PUMP1 AND PUMP3                                                     00029600
 9                                                                          00029700
-1.0  2.00        -0.95 1.81        -0.62 1.52        -0.50 1.39            00029800
 0.0  1.181        0.27 1.18         0.47 1.16         0.64 1.13            00029900
 1.0  1.0                                                                   00030000
 2                                                                          00030100
-1.0 -1.0           1.0  1.0                                               00030200
 6                                                                          00030300
-1.0 -1.0           0.0 -0.56         0.41 -0.16        -0.51 -0.05          00030400
 0.76 0.48          1.0  1.0                                               00030500
 6                                                                          00030600
-1.0  2.0         -0.79  1.53        -0.63  1.25        -0.30  0.93          00030700
 0.0  0.72          1.0  1.0                                               00030800
 2                                                                          00030900
-1.0  2.0           1.0  1.0                                               00031000
 2                                                                          00031100
-1.0  1.0           1.0  0.0                                               00031200
 2                                                                          00031300
-1.0 -1.0           1.0  1.0                                               00031400
 2                                                                          00031500
-1.0  2.0           1.0  0.0                                               00031600
 16                                                                         00031700
-1.0 -1.16        -0.90 -1.24        -0.80  -1.77       -0.70 -2.36         00031800
-0.6 -2.79        -0.5  -2.91        -0.40  -2.67       -0.25 -1.69         00031900
-0.1 -0.50         0.0   0.0          0.10   0.83        0.20  1.09         00032000
 0.5  1.02         0.7   1.01         0.90   0.94        1.00  1.0          00032100
 2                                                                          00032200
-1.0  0.0           1.0  0.0                                               00032300
 9                                                                          00032400
-1.0  0.0           0.0  0.0          0.10  -0.04        0.20  0.0          00032500
 0.3  0.1           0.40 0.21         0.80   0.67        0.90  0.80         00032600
 1.0  1.0                                                                   00032700
 11                                                                         00032800
-1.0 -1.16        -0.90 -0.78        -0.80  -0.50       -0.70 -0.31         00032900
-0.6 -0.17        -0.50 -0.08        -0.35   0.0        -0.20  0.05         00033000
-0.1  0.08         0.0   0.11         1.0   0.0                             00033100
 0                                                                          00033200
 0                                                                          00033300
 0                                                                          00033400
 0                                                                          00033500
 11                                                                         00033600
 0.0    0.0       0.1   0.0        0.15  0.05        0.24   0.08           00033700
 0.3    0.96      0.4   0.98       0.60  0.97        0.80   0.90           00033800
 0.90   0.80      0.96  0.50       1.0   0.0                               00033900
```

```
  2
  0.0     0.0         1.0     0.0
  2  2
        0.0     1.0
  0.0   0.0     0.0
  1.0   0.0     0.0
SB1102
 2    / PUMP2
 10
 -1.0  2.00          -0.95 1.81           -0.62 1.52           -0.50 1.39
  0.0  1.136          0.20 1.135           0.40 1.12            0.60 1.10
  0.8  1.055          1.0  1.0
 2
 -1.0 -1.0            1.0  1.0
 8
 -1.0 -1.0            0.0  -0.56           0.20 -0.385          0.40 -0.18
  0.5 -0.055          0.6   0.145          0.80  0.565          1.0   1.0
 6
 -1.0  2.0           -0.79  1.53          -0.63  1.25          -0.30  0.93
  0.0  0.72           1.0   1.0
 2
 -1.0  2.0            1.0   1.0
 2
 -1.0  1.0            1.0   0.0
 2
 -1.0 -1.0            1.0   1.0
 2
 -1.0  2.0            1.0   0.0
 16
 -1.0 -1.16         -0.90  -1.24          -0.80   -1.77        -0.70 -2.36
 -0.6 -2.79         -0.5   -2.91          -0.40   -2.67        -0.25 -1.69
 -0.1 -0.50          0.0    0.0            0.10    0.83         0.20  1.09
  0.5  1.02          0.7    1.01           0.90    0.94         1.00  1.0
 2
 -1.0  0.0            1.0   0.0
 9
 -1.0  0.0            0.0   0.0            0.10   -0.04         0.20  0.0
  0.3  0.1            0.40  0.21           0.80    0.67         0.90  0.80
  1.0  1.0
 11
 -1.0 -1.16          -0.90 -0.78          -0.80   -0.50        -0.70 -0.31
 -0.6 -0.17          -0.50 -0.08          -0.35    0.0         -0.20  0.05
 -0.1  0.08           0.0   0.11           1.0     0.0
  0
  0
  0
  0
 11
  0.0     0.0        0.1    0.0          0.15    0.05         0.24     0.08
  0.3     0.96       0.4    0.96         0.60    0.97         0.80     0.90
  0.90    0.80       0.96   0.50         1.0     0.0
  2
  0.0     0.0        1.0    0.0
  2  2
        0.0     1.0
  0.0   0.0     0.0
  1.0   0.0     0.0
/
/ BREAK DATA
SB13
  50    1.0    0.1          .0    .0    .0
                            .5    .6    .6      3.8E3  3.8E3  3.8E3  3.8E3
   2
  0.   4.      1000.   4.
/
/ STEAM GENERATOR DATA
SB15
```

```
SB1501                                                                  00040700
 55  139  45 45 1  1                                                    00040800
 5.5   18.9  0.7  0.5    0.02     0.004      10.4  1.0   30.      1.3    00040900
 0.1  0.9999 1.   0.2  0.1                                              00041000
-7.0                                                                    00041100
 0.001  80.  0.5  0.5  0.5                                              00041200
 3                                                                      00041300
 0.0 1.0 1.0 1.0 1.0 1.0 1.0 1.0 1000.0 1.0 1.0 0.0                     00041400
/                                                                       00041500
/ CORE DATA                                                             00041600
BB16                                                                    00041700
/ AVERAGE HEATER ROD                                                    00041800
SB1601                                                                  00041900
   1                                                                    00042000
  35    2   13    12   0   1  2  2  3                                   00042100
  0.006125      0.016896      0.                                        00042200
2     3     4     5     6     7     8     9     10    11    12    13     00042300
 0.071 0.368 0.368 0.368 0.368 0.368 0.368 0.368 0.368 0.368 0.368 0.18200042400
/0.     108.9 154.1 170.7 180.5 180.5 170.7 170.7 154.1 129.5  72.3 0.   00042500
 0.     119.7 169.3 187.6 198.4 198.4 187.6 187.6 169.3 142.3  79.4 0.   00042600
/ MATERIAL INDEX                                                        00042700
/  1  2  3  4  5                                                       00042800
   1  1  1  1  2                                                       00042900
   0. 0. 0. 0. 1.                                                     00043000
/                                                                       00043100
/ HOTTEST HEATER ROD                                                    00043200
SB1602                                                                  00043300
   2                                                                    00043400
   1    2   13    12   0                                              00043500
  0.006125      0.016896      0.                                        00043700
2     3     4     5     6     7     8     9     10    11    12    13     00043800
 0.071 0.368 0.368 0.368 0.368 0.368 0.368 0.368 0.368 0.368 0.368 0.18200043900
/0.     112.8 159.4 179.7 186.9 186.9 176.7 176.7 159.4 134.0  74.8 0.   00044000
 0.     123.9 175.2 194.2 205.4 205.4 194.2 194.2 175.2 147.3  82.2 0.   00044100
/ MATERIAL INDEX                                                        00044200
/  1  2  3  4  5                                                       00044300
   1  1  1  1  2                                                       00044400
   0. 0. 0. 0. 1.                                                     00044500
/ PHYSICAL PROPERTIES OF HEATER ROD MATERIALS                           00044600
BB17                                                                    00044700
/ NORMALIZED CORE POWER                                                 00044800
  11                                                                    00044900
   0.0    1.0        1.0    1.0         2.0    0.98        2.7    0.8   00045000
   4.5    0.6        7.0    0.4        11.5    0.2        16.5    0.1   00045100
  21.0    0.065     31.0    0.05        1.E4   0.035                    00045200
/------ DENSITY (MGO) -----                                            00045300
   2                                                                    00045400
   0.0    3.E3     2000.0   3.E3                                        00045500
/------ DENSITY (INCONEL 600) -----                                    00045600
   2                                                                    00045700
   0.0    1.0      2000.0   1.0                                         00045800
/------ SPECIFIC HEAT CAPACITY (MGO) -----                             00045900
   6                                                                    00046000
   0.0   0.287                                                         00046100
 100.0   0.287      450.0   0.291      650.0   0.318      800.0   0.323 00046200
1000.0   0.323                                                         00046300
/------ VOLUMETRIC HEAT CAPACITY (INCONEL 600) -----                   00046400
  20                                                                    00046500
 -17.8  323.5       93.3  919.9       148.8  953.6       204.4  979.9  00046600
 260.0 1000.8      315.6 1018.3       371.1 1034.5       426.7 1051.0  00046700
 482.2 1068.4      537.8 1093.3       593.3 1122.7       648.9 1160.4  00046800
 704.4 1208.1      760.0 1267.9       815.6 1341.5       871.1 1431.1  00046900
 926.7 1538.4      982.2 1665.4      1037.8 1814.3      1093.3 1986.5  00047000
/------ THERMAL CONDUCTIVITY (MGO) -----                               00047100
   7    2                                                              00047200
   0.0              100.0              450.0              500.0         00047300
 700.0              800.0             1000.0                           00047400
```

```
  14(3.E3)                                                                    00047500
 0.00149  0.00149  0.00149  0.00149  0.00084  0.00084  0.00076  0.00076 00047600
 0.00062  0.00062  0.00057  0.00057  0.00057  0.00057                       00047700
/------ THERMAL CONDUCTIVITY (INCONEL 600) -----                           00047800
  20    2                                                                   00047900
 -17.8              93.3             148.8             204.4              00048000
 260.0             315.6             371.1             426.7              00048100
 482.2             537.8             593.3             648.9              00048200
 704.4             760.0             815.6             871.1              00048300
 926.7             982.2            1037.8            1093.3              00048400
  40(1.0)                                                                  00048500
 0.003484 0.003484 0.003716 0.003716 0.003925 0.003925 0.004105 0.00410500048600
 0.004299 0.004299 0.004506 0.004506 0.004721 0.004721 0.004946 0.00494600048700
 0.005180 0.005180 0.005419 0.005419 0.005663 0.005663 0.005911 0.00591100048800
 0.006163 0.006163 0.006411 0.006411 0.006660 0.006660 0.006902 0.00690300048900
 0.007143 0.007143 0.007379 0.007379 0.007606 0.007606 0.007821 0.00782100049000
/ HEAT SLAB CONTROL DATA                                                   00049100
BB21                                                                       00049200
 1 1                                                                       00049300
/                                                                          00049400
/ HEAT SLAB DATA                                                           00049500
BB22                                                                       00049600
SB2201                                                                     00049700
 1 2 1 1 0 36     0.475 0. 0.006   69.0   .0   .0                         00049800
   1 1 5 1                  0.006    2.23E4                                00049900
/  1 1 5 1                  0.006    1.98E4                                00050000
SB2202                                                                     00050100
 2 2 1 1 0 37     0.940 0. 0.006  100.2   .0   .0                         00050200
   1 1 5 1                  0.006    3.24E4                                00050300
/  1 1 5 1                  0.006    2.88E4                                00050400
SB2203                                                                     00050500
 3 2 1 1 0 38     0.935 0. 0.006  161.2   .0   .0                         00050600
   1 1 5 1                  0.006    5.20E4                                00050700
/  1 1 5 1                  0.006    4.62E4                                00050800
SB2204                                                                     00050900
 4 2 1 1 0 39     0.929 0. 0.006  100.2   .0   .0                         00051000
   1 1 5 1                  0.006    3.24E4                                00051100
/  1 1 5 1                  0.006    2.88E4                                00051200
SB2205                                                                     00051300
 5 2 1 1 0 40     0.625 0. 0.006   61.5   .0   .0                         00051400
   1 1 5 1                  0.006    1.99E4                                00051500
/  1 1 5 1                  0.006    1.77E4                                00051600
/                                                                          00051700
/ SLAB MATERIAL DATA                                                       00051800
BB23                                                                       00051900
SB2301                                                                     00052000
 1                                                                         00052100
 STAINLESS STEEL ( 18CR 8NI )                                              00052200
/ DENSITY                                                                  00052300
 2                                                                         00052400
  20.0  7820.0       1000.0  7820                                         00052500
/ SPECIFIC HEAT                                                            00052600
 2                                                                         00052700
  20.0  0.118        1000.0 0.118                                         00052800
/ THERMAL CONDUCTIVITY                                                     00052900
 6                                                                         00053000
  20.0  0.35          100.0  0.38         200.0  .40         400.0  0.47  00053100
 600.0  0.55         1000.0  0.70                                         00053200
/                                                                          00053300
BB24                                                                       00053400
SB2401                                                                     00053500
 1                                                                         00053600
/ NORMALIZED BYPASS HEATER POWER                                           00053700
  11                                                                       00053800
   0.0   1.0         1.0   1.0         1.2   0.8         1.75  0.6        00053900
   2.5   0.5         4.5   0.4         8.4   0.3        11.3   0.2        00054000
  13.0   0.1        13.6   0.0         1.E4  0.0                          00054100
```

```
/ VALVE DATA                                                          00054200
BE25                                                                  00054300
SB2501                                                                00054400
  2  42  0.06 0.06  2.78   1.E5  0.   0.  0.  0.                      00054500
/ 2  42  0.08 0.08  2.35   1.E5  0.   0.  0.  0.                      00054510
SB2502                                                                00054600
  2  47  0.08 0.08  2.78   1.E5  0.   0.  0.  0.                      00054700
/ 2  47  0.08 0.08  2.35   1.E5  0.   0.  0.  0.                      00054710
SB2503                                                                00054800
  2  49  0.08 0.08  2.78   1.E5  0.   0.  0.  0.                      00054900
/ 2  49  0.08 0.08  2.35   1.E5  0.   0.  0.  0.                      00054910
SB2504                                                                00055000
 -2  51  0.06 0.06  1.E4   1.E5  0.   0.  0.  0.                      00055100
/                                                                     00055200
/ MISCELLANEOUS DATA                                                  00055300
BB26                                                                  00055400
   0. 1.4  1.4  0.                                                    00055500
BEND                                                                  00055600
6                                                                     00055700
  0    0    0    0    0    0.                                        00055800
  0. 1.E-4  0. -1.E4  -1.E-4  1.E-4                                   00055900
  0                                                                   00056000
  0  0.08                                                             00056100
  0  0.08                                                             00056200
```

Appendix B Description and Geometrical Data of components in FIX II Loop

Item no	Description	Figure no reference	Lowest level**) (m)	Highest level**) (m)	Diameter or hydr.diameter* (m)	Material thickness (mm)	Min flow area (cm^2)	Flow length (m)	Volume (dm^3)	Comments
1	Lower plenum	2:5	0.835	1.603	0.264	30	322.1	0.768	30.6	
2	Lower plenum baffle inlet	2:5	0.986	1.310	0.0815*	3/30	158.4	0.324	4.52	Section within baffle
3	Bundle inlet section	2:6	1.501	1.582	0.0136*	3-20	64	0.081	0.76	
4	Test section	2:5	1.582	5.326	0.0136*	2	60.34	3.744	22.7	Up to top plate
5	Upper plenum, lower part	2:5	5.330	5.444	0.120*	30	530	0.114	6.0	
6	Upper plenum, upper part	2:5	5.444	5.509	0.184	68	240	0.065	1.56	
7	Steam separator	2:15	5.509	7.357	0.150/0.100	2	78.5	1.848	16.7	
8	Spray condenser	2:15	5.514	9.705	0.264/0.5	53	361	4.191	678.0	
9	Downcomer, upper horizontal part	2:3	5.094	5.564	0.0986/0.1095	15.9	76	3.42	31.4	One 90^{o}-elbow at end incl
10	Downcomer, vertical part, to pump P1	2:3	0.365	5.094	0.0737/0.1095	15.9	42.6	5.22	48.7	One 90^{o}-elbow at pump inlet

Item no	Description	Figure no reference	Lowest level** (m)	Highest level** (m)	Diameter or hydr.diameter* (m)	Material thickness (mm)	Min flow area (cm^2)	Flow length (m)	Volume (dm^3)	Comments
11	Pump P2 suction line from downcomer	2:3	0.295	1.115	00492/ 0.0737	7.6	19.0	2.29	7.69	Two T-connections plus one 90°-elbow
12	Pump P1	2:3	0.365	0.648	-	-	-	-	10.1	
13	Pump P2	2:3	0.295	0.523	-	-	-	-	5.0	
14	Intact recirculation line pressure side	2:3	0.648	1.201	0.0737/ 0.0986	7.6	42.6	6.15	28.8	One 65°-elbow, two 90° - elbows plus pump exit restriction orifice (see table 2:2)
15	Broken recirculation line, pump P2 to split break T-connection	2:3	0.523	0.940	0.0492	5.5	19.0	1.41	2.8	One 90° - elbow and pump exit restriction plus meas. orif (see Table 2:2)
16	As above, from break T-connection to break line from lower plenum	2:3	0.940	1.201	0.0492	5.5	19.0	3.06	5.82	Three 90° - elbows
17	Broken rec. line back to lower plenum	2:3	1.201	1.201	0.0737/ 0.0986	7.6	42.6	1.42	7.57	One 25° - turn

Item no	Description	Figure no reference	Lowest level** (m)	Highest level** (m)	Diameter or hydr.diameter* (m)	Material thickness (mm)	Min flow area (cm^2)	Flow length (m)	Volume (dm^3)	Comments
18	Bypass channel lower horizontal part	2:3	1.311	1.311	0.0248/ 0.0477	6.3	4.8	1.16	1.41	Measuring orifice (see Table 2:2)
19	Guide tube simulator volume	2:3/ 2:13	0.090	1.311	0.0777/ 0.226	12	47.4	1.22	32.3	See Fig 2:13 for details
20	Bypass channel, vertical part	2:3/ 2:13	1.311	5.449	0.972/* 0.0673	8.6	70.7	4.14	29.3	Heater included
21	Bypass channel, upper horizontal part	2:3/ 2:13	5.421	5.421	0.0477	5.5	17.9	1.16	2.14	
22	Split break line, from T-connection to break flow restrictor K12	2:1/ 2:3	0.940	0.940	0.0737	7.6	42.6	1.48	6.29	Flow restrictor see Fig 2:19 and Table 2:2
22a	As above, to tank T2	2:1/ 2:3	0.940	0.940	0.0737/ 0.1317	4	42.6	0.850	9.7	
23	Guillotine break line from pump P2 suction line to break flow restrictor K11	2:1/ 2:3	1.115	1.115	0.0649/ 0.0737	7.6	33.1	2.44	9.09	Flow restrictor see Fig 2:19 and Table 2:2
24	As above, to tank T1	2:1/ 2:3	1.115	1.115	0.1071	3.6	90.1	3.24	29.2	

Item no	Description	Figure no reference	Lowest level**) (m)	Highest level**) (m)	Diameter or hydr.diameter* (m)	Material thickness (mm)	Min flow area (cm^2)	Flow length (m)	Volume (dm^3)	Comments
25	Guillotine break line from T-connection before valve V116 to break flow restrictor K13	2:1/ 2:3	1.201	1.201	0.0649/ 0.0737	5	33.1	1.43	4.7	Flow restrictor see Fig 2:19 and Table 2:2
26	As above, to tank T3	2:1/ 2:3	1.201	1.201	0.0661/ 0.1317	4	34.3	1.44	14.9	
27	Coolant flow line from down-comer to pump P3	2:1/ 2:3	0.365	1.415	0.071	9.5	39.6	3.07	15.5	Two 90^{o} - elbows
28	Pump P3	2:1/ 2:3	0.365	0.648	-	-	-	-	10.1	
29	From pump P3 to evaporation cooler	2:1/ 2:3	0.648	0.165	0.071	9.5	39.6	2.46	10.08	Three 90^{o}- elbows
30	Evaporation cooler	2:1	0.706	0.706	139x0.008*	1	0.50	947.2	47.6	139 U-tubes
31	Outlet from evap cooler to feedwater line	2:1/ 2:3	0.706	5.408	0.071	9	39.6	6.90	27.9	

Item no	Description	Figure no reference	Lowest level**) (m)	Highest level**) (m)	Diameter or hydr.diameter* (m)	Material thickness (mm)	Min flow area (cm^2)	Flow length (m)	Volume (dm^3)	Comments
32	Feedwater line	2:1/ 2:3	5.408	5.564	0.0383/ 0.0492	5.4	11.5	6.27	10.74	Two 90^{o} - elbows measuring orifice (see Table 2:2)
33	Spray water lines, up to V109	2:1/ 2:3	5.408	7.9	0.0294/ 0.0492	5.0	12.2	2.49	6.81	Including connections to the three separate lines. Measureing orifice, see Table 2:2
34	Spray lines(3) from V109 to spray condenser	2:1/ 2:3	7 900	~9.5	2*0.0492 1*0.0243	5.5	42.6	8.1 7.1 7.4	32.4	Three 90^{o}-elbows. Volume for three lines
35	Steam line to V111	2:1/ 2:3	9.198	9.198	0.0737/ 0.0986	7.6	42.6	1.89	9.72	Measuring orifice, see Table 2:2

*) Hydraulic diameter is given for non-circular cross-sections

**) Level reference plane is the bottom plate

Appendix C Brief Description of Code Characteristics And Information on Computer Resources Utilized in Present Calculation

Table C.1 shows the brief description of the computer code characteristics. The detailed information of the utilized computer resources in the present calculationis is shown in Table C.2. These tables have been made for the submittal to the ISP No.15.

Table C.1
Computer Code Characteristics

1 Participant Identification

- JAPAN 'B'

2 Name and Version of Computer Code

- THYDE-P1 (SV03L03)

3 Change in Computer Code not Included in Basic Code Description

- Relief valve modeling for FIX-II calculation
- Phase separator modeling
  (THYDE-P1 has originally been developed for PWR LOCA anlyses.)

4 Classification of Hydrodynamic Model

- Drift flux model
- Relaxation model considering thermal non-equilibrium

5 Slip-Model

- Drift flux model

- $V_{gj}=1.14\left[\frac{\sigma g(\rho_{fs}-\rho_{gs})}{\rho_{fs}^2}\right]^{1/4}$

6 Critical Flow Model

- Modified Zaloudek for subcooled state
- Moody for saturated state (Cd=0.6)
- Transition quality : 0.02

7 Interphase Drag Model

See item 4

8 Wall Friction Model

- Single phase friction factor :
  - 16/Re for laminar flow
  - Blausius formula for turbulent flow
- Two-phase multiplier : Thom

9 Flashing/Condensation Model

See item 4

10 Heat Transfer Models

- Present option selected :
  - Dittus-Boelter for subcooled forced convection
  - Thom for nucleate boiling
  - Bromley-Pomerantz for low flow film boiling
  - Groenevelt and Dougall-Rohsenow for high flow film boiling
  - McEligot for superheated steam forced convection
  - Interpolation for transition boiling

11 CHF Correlation

- Present option selected :
  - Biasi for forced flow condition (high flow)
  - Zuber for pool flow condition (low flow)

Table C.2
Details of the utilized computer resources in the calculation

1 Participant Identification

JAPAN 'B'

2 Computer code

THYDE-P1 (SV03L03)

3 Number of nodes

54

4 Number of junctions

50

5 Number of heat slabs

- Core : 24 (12 for average rod and 12 for hottest rod)
- Core bypass heater : 5
- Cooler : 1

6 Computer utilized

FACOM M-380

7 Computer time required for the transient

CPU time : 2260 s

8 Number of calculated time steps

7800 steps

9 Remarks

- Ambient heat loss is not taken into consideration :
  - Initial core power : 3.5 MW
  - Initial core bypass power : 62.5 kW
  - No heat slab except core, core bypass and cooler

Appendix D Pump Characteristic Curves Used in Present Calculation

In this appendix, the pump characteristic curves used in the present calculation are presented. These data are taken from Ref. (13) in the text.

Homologous pump curves for pump P1 used in Studsvik's RELAP 5 calculations

Curve type	α/ν or ν/α	h/ν^2 or h/α^2
HAN (1)	0	1.181
	0.27	1.180
	0.47	1.160
	0.64	1.130
	1.00	1.000
HVN (2)	0.0	-0.56
	0.41	-0.16
	0.51	-0.05
	0.76	0.48
	1.00	1.00
HAD (3)	-1.00	2.00
	-0.95	1.81
	-0.62	1.52
	-0.50	1.39
	0.00	1.181
HVD (4)	-1.00	2.00
	-0.79	1.53
	-0.63	1.25
	-0.30	0.93
	0.00	0.72

Torque curves are not needed (speed given).

Homologous pump curves for pump P2 used in Studsvik's RELAP 5 calculations

Curve type	α/ν or ν/α	h/ν^2 or h/α^2
HAN (1)	0	1.136
	0.2	1.135
	0.4	1.120
	0.6	1.100
	0.8	1.055
	1.0	1.000
HVN (2)	0.0	-0.56
	0.2	-0.385
	0.4	-0.180
	0.5	-0.055
	0.6	0.145
	0.8	0.565
	1.0	1.000
HAD (3)	-1.00	2.00
	-0.95	1.81
	-0.62	1.52
	-0.50	1.39
	0.00	1.136
HVD (4)	-1.00	2.00
	-0.79	1.53
	-0.63	1.25
	-0.30	0.93
	0.00	0.72

Torque curves are not needed (speed given).

Head multiplier for pumps P1 and P2 used in Studsvik's RELAP 5 calculations

α	M (α)
0.08	0.00
0.10	0.00
0.15	0.05
0.24	0.08
0.30	0.96
0.40	0.98
0.60	0.97
0.80	0.90
0.90	0.80
0.96	0.50
1.00	0.00

Dimensionless head ration difference data (Semiscale) for pumps P1 and P2

Curve type	x	y
HAN (1)	0.0	0.00
	0.1	0.83
	0.2	1.09
	0.5	1.02
	0.7	1.01
	0.9	0.94
	1.0	1.0
HVN (2)	0.0	0.0
	0.1	-0.04
	0.2	0.00
	0.3	0.10
	0.4	0.21
	0.8	0.67
	0.9	0.80
	1.0	1.00
HAD (3)	-1.0	-1.16
	-0.9	-1.24
	-0.8	-1.77
	-0.7	-2-36
	-0.6	-2.79
	-0.5	-2.91
	-0.4	-2.67
	-0.25	-1.69
	-0.1	-0.50
	0.0	0.00
HVD (4)	-1.0	-1.1b
	-0.9	-0.78
	-0.8	-0.50
	-0.7	-0.31
	-0.6	-0.17
	-0.5	-0.08
	-0.35	0.00
	-0.2	0.05
	-0.1	0.08
	0.0	0.11